REGULATION DER EPITHELIALEN *TIGHT JUNCTIONS* DURCH DEN HUMANEN SOMATOSTATINREZEPTOR-SUBTYP 3

Dissertation

zur Erlangung des Doktorgrades

des Fachbereichs Biologie

der Universität Hamburg

vorgelegt von

CHONG WEE LIEW
aus MALAYSIA

Hamburg 2004

REGULATION OF EPITHELIAL TIGHT JUNCTIONS BY HUMAN SOMATOSTATIN RECEPTOR SUBTYPE 3

A DISSERTATION

SUBMITTED FOR THE DOCTORAL DEGREE
FACULTY OF BIOLOGY
UNIVERSITY OF HAMBURG

BY

CHONG WEE LIEW
from MALAYSIA

Hamburg 2004

fürBibi

Genehmigt vom
Fachbereich Biologie der
Universität Hamburg
auf Antrag von Herrn Professor Dr. D. RICHTER
Weitere Gutachter der Dissertation:
Herr Professor Dr. H. BRETTING

Tag der Disputation: 26. November 2004

Hamburg, den 12. November 2004

Universität Hamburg
14/1
Fachbereich Biologie

Professor Dr. Arno Frühwald
Dekan

ACKNOWLEDGMENTS

First of all, I would like to thank Herrn Prof. Dr. Dietmar Richter for giving me the opportunity to do my research and complete my PhD in his institute and in Germany.

Most importantly, I would like to thank my supervisors, Herrn Dr. Hans-Juergen Kreienkamp for his supervision, guidance, encouragement, ideas, helping hand and everything throughout the entire projects.

Not forgetting Dr. Stefan Kindler and Dr. Dietmar Baechner for their guidance, ideas and encouragement.

I would also like to give my special thanks to Dr. Johanna Brandner for her helpful discussions, her Millicell apparatus and all the antibodies for this study.

Many thanks also go to Soenke Harder and Dr. Fritz Buck for mass spectroscopy and primer synthesis.

Special thank to Frau Maria Kienle for her help in all the administrative works as well as my registration as PhD student with the university.

I would like to thank past and present members of our lab: Hans-Hinrich, Gwen, Kerstin, Peter, Arne, Felix, Marina, Marie, Agata and Nina; as well as members from other labs in the institute: John, Krishna, Cornelia, Brigitte, Konstanze, Stefanie, Carola, Heidje, Bettina and Monica for their help and support.

I am most thankful to Bibi for her understanding, support and patience.

Last but not least, I would like to thank my parents and sisters for their constant love, care and support.

TABLE OF CONTENTS

		Page
Table of Contents		I
Abbreviations		IV
Chapter 1	**Introduction**	1
1.1	The Peptides	1
1.2	The Receptors	3
1.3	Expression of SSTR Subtypes	5
1.4	Signal Transduction Through Somatostatin Receptor	6
1.5	PDZ Domains and Binding Motifs	8
1.6	Purpose of This Study	11
Chapter 2	**Materials and Methods**	12
2.1	**Materials**	12
2.1.1	Chemicals	12
2.1.2	Microbial Strains and Cell Lines	12
2.1.3	cDNA Libraries and Genomic DNAs	12
2.1.4	Plasmid DNAs	13
2.1.5	Antibodies	13
2.1.6	Oligonucleotides	14
2.2	**Methods**	14
2.2.1	Molecular Biology Techniques	14
2.2.1.1	Polymerase Chain Reaction (PCR)	14
2.2.1.2	Splice Variants Expression Profiles Assays	15
2.2.1.3	Restriction Endonuclease Digestions of DNA samples	16
2.2.1.4	Agarose Gel Electrophoresis	16
2.2.1.5	Purification of DNA Fragments from Agarose Gel	16
2.2.1.6	DNA Ligation	16
2.2.1.7	pGEM®-T Easy Vector Systems and TOPO TA Cloning® Kits	17
2.2.1.8	Preparation of Competent *E. coli* cells	17
2.2.1.9	*E. coli* Transformation	17
2.2.1.10	Plasmid DNAs Isolation	18
2.2.1.10.1	Mini-preparation with TELT-Lysis (Rapid Boiling Method)	18
2.2.1.10.2	Midi-preparation	18
2.2.1.11	Nucleic Acids Concentration Determination	18
2.2.1.12	DNA Sequencing	18
2.2.2	Yeast Two Hybrid System	19
2.2.2.1	Yeast Transformation	19

2.2.2.2 Yeast Two Hybrid Screening 19
2.2.2.3 β-Galactosidase Colony-lift Filter Assay 20
2.2.2.4 Plasmid Isolation from Yeast 20

2.2.3 Cell Biology Techniques 21
2.2.3.1 Cell Culture 21
2.2.3.2 Transient Transfection 22
2.2.3.3 Stable Transfection 22

2.2.4 Immunofluorescence Techniques 22
2.2.4.1 Immunocytochemistry 22
2.2.4.2 Immunohistochemistry 23
2.2.4.3 Microscopy 23

2.2.5 Biochemical Techniques 24
2.2.5.1 SDS-Polyacrylamide-Gel-Electrophoresis (SDS-PAGE) 24
2.2.5.2 Coomassie Staining of SDS-PAGE Gel 24
2.2.5.3 Protein Concentration Determination 24
2.2.5.4 Western Blot Analyses 25
2.2.5.5 Expression and Purification of Fusion Protein 25
2.2.5.6 Antibody Affinity Purification 26
2.2.5.7 Covalent Coupling of Antibody to Protein A/G Agarose 26
2.2.5.8 Precipitation Assays 27
2.2.5.8.1 Co-immunoprecipitation from Mammalian Cells 27
2.2.5.8.2 Affinity Precipitation with Synthetic Peptide 27
2.2.5.9 Mass Spectroscopy 28
2.2.5.10 Overlay Assays 28
2.2.5.11 Transepithelial Electrical Resistance (TER) Measurement 29
2.2.5.12 Calcium Switch Assays 30
2.2.5.13 Statistical Analysis 30

Chapter 3 Results 31
3.1 Identification of Interaction Partners for Human Somatostatin Receptor 3 with the Yeast Two-Hybrid System 31
3.2 Identification of Novel Splice Variants for MUPP1 35
3.3 Interaction of hSSTR3 with MUPP1 In Immunoprecipitation Assay 39
3.3.1 Co-Immunoprecipitation from Overexpressed Cells 39
3.3.2 Generation and Purification of Anti-PDZ10 Antibody 41

3.3.3	Co-Immunoprecipitation from Non-overexpressed Cells	41
3.4	Localization of MUPP1 in Epithelial Cell Lines and Choroid Plexus	43
3.5	Affinity Purification of MUPP1 Associated Macromolecular Complexes	44
3.5.1	Affinity Purification with hSSTR3 Peptide Coupled NHS-Sepharose	44
3.5.2	Identification of MUPP1 Macromolecular Complexes	45
3.6	Differential Binding Affinity of SSTR3 Homolog Dictated by Amino Acid Composition of the PDZ Binding Domain at the C-terminus	50
3.7	Localization of hSSTR3 in Stably Transfected Epithelial Cell Lines	52
3.7.1	Mapping of Regions Responsible for Apoptotic Effects of hSSTR3	52
3.7.2	Localization of hSSTR3 in MCF-7 Cells	54
3.7.3	Localization of hSSTR3 and the Fusion Receptor in MDCK II Cells	55
3.8	Functional Relevance of the Interaction between the Receptor and the TJ Protein, MUPP1	59
3.8.1	Regulation of the TJ Integrity in the MCF7-hSSTR3 Stable Cell Line	59
3.8.2	Regulation of the TJ Integrity in MDCK II Stable Cell Line	64
3. 9	Biochemical Analysis of Wild Type and Stable MDCK II Cell Line after Calcium Switch Assays	68
Chapter 4	**Discussion**	75
Chapter 5	**Summary**	89
Chapter 6	**References**	90
Appendices		
Appendix I	List of Constructs	i
Appendix II	List of Primers	iii
Bibliography		vi

ABBREVIATIONS

Acc.	accession number in GenBank (www.ncbi.nlm.nih.gov)
Amp	ampicillin
bp	base pair(s)
β-gal	β-galactosidase
BSA	bovine serum albumin
°C	degree Celsius
C-terminal	carboxy terminal
COS-7	African green monkey kidney
DMEM	Dulbecco's modified Eagle's medium
DMSO	dimethylsulfoxide
DNA	deoxyribonucleic acid
dNTP	deoxyribonucleoside 5'-triphospate
DO	dropout
EDTA	ethylenediamine tetraacetic acid
EGFP	enhanced green fluorescence protein
ERK	extracellular signal-regulated protein kinase
FBS	fetal bovine serum
g	gram(s)
GST	glutathione S-transferase
GPCR	G protein-coupled receptor
h	hour(s)
HEK	human embryonic kidney
Ig	immunoglobulin
IPTG	isopropyl-β-D-thiogalactopyranoside
kb	kilobase(s)
kDa	kilodalton(s)
l	liter(s)
M	molarity
min	minute(s)
mol	mole(s)
MAPK	mitogen-activated protein kinase
MEK1/2	mitogen-activated extracellular signal-regulated protein kinase kinase
MDCK	Madin-Darby canine kidney
MCF-7	human breast epithelial
N-terminal	amino terminal
NHS	*N*-Hydroxy-Succinimidyl

OD	optical density
PCR	polymerase chain reaction
PDZ	PSD-95/Discs-large/ZO-1
PTX	pertussis toxin
rpm	revolutions per minute
s	second(s)
S.D.	standard deviation
SDS	sodium dodecyl sulfate
SST	somatostatin
SSTR	somatostatin receptor
TAE	Tris-acetate/EDTA
TEMED	N,N'N,N' -Tetramethylethylendiamine
TER	transepithelial electrical resistance
TJ	tight junction
Tris	2-amino-2-(hydroxymethyl)-1,3-propanediol
U	unit(s) of enzyme activity
UV	ultraviolet
V	volt(s)
v/v	volume per volume
w/v	weight per volume
X-Gal	5-Bromo-4-Chloro-3-Indolyl-β-D-Galactopyranoside
ZO-1	*Zonulae Occludentes*-1

CHAPTER ONE INTRODUCTION

1.1 The Peptides

Somatostatin (SST) also known as somatotropin release-inhibiting factor (SRIF), was first identified in hypothalamic extracts as a tetradecapeptide that inhibits the release of growth hormone (Krulich *et al*., 1968). Subsequently, it was found that SST14 is produced not only in the hypothalamus but also throughout the central and peripheral nervous system (CNS & PNS) as well as in many peripheral organs such as the endocrine pancreas, gut, thyroid, adrenals, submandibular glands, kidneys, prostate and placenta (Hokfelt *et al*., 1975; Patel & Reichlin, 1978; Reichlin, 1983). In addition to that, many tumor cells as well as inflammatory and immune cells also produce SST (Reichlin, 1983).

Besides SST14, the cyclic 14 amino acid peptide originally identified in the hypothalamus, a second bioactive form with a N-terminal extension of 14 amino acids, SST28 was subsequently discovered and characterized (Pradayrol *et al*., 1980). Different SST producing cells in both CNS and PNS produces these two peptides in various proportions.

In mammals, SST is derived by tissue specific proteolytic maturation from a large preprosomatostatin precursor (116 amino acids) (Patel & Galanopoulou, 1995), which in turn is the product of a single gene (human chromosome 3q28). The signal peptide of preprosomatostatin is first cleaved to yield the prosomatostatin (92 amino acids) which can then be processed predominantly at the C-terminal segment by the appropriate prohormone processing enzymes to release either SST28 or SST14 (Epelbaum *et al*., 1994) (Figure 1.1).

Some SST-related peptides have been found including cortistatin (CST) from human and rodent, Drostatin from *Drosophila melanogaster* and allatostatin C from *Manduca sexta*. Unlike Drostatin and allatostatin C, two of the SST-related peptides found in invertebrate in which only bear superficial similarity to somatostatin-14, the cortistatin gene encodes for a 112 amino acid preprohormone that gives rise to two cleavage products comparable to SST14 and SST28. These cleavage products consist of human CST17 and its rodent homologue CST14 and CST29 in both human and rodent (de Lecea *et al*., 1996; Fukusumi *et al*., 1997) (Figure 1.1). The gene expression of CST is however restricted to the cerebral cortex and hippocampus. CST was not found in the hypothalamus and some peripheral tissues (de Lecea *et al*., 1996).

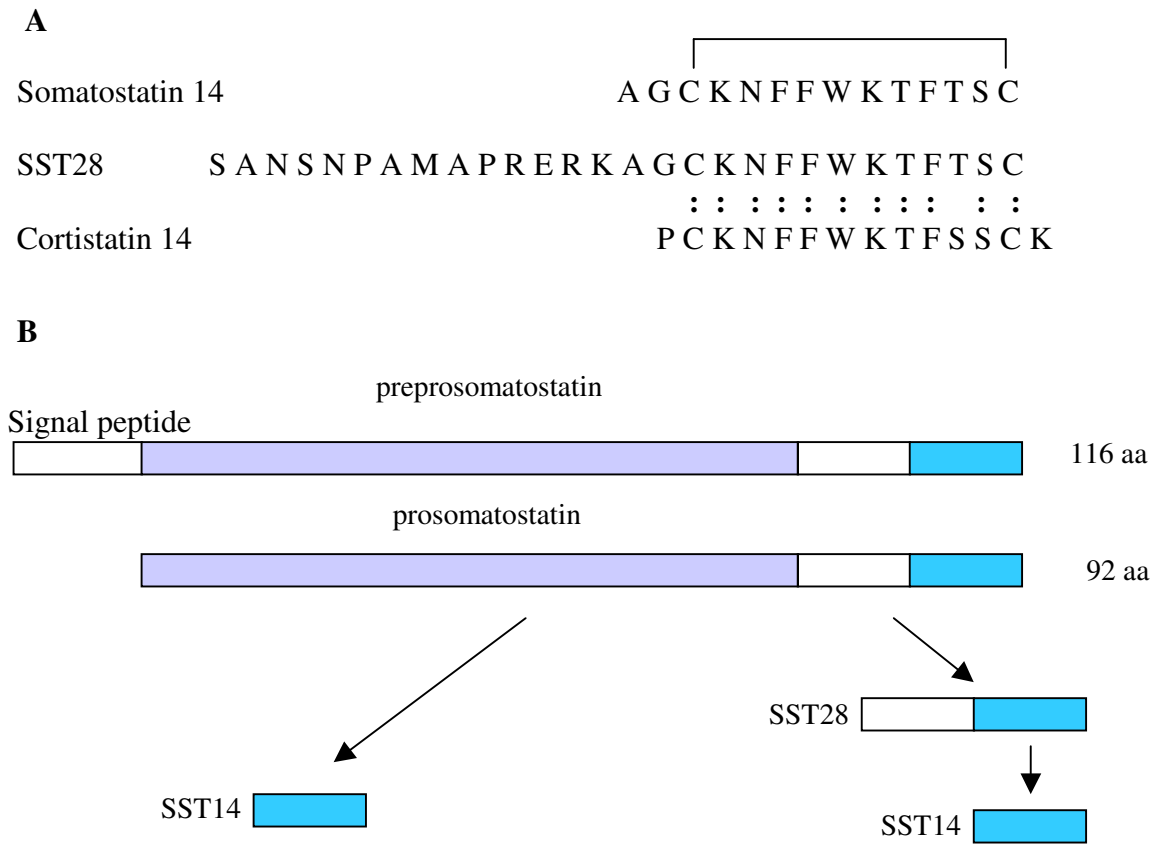

Figure 1.1 Structure and biosynthesis of bioactive somatostatin peptides

(A) Primary structure of the bioactive somatostatin peptides SST14, SST28 and cortistatin14. The position of a conserved disulfide loop is indicated in the sequence of SST14. '**:**' Indicate identical sequence between somatostatin and cortistatin.
(B) Prosomatostatin (92 amino acids) is derived from preprosomatostatin (116 amino acids) after cleavage of the signal peptide. Further cleavage at typical prohormone cleavage sites yields either SST28 or SST14.

Besides its function as a regulator of growth hormone release, somatostatin also has broad inhibitory effects on both endocrine secretion, for example insulin, glucagon, gastrin, cholecystokinin, vasoactive intestinal peptide and secretin; and exocrine secretion, for example gastric acid, intestinal fluid and pancreatic enzymes (Reichlin, 1983). Furthermore, it has been shown that SST functions as a neurotransmitter in the CNS with effects on cognitive, locomotor, sensory and autonomic functions (Epelbaum *et al.*, 1994; Patel, 1992; Reichlin, 1983). It inhibits the release of dopamine from the midbrain and of norepinephrine, thyroid releasing hormone, corticotrophin-releasing hormone, and endogenous SST from the hypothalamus (Patel, 1999). This pan-antisecretory profile has led to the use of SST14 or the metabolically stabilized cyclo-octapeptide, SMS 201-995 (Octreotide) (Bauer *et al.*, 1982) for the treatment of a range of conditions including diabetes type I and II; hypersecretory tumors

such as growth hormone-secreting pituitary adenomas, gastrinomas, insulinomas, glucagonomas and vipomas; and some gastrointestinal disorders (Reichlin, 1983). In addition, a benign side effect of this treatment was the shrinkage of tumors, which could be achieved by the octreotide therapy. These antiproliferative effects of SST have also been demonstrated in normal dividing cells (Reichlin, 1983; Aguila *et al*., 1996; Karalis *et al*., 1994) and *in vivo* in solid tumors (Weckbecker *et al*., 1993). In addition to its cytostatic effect, SST also induces apoptosis as first demonstrated in the AtT-20 and MCF-7 tumor cell lines treated with octreotide (Pagliacci *et al*., 1991; Sharma & Srikant; 1998; Srikant, 1995).
All these actions are mediated by a family of seven transmembrane domains G-protein-coupled receptors, which bind the natural SST peptides, SST14 and SST28, with low nanomolar affinity.

1.2 The Receptors

In the early 1990s, about 20 years after the discovery of SST, the first cDNA of a somatostatin receptor (SSTR) was described to encode a novel putative G-protein-coupled receptor in brain (Meyerhof *et al*., 1991). It was later identified as the rat sstr1 by sequence homology to the human sstr1 and the mouse sstr1 gene (Yamada *et al*., 1992). At the same time, the rat sstr2 gene was identified by expression cloning by Kluxen *et al*. (1992). By a polymerase chain reaction (PCR) based approach using degenerate primers directed at the conserved transmembrane regions which are shared by all G-protein-coupled receptors of the rhodopsin family, the cDNA of rat sstr3 (Meyerhof *et al*., 1992) and rat sstr5 (O'Carroll *et al*., 1992) were isolated. Subsequently, based on their highly conserved sequence, most members of the somatostatin receptor family from various species was rapidly isolated (Meyerhof, 1998). The genes of sstr1, sstr3, sstr4 and sstr5 are not interrupted by introns in their protein coding regions, whereas the sstr2 gene contains a cryptic intron at the 3' end of the coding segment, which gives rise to two spliced variants, a long form named SSTR2A (which corresponds to the unspliced version of the mRNA) and a short form named SSTR2B (which carries the alternative exon coding for a slightly shorter C-terminus) (Vanetti *et al*., 1992).
A comparative amino acid sequence analysis revealed that the five SSTRs exhibit the typical profile of G-protein-coupled receptors with seven hydrophobic α helical transmembrane (TM) domains (about 25 amino acids), an extracellular N-terminus and an intracellular C-terminus. They constitute their own subfamily within the larger family of type I (Rhodopsin-like) G-protein-coupled receptors (GPCR), the closest relatives being the four known opioid

receptors (μ, κ, δ, ORL). Thus the δ-opioid receptor subtype shows 37% sequence similarity to the mouse SSTR1 (Evans *et al*., 1992).

Functional expression of the SSTRs cDNA in HEK or COS cells yielded receptors which exhibit high affinity for both of the endogenous ligands SST14 and SST28. Only SSTR5 consistently showed some preference for SST28 over SST14 (O'Carroll *et al*., 1992). Cortistatin was shown to be a high affinity agonist for all five receptor subtypes (Siehler *et al*., 1998). On the basis of structural, phylogenetic and pharmacological features, SSTR subtypes can be subdivided into two main classes: SRIF1, which comprises SSTR2, SSTR3 and SSTR5; and SRIF2, which includes SSTR1 and SSTR4. SSTR2, 3 and 5 exhibit high to moderate affinity for the synthetic peptide derivatives SMS 201 995 and MK678, whereas SSTR1 and 4 do not bind SMS and MK678 (Raynor et al., 1993a; Raynor et al., 1993b; Patel and Srikant, 1994; Hoyer et al., 1995).

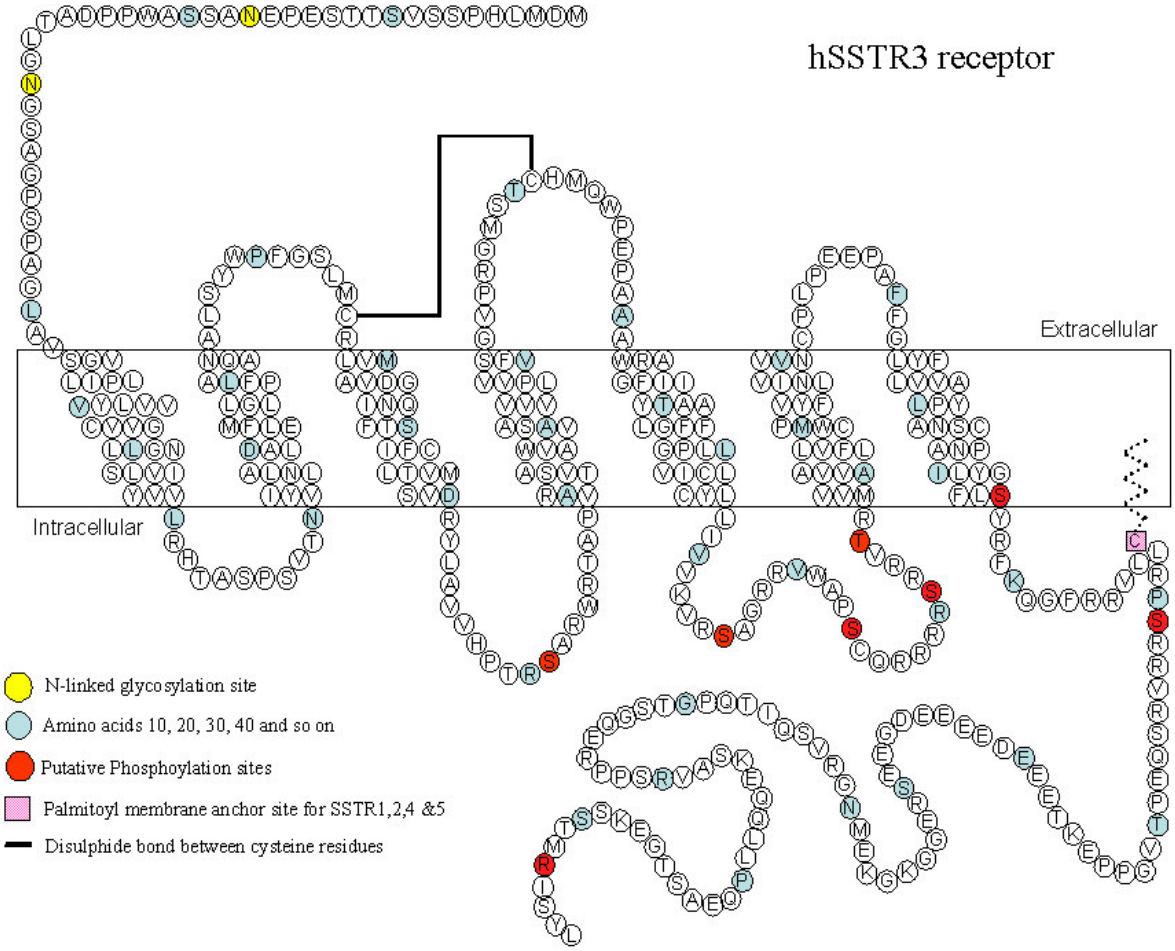

Figure 1.2 Structure of SSTR exemplified by the SSTR3 subtype.
Sites for potential N-linked glycosylation (blue) and phosphorylation (pink) are indicated. A predicted disulphide bond is shown.

The human receptors proteins range in size from 356 (hSSTR2B) to 418 (hSSTR3) amino acids residues, show the greatest sequence similarity in the putative TMs (55-70%) and diverge the most at their amino- and carboxyl-terminal (Patel, 1999). Overall, there is 39-58% sequence identity among the various members of the SSTR family.

All SSTR isoforms that have been cloned so far from human as well as other species possess a highly conserved sequence motif, YANSCANPI/VLY in the 7th TM domain, which serves as a signature sequence for this receptor family. The five hSSTRs display one to four sites for N-linked glycosylation within the amino-terminus, second extracellular loop (ECL) (SSTR5) and the upper part of the 6th TM domain (SSTR2). hSSTR1, 2, 4 and 5 display a conserved cysteine residue 12 amino acids downstream from the 7th TM, which may be the site of a potential palmitoyl membrane anchor as observed in several other members of the GPCR superfamily such as β2- and α2-adrenergic receptors (O'Dowd *et al*., 1989; Kennedy & Limbird, 1993). Interestingly, hSSTR3, which uniquely lacks the cysteine palmitoylation membrane anchor, features a much longer C-tail than the other four members of the family. Besides that, SSTR3 also contains a glutamic acid rich region in its C-terminus of unknown significance (Figure 1.3).

1.3 Expression of SSTR Subtypes

The regional and temporal expression patterns of the receptors have been studied extensively by in-situ hybridization, reverse transcriptase PCR, Northern blotting and radio-ligand binding assays (Wulfsen *et al*., 1993; Breder *et al*., 1992; Bruno *et al*., 1993; Kong *et al*., 1994; Epelbaum *et al*., 1986; Schoeffter *et al*., 1995). Recently, the advent of subtype- and species-selective SSTR antibodies, which were raised against fusion proteins or synthetic peptides, has provide the opportunities to directly localize the SSTR proteins by immunohistochemistry (Dournaud *et al*., 1996; Schindler *et al*., 1997; Kumar *et al*., 1999; Schulz *et al*., 2000; Kulaksiz *et al*., 2002).

It became obvious that the expression patterns of the subtypes are clearly distinct, but overlapping in many regions of the brain. mRNAs from SSTR1-4 have been shown to be present in the hippocampus and the cortex of rats in various studies. In the cortex, SSTR2 is more restricted to the deeper layers, while SSTR1 mRNA is present in all cortical layers; SSTR3 was shown to be the only subtype present in the cerebellum of adult animals, while SSTR1 exhibits a transient expression in this region shortly before and after birth. SSTR4 appears to be the only receptor subtype that is relatively brain-specific. SSTR5 mRNA is only moderately expressed in the rat brain, primarily in the preoptic area and the hypothalamus

(Raulf *et al*., 1994) but there is negligible expression of SSTR5 mRNA in the human brain (Panetta *et al*., 1994; Thoss *et al*., 1996). Other than that, variations in sstr1 mRNA levels between mouse and human cerebrum (Li *et al*., 1992; Yamada *et al*., 1992) as well as differences in localization of SSTR3 in rat and human cerebral cortex revealed by immunohistochemistry (Cervera *et al*., 2002), indicate the existence of species-specific differences in SSTRs gene expression.

An overlapping pattern of sstr1-5 mRNAs has been observed in many peripheral tissues. In the rat pancreatic islets, all five SSTRs mRNAs have been detected (Patel *et al*., 1995). mRNAs for all the SSTR subtypes have also been identified in the rat stomach, duodenum, jejunum, ileum and colon by *in situ* hybridization (Krempels *et al*., 1997). In addition to normal tissues, many tumor cell lines such as AtT-20, GH_4C_1, AR42J, MCF7, Jurkat and etc are rich in multiple SSTR mRNA subtypes (Patel, 1999).

Recent advances in subtype- and species-selective SSTR antibodies development allows more detailed studies of SSTR subtypes at the cellular and subcellular level. A previous immunohistochemical study in adult rat brain showed that SSTR1 is primarily localized to the axon, SSTR2s are confined to the plasma membrane of neuronal somata and dendrite, SSTR3 is selectively targeted to neuronal cilia and SSTR4 is distributed to distal dendrite. SSTR5 was found in the pituitary but not in the central nervous system (Schulz *et al*., 2000). These results demonstrated that even with the overlapping distribution of the receptor subtypes, there appears to be a high degree of specialization in terms of subcellular targeting among the somatostatin receptor subtypes.

1.4 Signal Transduction Through Somatostatin Receptor

Somatostatin receptors elicit their cellular responses through heterotrimeric G-protein-linked modulation of multiple second-messenger systems including adenylyl cyclase, Ca^{2+} and K^+ ion channels, Na^+/H^+ exchanger, phospholipase C, phospholipase A2, MAP kinase (MAPK), serine/threonine phosphates and phosphotyrosine phosphates (PTP). It is believed that just like other GPCRs, binding of agonists to the SSTR would result in a conformational change of the receptor. This conformational change leads to the exchange of the GDP of the $G\alpha$ subunit of a heterotrimeric G-protein to GTP and subsequently results in dissociation of the activated GTP-$G\alpha$ subunit from the $G\beta\gamma$ subunits. Dissociated and activated $G\alpha$ and $G\beta\gamma$ subunits bind directly to effector molecules and modulate their respective second messenger systems.

All SSTR subtypes preferentially couple to pertussis toxin-sensitive Gαi and Gαo containing G-proteins. In addition, in some cases coupling to $G\alpha_{14}$ has been observed. All somatostatin receptors are functionally coupled to inhibition of adenylate cyclase via a pertussis toxin-sensitive G-protein ($G\alpha_{i1-3}$) and hence decrease the cAMP level (Patel *et al*., 1994). This effect may participate in the anti-secretory action of somatostatin. However, somatostatin-induced inhibition of peptide secretion mainly results from a decrease in intracellular Ca^{2+}, which is achieved by either opening K+ channels and secondarily inhibiting voltage-dependent Ca^{2+} current or closing the voltage-dependent Ca^{2+} channels via Gαo protein. All SSTRs except SSTR1 are also coupled to the G-protein gated inwardly rectifying potassium channel (GIRK) (Kreienkamp *et al*., 1997). Gβγ dimers associated with Gαi3 appeared to be responsible for the activation of the inward rectified K^+ current by SSTRs (Takano *et al*., 1997). All five human SSTRs stimulate the PTP via a pertussis toxin sensitive pathway (Patel, 1999) but the nature of the G protein involved is not known. Besides these, activation of G proteins has also been shown to modulate various other effectors directly or indirectly such as phospholipase C, MAPK and Na^+/H^+ exchanger (reviewed in Patel, 1995; Meyerhof, 1998; Patel, 1999).

In addition, activated serine/threonine phosphatase calcineurin has also been suggested to mediate SSTR action on secretory processes (Gromada *et al*., 2001). Anti secretory effects on growth hormone by SSTR1; insulin and glucagons by SSTR2 as well as insulin by SSTR5 have been demonstrated by the respective knock-out mice (Kreienkamp *et al*., 1999; Strowski *et al*., 2000 & 2003).

In responsive normal or transformed cells grown in cell culture or as tumors in experimental animals, SSTR receptor activation can directly lead to cell-growth arrest and/or apoptosis (Mascardo *et al*., 1984; Srikant, 1995; Sharma *et al*., 1996). However, growth inhibition by SSTR is usually incomplete even after prolonged exposure of highly susceptible cells (Weckbecker *et al*., 1993). Multiple in vitro proliferation studies that mostly used cell lines transfected with SSTR receptors have shown that all receptor subtypes can mediate effects on cell growth (Sellers *et al*., 2000), whereas apoptosis is induced via SSTR3 (Sharma *et al*., 1996) and SSTR2 (Guillermet *et al*., 2003). Antiproliferative signaling triggered by SSTR receptor activation leads to activation of PTPase such as SHP-1, SHP-2 and rPTP-η via a pertussis toxin and orthovanadate sensitive pathway, which in turn leads to the modulation of MAPK/ERK pathway (Cordelier *et al*., 1997; Weckbecker *et al*., 2003).

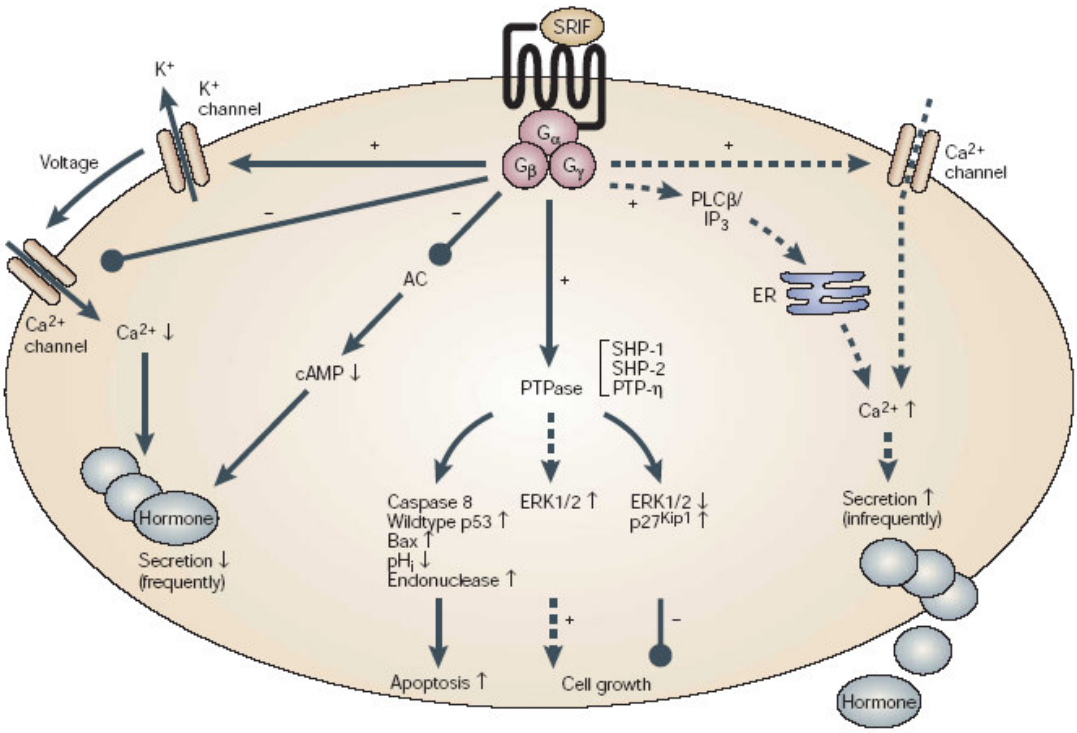

Figure 1.3 SSTR receptor mediated modulation of signaling cascades leading to changes in hormone secretion, apoptosis and cell growth. (from Weckbecker *et al*., 2003)
In most cells, SSTR inhibits hormone as well as other secretions. Increased secretion is observed, for example, in B-lymphocytes. SSTR plays a role in the control of cell growth and apoptosis. In a G-protein-dependent manner, PTPases, such as SHP-1, are activated, leading to dephosphorylation of signal-transducing proteins. SRIF-induced inhibition of ERK1/2 blocks degradation of the cyclin-dependent kinase inhibitor p27kip1, leading to growth arrest. In rare cases, SRIF can stimulate proliferation. Solid arrows: Effects observed in most systems and receptor subtypes; Broken arrows: Effects observed in specific system or specific subtypes. AC, adenylyl cyclase; ER, endoplasmic reticulum; ERK, extracellular signal-regulated kinase; Gα, Gβ, Gγ, G-protein subunit; PLC, phospholipase C; IP3, inositol trisphosphate; pHi, intracellular pH; PTPase, phosphotyrosine phosphatase.

1.5 PDZ Domains and Binding Motifs

All known SSTR receptor subtypes so far contain a classical PDZ domain binding motif at their extreme C-terminal end. Many GPCRs such as the β2-adrenergic receptor, mGluR5, GluR2, 5HT2C and SSTR2 have been shown to interact with PDZ containing proteins through their PDZ binding motifs (Hall *et al*., 1998; Tu *et al*., 1999; Dong *et al*., 1997; Xia *et al*., 1999; Ullmer *et al*., 1998; Zitzer *et al*., 1999), which in turn has an influence on the receptor functions and localization. So, what is a PDZ domain?

PDZ domains were originally recognized as ~90 amino acid-long repeated sequences in the synaptic protein PSD-95/SAP90 (PSD for postsynaptic density), the Drosophila septate junction protein Disc-large, and the epithelial tight junction protein ZO-1 (hence the acronym PDZ). They are among the most common protein domains in *Caenorhabditis elegans* (92

proteins), *Drosophila melanogaster* (131 proteins), *Homo sapiens* (more than 400 proteins), plants (33 proteins) and bacteria (307 proteins).

A canonical PDZ domain is composed of six antiparallel β-strands (βA-βF) with its open sides each capped with an α-helix (αA and αB) (Figure 1.4). An isolated domain can bind specifically to a short peptide at the extreme end of the C-terminus of target proteins (Kim *et al*., 1995) and/or an internal sequence with restrained conformation (Hillier *et al*., 1999; Im *et al*., 2002). Peptide binding occurs in a groove (carboxylate-binding loop) between the βB strand and the αB helix.

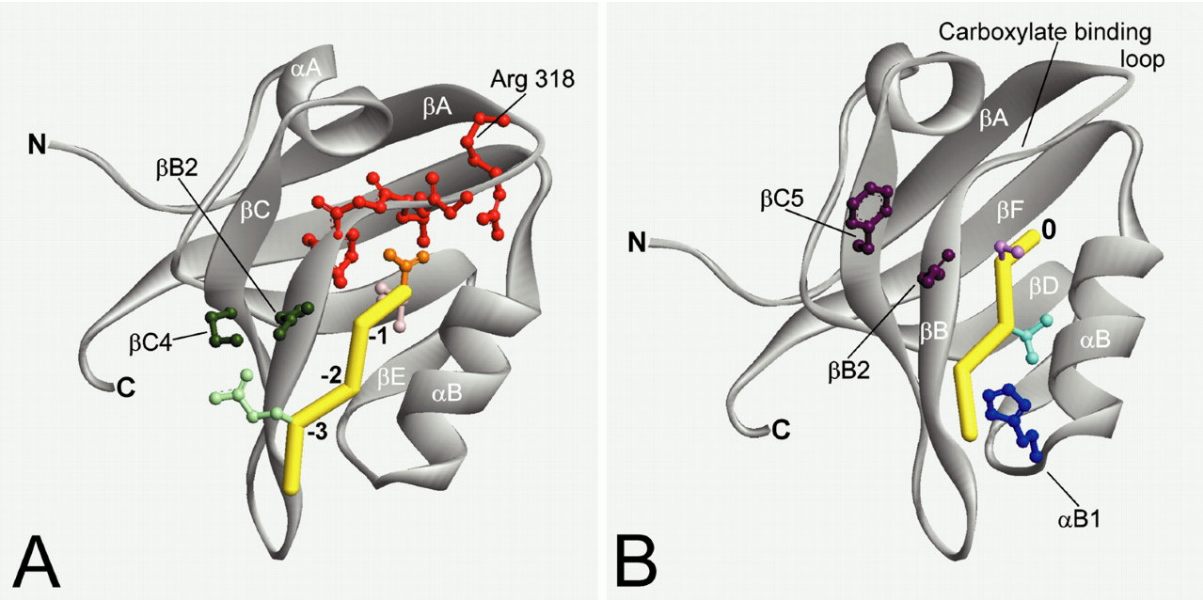

Figure 1.4 Structure of a PDZ domain complexed with a C-terminal peptide ligand, based on PDZ3 of PSD-95 complexed with CRIPT (from Sheng & Sala, 2001).
The ribbon diagram of the PDZ domain (gray) is shown bound to the peptide ligand (main chain represented in yellow). The structures in A and B are slightly rotated relative to each other to better show particular sets of interactions. A. The free carboxylate group (orange) of the C-terminal residue (P0) of the peptide interacts with the conserved amino acids (Arg-318 and Gly-Leu-Gly-Phe) of the carboxylate binding loop (red). The side chain of the P-3 residue (glutamine; light green) interacts with βB2 (asparagine) and βC4 (serine; dark green). B. The hydroxyl group of the P-2 residue (threonine; light blue) interacts with the sidechain of αB1 (histidine; dark blue). The side chain of the P-1 residue (serine; light purple) of the CRIPT peptide shows no interactions with the PDZ domain. However, βB2 and βC5 residues (dark purple) are likely to influence selectivity at the P-1 position of the peptide ligand.

PDZ domains recognize specific C-terminal sequence motifs that are usually about 4 residues in length, although in some cases specificity of recognition extends beyond these four residues (Songyang *et al*., 1997; Niethammer *et al*., 1998). The nomenclature for residues within the PDZ-binding motif is as follows: the C-terminal residue is referred to as the P0 residue; subsequent residues towards the N-terminus are termed P-1, P-2, P-3 and etc. Extensive peptide library screens pioneered by Songyang et al. (1997) have revealed the specificities of distinct PDZ domains (Songyang *et al*., 1997; Schultz *et al*., 1998). Together, these studies suggest that the P0 and P-2 residues are most critical for recognition and also show that PDZ domains can be divided into three main classes on the basis of their preferences for residues at these two sites: Class I PDZ domains recognize the motif –X-S/T-X-ϕ-COOH (where ϕ is a hydrophobic amino acid with preference for valine, leucine and isoleucine and X is any amino acid); class II PDZ domains recognize the motif -X-ϕ-X-ϕ-COOH; and class III PDZ domains recognize the motif –X-D/E-X-ϕ-COOH (Hung & Sheng, 2002). Special preference for a hydrophobic residue at P0 is due to the hydrophobic nature of the carboxylate-binding loop where the side chain of the P0 residue would lie. Residue selection at the position P-2 is largely based on the degree of the hydrophobicity of the residues at the αB1 position (Songyang *et al*., 1997; Tochio *et al*., 1999) (Figure 1.4). Results from structural studies showed that the amino acid at the P-3 position of the peptide ligand also makes specific contact with the PDZ domain. In general, the P-3 amino acid in the peptide ligand is less stringently specified by individual PDZ domains than is the residue P-2 (Songyang *et al*., 1997). The side chain of the P-1 residue for example of CRIPT showed no interaction with the PDZ domain (Doyle *et al*., 1996) (Figure 1.4), which suggests that the P-1 plays no role in PDZ specificity. However, Niethammer *et al*. (1998) showed that substitution of P-1 of CRIPT with another amino acid changes the binding specificity of the ligand. Furthermore, in the peptide library screening approach, most PDZ domains selected for specific amino acids at the position, albeit not as strong as at the P-2 (Songyang *et al*., 1997; Stricker *et al*., 1997). Thus there is no doubt that many PDZ domains can discriminate between amino acids at the P-1 position of the C-terminal peptide. Results from various studies have also shown that residues N-terminal to P-3 (even up to P-8) are also important for the PDZ binding in term of both binding affinity and specificity (Songyang *et al*., 1997; Niethammer *et al*., 1998; Kozlov *et al*., 2000). Other than that, the ability of the PDZ domain to bind to another PDZ domain, as observed for GRIP (Dong *et al*., 1999) and INAD (Xu *et al*., 1998) allows the formation of macromolecular complexes, which is one of the important functions of PDZ domain containing proteins.

PDZ containing proteins appear to function *in vivo* by acting as scaffolds for the assembly of large multiprotein complexes that function in signaling, as well as establishing and maintenance of cell polarity at specific subcellular locations such as the synapses of neuron and the cell-cell junctions of epithelial cells. In recent years, some PDZ proteins have been shown to plug together receptors, signaling molecules and proteins with different functional abilities to specific subcellular compartments such as photoreceptor cells (INAD) (Tsunoda *et al*., 1997), postsynaptic density of the synapses (PSD-95 and Shank) (reviewed in Sheng & Kim, 2000; Kennedy, 2000), apical domain of epithelial cells (Harris & Lim, 2001) and tight junction of epithelial cells (ZO-1, Pals1, Par6) (reviewed in Tsukita *et al*., 2001; Doe, 2001; Bilder, 2003).

1.6 Purpose of This Study

More than 10 years after the first somatostatin receptor was cloned, the individual *in vivo* functions of the SSTR subtypes are still poorly understood. The recent development of highly selective agonists and antagonists, subtype specific antibodies, improved genetic technologies and the generation of knock out mice provided a major step forward to overcome this problem. However, a different approach might be required to overcome these problems.

Results from different studies show that despite the overlapping expression, the receptor subtypes are highly specialized with respect to subcellular targeting as discussed earlier. Furthermore, the receptor subtypes have demonstrated differential coupling to signaling molecules even though sharing a similar set of effector molecules.

All these results suggest the involvement of additional intracellular factors, which might determine localization and function of subtypes. Moreover, all SSTR subtypes contain a PDZ binding motif at their extreme C-terminus, which might directly interact with PDZ domain containing protein (Zitzer *et al*., 1999).

So, the purpose of this study is to identify the interaction partner(s) of hSSTR3 using either the yeast-two-hybrid analysis or the affinity purification with synthetic peptides. Through this, it might be possible to elucidate the localization and functions of the receptor.

CHAPTER TWO MATERIALS AND METHODS

2.1 Materials

2.1.1 Chemicals

All chemicals unless stated otherwise were purchased from Merck, Sigma or Roth and are of analytical grade.

2.1.2 Microbial Strains and Cell Lines

	Name	Source
Bacterial strain	*Escherichia coli* TOP10 F'	Invitrogen
Yeast Strain	*Saccharomyces cerevisiae* Y187	Clontech
	S. cerevisiae AH109	Clontech
Cell Lines	Human Embryonic Kidney 293 (HEK293)	ATCC
	African green monkey kidney (COS-7)	ATCC
	Human breast epithelial (MCF-7)	ATCC
	Madin-Darby canine kidney II (MDCK II) Tet-Off	Clontech
	Madin-Darby canine kidney (MDCK)	Dr. Thomas Braulke, Dept. of Biochemistry, University of Hamburg
	Madin-Darby canine kidney II (MDCK II)	Prof. Kai Simons, MPI-Molecular Cell Biology and Genetics, Dresden

Table 2.1 Bacterial strains and mammalian cell lines used in this study.

2.1.3 cDNA Libraries and Genomic DNAs

	Source
Human brain cDNA library	Clontech
Rat brain cDNA library	Clontech
Human MTC™ (Multiple Tissue cDNA) panel I	Clontech
Mouse brain cDNA	Our laboratory
Human genomic DNA	Our laboratory
MDCK II genomic DNA	This study

Table 2.2 cDNA libraries and genomic DNAs used in this study as template for polymerase reaction for cloning of various genes and for MUPP1 splice variants expression study (MTC™ panel).

2.1.4 Plasmid DNAs

Plasmid	Source	Accession number (Acc.)
pAS2.1	Clontech	U30497
pACT2	Clontech	U29899
pGBK-T7	Clontech	
pGEX-4T-1	Amersham Biosciences	U13853
pGEX-6P-1	Amersham Biosciences	U78872
pEGFP-C3	Clontech	U66474
pcDNA3-T7-Ntag	Roth *et al*. (1997)	
pcDNA3.1A/*Myc*-His	Invitrogen	
pCR®II-TOPO®	Invitrogen	
pGEM®-T Easy	Promega	
pCMV-Tag-2C	Stratagene	
p3XFLAG-*myc*-CMV™-26	Sigma	
pTRE2-hyg	Clontech	

Table 2.3 Plasmid vectors used in this study for cloning of PCR products and for construction of expression constructs for yeast two hybrid, mammalian cells expression and fusion protein expression in bacteria. Sequences of the corresponding vectors are available at GenBank (www.ncbi.nlm.nih.gov) thru their accession number listed above as well as from the respective sources.

2.1.5 Antibodies

	Working concentration		
Primary antibody	**Western blot**	**Cytochemistry**	**Source**
mAnti-T7-tag	1:10000	1:10000	Novagen
mAnti-EGFP	1:5000	1:5000	BabCO
mAnti-*myc*	1:10000	-	Sigma
rbAnti-GST	1:5000	-	Our laboratory
rbAnti-PDZ10	1:500	1:50	This study
gAnti-MUPP1	1:2000	1:500	Upstate
rbAnti-hSSTR3	1:5000	1:500	S. Schulz; Magdeburg
rbAnti-ZO1	1:2000	1:500	Zymed
rbAnti-ZO2	1:250	-	Zymed
rbAnti-Claudin-1 (MH25)	1:500	-	Zymed
rbAnti-Claudin-2 (MH44)	1:500	-	Zymed
rbAnti-Claudin-3 (Z23.JM)	1:500	-	Zymed

gpAnti-Claudin-4	1:200	-	J. Brandner; Hamburg
rbAnti-p44/42 MAP Kinase	1:1000	-	Cell Signaling
mAnti-phospho-p44/42 MAPK (E10)	1:1000	-	Cell Signaling
mAnti-α-Tubulin (DM1A)	1:5000	-	Abcam

	Working concentration		
Secondary antibody	**Western blot**	**Cytochemistry**	**Source**
Cy™3-gAnti-rbIgG		1:400	Dianova
Cy™2-gAnti-mIgG		1:400	Dianova
Alexa488-gAnti-mIgG		1:400	Molecular Probes
HRP-Anti-rbIgG		1:2,500	Amersham Biosciences
HRP-Anti-mIgG		1:2,500	Amersham Biosciences
HRP-Anti-gIgG		1:10,000	Dianova

Table 2.4 Antibodies used in this study for Western blot and immunocytochemistry with the working concentration used. The species origin of the immunoglobulin is indicated by the abbreviation preceding IgG in the antibody name: g: goat, m: mouse, rb: rabbit, gp: guinea pig.

2.1.6 Oligonucleotide

All the oligonucleotides listed in the appendix were synthesized at the analytical laboratory in Institute for Cell Biochemistry and Clinical Neurobiology (University Hospital Eppendorf, Hamburg) with a DNA/RNA Synthesizers (Applied Biosystems). The oligonucleotides were suspended in sterile H_2O, concentration determined (2.2.1.10) and diluted to either 15 pmol/µl for sequencing or 20 pmol/µl for polymerase chain reaction.

2.2 Methods

2.2.1 Molecular Biology Techniques

2.2.1.1 Polymerase Chain Reaction (PCR)

All the PCR reactions were either performed with AmpliTaq (Perkin Elmer) or Pfu Turbo® (Stratagene) DNA polymerase in either Biometra T Gradient Thermocycler 96 (Whatman) or GeneAmp PCR System 2400 Thermocycler (Perkin Elmer) with the following reaction components and cycling conditions:

AmpliTaq DNA polymerase	Pfu Turbo® DNA polymerase
1x polymerase buffer	1x polymerase buffer
1.5 mM $MgCl_2$	
2.5 mM of each dNTP (dATP, dCTP, dGTP, dTTP)	2.5 mM of each dNTP (dATP, dCTP, dGTP, dTTP)
5 % DMSO	
20 pmol of each primer	20 pmol of each primer
50 ng of template plasmid DNA or 200 ng of cDNA library	50 ng of template plasmid DNA or 200 ng of cDNA library
2.5 U Polymerase	2.5 U Polymerase

	AmpliTaq	Pfu Turbo®
Initial denaturation	94°C; 3 min	95°C; 2 min
Denaturation } 35 cycles	94°C; 30 s	95°C; 30 s
Annealing } 35 cycles	4-6°C below melting temperature (Tm) of primers used	
Extension } 35 cycles	72°C; 1 min per kb of intended PCR product	
Final extension	72°C; 7 min	
	4°C; indefinite	

$Tm = 2 \times N_{(A+T)} + 4 \times N_{(G+C)}$ (N: Number of Bases)

To check for the PCR product, an aliquot of the reaction was analyzed with gel electrophoresis (2.2.1.3) and the DNA fragments were then purified (2.2.1.4) for subsequent experiments.

2.2.1.2 Splice Variants Expression Profiles Assays

In order to study the MUPP1 splice variants expression profiles in different human tissues, Human MTC™ Panel I (Clontech) was purchased and the primers were synthesized (2.1.6). TITANIUM™ Taq DNA polymerase (Clontech) was used as recommended by the manufacturer.

2.2.1.3 Restriction Endonuclease Digestions of DNA samples

(Sambrook *et al*., 1989)

Restriction endonuclease digestions of DNA samples were carried out in the optimal buffers and incubation conditions as recommended by the manufacturers (Invitrogen, MBI Fermentas, New England Biolabs and Roche). At the end of incubation, the samples were then analyzed on agarose gel (2.2.1.3) and purified (2.2.1.4) for subsequent experiments.

2.2.1.4 Agarose Gel Electrophoresis

(Sambrook *et al*., 1989)

Aliquots of restriction endonuclease digestions or PCR reactions were analyzed in submerged horizontal non-denaturing agarose gel electrophoresis. Agarose (Invitrogen) was dissolved in 1x TAE (100 mM Tris/Acetate, 5 mM EDTA; pH8.0) at a concentration of 1 to 2 % (w/v). 0.2 g/ml of ethidium bromide was added. DNA samples prepared with 1x gel loading buffer (6 % (w/v) glycine, 8 mM Tris/HCl, 0.05 % bromophenol blue; pH8.0) added to them were loaded into the wells of the gel and EcoRI+HindIII-digested lambda markers or Gene Ruler^{TM} 100bp DNA Ladder (MBI Fermentas) was used as the standard DNA molecular weight markers. The gel was electrophorezed in 1x TAE buffer at a constant voltage of 80-100 volts. The gel was then viewed and photographed under ultraviolet light from a UV transilluminator (UVT 2035, Herolab).

2.2.1.5 Purification of DNA Fragments from Agarose Gel

Purification of DNA fragments from agarose gel was carried out using QIAEX II Agarose Gel Extraction Kits (Qiagen) according to manufacturer's recommendation. An aliquot of the eluate was then analyzed on a gel for concentration determination.

2.2.1.6 DNA Ligation

An approximate molar ratio of 3:1 of digested insert to linearized vector was used for each ligation. 1 U of T4 DNA ligase (Roche) and a final concentration of the provided 1x ligase buffer were added for each 10 µl ligation reaction mixture. Ligation was carried out either overnight at 16°C waterbath or at RT for 2 h.

2.2.1.7 pGEM®-T Easy Vector Systems and TOPO TA Cloning® Kits

pGEM®-T Easy Vector systems (Promega) and TOPO TA Cloning® kits (Invitrogen) were used for the cloning of the PCR products with an A tail at the 3'of the DNA fragments. The reactions were done according to manufacturer's recommendation.

2.2.1.8 Preparation of Competent *E. coli* cells

(Sambrook *et al*., 1989)

E. coli (TOP 10F') competent cells were prepared according to the rubidium chloride methodology described below. A single colony of TOP10F' cells was precultured in 5 ml of LB medium (10 g/l bacto-peptone, 10 g/l NaCl, 5 g/l yeast extract; pH7.5) with 15 g/ml of tetracycline overnight at 37°C. On the following day, the overnight culture was inoculated into a 200 ml LB medium without tetracycline and grown at 37°C until the optical density (OD_{600}) reached 0.4. Harvesting was done at 5,000 rpm for 5 min at 4°C, after which the cell pellet was resuspended in 60 ml of TFB I (30 mM KOAc, 50 mM $MnCl_2$, 100 mM RbCl, 10 mM $CaCl_2$, 15 % (v/v) glycine; pH5.8). This was followed by centrifugation at 5,000 rpm for 5 min at 4°C and then resuspension in 8 ml TFB II (10 mM MOPS, 75 mM $CaCl_2$, 10 mM RbCl, 15 % (v/v) glycine; pH7.0). 200 µl aliquots of the competent cells were then stored at -70°C after being snapped frozen in liquid nitrogen. To check for the transformation efficiency, 0.1 ng of supercoiled plasmid DNA (pUC19) was used with 100 µl of the competent cells for transformation (2.2.1.8). A transformation efficiency of at least $1x10^6$ cfu per µg of DNA was desired for transformation of ligation reaction.

2.2.1.9 *E. coli* Transformation

(Hanahan, 1983)

100 µl of TOP 10F' competent cells were thawed on ice before 2 µl of the ligation reaction was added and mixed well. After 20 min incubation on ice, the cells were then heat-shocked at 42°C for 1 min and immediately chilled on ice for 3 min. 400 µl of LB medium was then added and the cells were recovered with slight shaking in a 37°C shaker incubator for at least 45 min. After recovery, the cells were then spread onto a LB selection agar plate (10 g/l bacto-peptone, 10 g/l NaCl, 5 g/l yeast extract, 15 g/l bacto-agar) supplemented with either 100 µg/ml ampicillin or 30 µg/ml kanamycin and the plates were then incubated at 37°C overnight.

2.2.1.10 Plasmid DNAs Isolation

2.2.1.10.1 Mini-preparation with TELT-Lysis (Rapid Boiling Method)

(Holmes and Quigley, 1981)

Cells of 1.5 ml of overnight bacterial culture at 37°C were harvested at 13,000 rpm for 1 min at RT. The cell pellet was resuspended in 250 µl of TELT-lysis buffer (50 mM Tris/HCl, 62.5 mM EDTA, 2.5 mM LiCl, 0.4 % (v/v) Triton X-100; pH 7.5) and 25 µl of lysozyme stock solution (10 mg/ml) was added. After 3 s of vortexing at maximum speed, the cell suspension was incubated on ice for 5 min before being heat-denatured at 95°C for 5 min and immediately put on ice for another 5 min. Denatured proteins were separated from the solution by centrifugation at 13,000 rpm for 15 min at RT and the pellet was then removed with a toothpick. 250 µl of isopropanol was added and the mixture was centrifuge at 13,000 rpm for 20 min at RT. The DNA pellet was then washed once with 70 % ethanol at 14,000 rpm for 5 min at 4°C before allowed to dry at RT. The DNA pellet was dissolved in 20 µl of sterile water, the sample was then ready for subsequent analysis for example restriction enzyme digestion.

2.2.1.10.2 Midi-preparation

To obtain an increased yield of supercoiled plasmid DNAs for certain downstream experiments for example transfection of mammalian cell and yeast transformation, Nucleobond® AX Kit (Macherey and Nagel) was used. Plasmid DNA purification was carried out according to manufacturer's recommendation.

2.2.1.11 Nucleic Acids Concentration Determination

The concentration of nucleic acids was determined by measuring the absorbance of the sample at wavelength of 260 nm on spectrophotometer Genequant (Amersham Biosciences)

2.2.1.12 DNA Sequencing

All the DNA sequencing reactions were done in the analytical laboratory of Institute for Cell Biochemistry and Clinical Neurobiology (University Hospital Eppendorf, Hamburg) according to the Dideoxy methodology (Sanger *et al*., 1977).

2.2.2 Yeast Two Hybrid System

2.2.2.1 Yeast Transformation

A single colony of *S. cerevisiae* AH109 strain was precultured in 50 ml of YPD (20 g/l difco-peptone, 10 g/l yeast extract, 2 % glucose; pH 5.8) at 30°C at 250 rpm overnight. The next day, up to 50 ml of YPD was inoculated with the overnight culture to an OD_{600} of 0.3. The culture was grown at 30 °C at 250 rpm until an OD_{600} of 0.4-0.5 was reached (about 4 h). The cells were harvested at 3,000 rpm for 5 min, then washed once with 25 ml of sterile H_2O. The pellet was the resuspended in 1 ml of 100 mM LiAc and transferred into 1.5 ml microfuge tube. The cells were again harvested at 8,000 rpm for 15 s before being resuspended in 400 µl of 100 mM LiAc. 50 µl of the cell suspension was then harvested for each reaction. The following were layered upon the pellet: 240 µl of 50 % polyethylenglycol 3350, 36 µl of 1 M LiAc, and 50 µl of freshly heat-denatured salmon sperm DNA at 2 mg/ml and 1 µg of plasmid DNA diluted into 34 µl with sterile H_2O. Mixtures were resuspended by vortexing and then incubated at 30°C for 30 min before being heat-shocked at 42°C waterbath for another 30 min. The cells were harvested by centrifugation at 7,000 rpm for 15 s. The pellet was then resuspended in 500 µl of sterile H_2O and 100 µl of the transformed cells were spread on each of the Synthetic Defined (SD) (6.7 g/l yeast nitrogen base, 20 g/l bacto-agar, 2 % glucose, appropriate dropout (DO) supplement mixture (Qbiogene); pH 5.8) selection plates (Yeast Protocols Handbook, Clontech) before being incubated at 30°C.

2.2.2.2 Yeast Two Hybrid Screening

One colony of yeast strain AH109 carrying the bait plasmid pGBKT7-hSSTR3-C was resuspended in 500 µl of SD medium (6.7 g/l yeast nitrogen base, 2 % glucose, complete supplement mixture (Qbiogene); pH 5.8) and inoculated into 50 ml of SD/-Trp medium before allowed to grow with shaking at 250 rpm at 30°C for 24 h. The cells were harvested at 1,000 g for 5 min. The pellet was then resuspended and inoculated into 45 ml of 2x YPDA medium (2x YPD, 0.003 % adenine hemisulfate) with 15 µg/ml of kanamycin in a 2 liter Erlenmeyer flask. One vial of the Matchmaker™ Human Brain Pretransformed Library (Clontech) was thawed at RT and then inoculated the whole volume of the library, excluding 10 µl for library titration, was inoculated into the 2x YPDA/Kan medium containing the bait harboring AH109 cells. The mating mixtures were incubated at 30°C at 40 rpm for 24 h. At the end of incubation, the cells were harvested by centrifugation at 1,000 g for 10 min and resuspended in 10 ml of 0.5x YPDA/Kan medium before spreading 200 µl of the cells

suspension onto 25 plates of SD/-Trp/-Leu/-His/-Ade and 25 plates of SD/-Trp/-Leu/-His (5 mM 3-AT (3-amino-1,2,4-triazole)). The plates were then incubated at 30°C for 7-21 days until the colonies appeared.

2.2.2.3 β-Galactosidase Colony-lift Filter Assay

Yeast clones were streaked in small patches onto SD/-Trp/-Leu/-His/-Ade agar plates and incubated at 30°C for 3-4 days. For each plate of transformants to be assayed, a piece of nitrocellulose filter (PROTRAN, Schleicher & Schuell) was placed onto the surface of colonies and followed by gentle rubbing with forceps. The evenly wetted filter with colonies facing up was then transferred to a pool of liquid nitrogen for about 10 s for fixing and permeabilizing the cells. After which the filter was allowed to thaw at RT before placing on a presoaked Whatman #5 paper in Z buffer (60 mM Na_2HPO_4, 40 mM NaH_2PO_4, 10 mM KCl, 1 mM $MgSO_4$, 0.27 % (v/v) mercaptoethanol, 33.4 mg/100 ml X-Gal). The filter was incubated at 30°C for 30-60 min and checked periodically for the appearance of blue colonies.

2.2.2.4 Plasmid Isolation from Yeast

Each colony was inoculated into 4 ml of SD/-Leu medium with cycloheximide (1 µg/ml) and grown for 2 days at 30°C at 250 rpm. The cells were harvested by centrifugation at 5,000 g for 5 min and resuspended in 100 µl of STET buffer (8 % sucrose, 50 mM Tris/HCl, 50 mM EDTA, 5 % Triton X-100; pH 8.0) together with 0.2 g of glass bead (425-600 microns, Sigma) by vortex vigorously for 5 min. After the addition of another 100 µl of STET buffer to the mixture, the cells were then heat denatured for 5 min at 95°C and immediately placed on ice for another 5 min. Denatured proteins were separated by centrifugation at 13,000 rpm for 30 min at RT and 180 µl of the supernatant was withdrawn and added to 90 µl of 7.5 M NH_4Ac before incubation at -20°C for 1 h. The samples were centrifuged again at 14,000 rpm at 4°C for 30 min, 180 µl of the supernatant was transferred and to a fresh 1.5 ml tube, 360 µl of absolute ethanol was added, followed with 30 min incubation at -80°C. The precipitate was recovered by centrifugation at 14,000 rpm at 4°C for 30 min and washed once with 300 µl of 70 % ethanol. The dried pellet was redissolved in 100 µl of H_2O and further purified with the QIAEX II Agarose Gel Extraction Kit (Qiagen). The purified plasmids were retransformed into *E. coli* TOP10F' cells (2.2.1.8) and the plasmids were reisolated using the miniprep

protocol (2.2.1.9.1). The plasmids were then analyzed with restriction enzyme digestion (2.2.1.2) and sequencing (2.2.1.11).

2.2.3 Cell Biology Techniques

2.2.3.1 Cell Culture

Human embryonic kidney 293 cells (HEK293), African green monkey kidney cells (COS-7) and Madin-Darby canine kidney strain II cells (MDCK II) were cultured in Dulbecco's modified Eagle's medium (DMEM, Cambrex) supplemented with 10 % heat-inactivated fetal bovine serum (FBS, Sigma), 100 U/ml penicillin and 100 g/ml streptomycin at 37°C in a humidified atmosphere of 5 % CO_2. Human breast epithelial cells (MCF-7) were cultured in DMEM supplemented with 10 % heat-inactivated FBS, 100 U/ml penicillin, 100 g/ml streptomycin, 10 mM HEPES (pH 7.4) and 10 µg/ml insulin at 37°C under a humidified atmosphere of 5 % CO_2. For normal maintenance of the cell lines, the cells were passaged every 3-5 days (HEK293, COS7 and MDCK II) or 7-10 days (MCF-7) by rinsing the cells monolayer once with Versene buffer (137 mM NaCl, 8.8 mM Na_2HPO_4, 2.7 mM KCl, 0.7 mM KH_2PO_4, 1mM EDTA; pH 7.4) and incubated with 0.25 % (w/v) trypsin (Invitrogen) in versene buffer at 37°C except for HEK293 cells until the cell layer was dispersed. Trypsinized cells were then replated in new culture dish with fresh culture medium in the dilution of 1:10.

For culturing cell in Costar® Transwell® insert (Corning) (Figure 2.1), medium was first added into both the lower (1.5 ml) and upper (0.5 ml) compartment of the permeable support (microporous membrane) for 8-16 h at 37°C to equilibrate the membrane to improve cell attachment prior to seeding. 1x 10^5 trypsinized MDCK II or MCF-7 cells were normally seeded onto a 12 mm Transwell® insert for optimum growth and polarization.

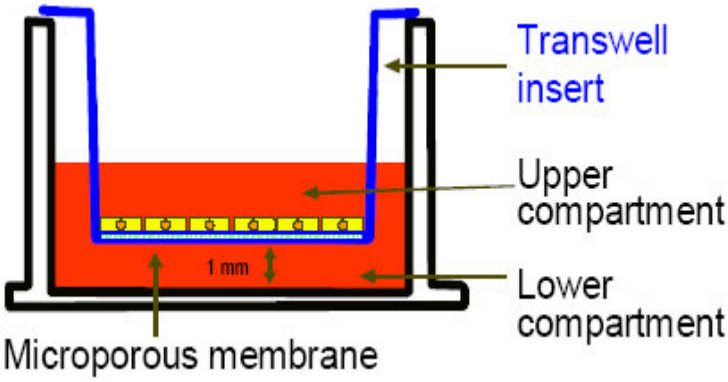

Figure 2.1 Cell monolayer grows on the porous support of the insert allowing independent access to medium.

2.2.3.2 Transient Transfection

HEK293 cells transient transfection was done according to the calcium phosphate precipitation method (Sambrook *et al*., 1989). 500 µl of the mixture (10 µg of plasmid DNA in 250 mM $CaCl_2$) was bubbled into 500 µl of 2x HBS buffer (280 mM NaCl, 10 mM KCl, 1.5 mM Na_2PO_4, 12 mM dextrose, 50 mM HEPES; pH 7.05) after which the precipitate was allowed to stand at RT for another 15 min before added onto cells with 50-80 % confluency. Transfection medium was changed with fresh culture medium 6-18 h after transfection to allow the cell to recover. As for COS-7 cells, transient transfections were done with Polyfect® transfection reagent (Qiagen) according to manufacturer's recommendation.

2.2.3.3 Stable Transfection

Transfections of MDCK II and MCF-7 were done with FuGENE 6 (Roche) and Effectene® (Qiagen) transfection reagents, respectively, according to manufacturer's recommendations for a 60 mm culture dish. 16-18 h after transfection, the transfected cells were passaged in 1:5 onto 100 mm culture dish with selection medium containing the appropriate concentration (400 µg/ml for MCF-7 and 600 µg/ml for MDCK II) of antibiotic geneticin (G418-sulfate) (Invitrogen). Selection medium was changed every 4-5 days until colonies appeared. An individual clone was picked by placing a suitable size of sterile Whatman paper soaked with 0.25 % trypsin in versene buffer onto the colony. After 3-5 min of incubation at 37°C, the Whatman paper containing cells were picked up and placed into a 6 wells plate containing selection medium. The plate was incubated at 37°C until the clone was grown.

2.2.4 Immunofluorescence Techniques

2.2.4.1 Immunocytochemistry

Transiently transfected cells or stable cell lines were plated either on 18 mm glass coverslips coated with 0.1 mg/ml poly-D-lysine (Sigma) in a 12 well plate or 12 mm Transwell® insert and incubated at 37°C. Growing cells were washed once in PBS (137 mM NaCl, 8.8 mM Na_2HPO_4, 2.7 mM KCl, 0.7 mM KH_2PO_4; pH 7.4) and fixed in 4 % paraformaldehyde in PBS for 10 min before washing off with PBS. The fixed cells were permeabilized with 0.1 % Triton X-100 in PBS for 15 min at RT. After blocking with 5 % horse serum (Sigma) in PBS for 1 h at RT, cells were incubated with the appropriate primary antibody diluted to the appropriate working concentration in blocking solution, overnight at 4°C. On the following day, the cells were washed three times with PBS with an interval of 5 min to allow diffusion

of the antibody, after which, the cells were again incubated with appropriate fluorophore-conjugated secondary antibody diluted 1:400 in 2 % horse serum in PBS for 1 h at RT. After the cells were washed three times with PBS, the coverslips with the cells facing down were mounted on a drop of glycerol gelatin (Sigma) on glass slide. The filter membranes of the Transwell® were cut from the holder and placed on a glass slide with the cells facing up where a drop of FlourSave™ reagent (Calbiochem) and glass coverslip were placed on the membrane.

2.2.4.2 Immunohistochemistry

To study the distribution of MUPP1 protein in the brain, a mouse was deeply anesthetized and the brain was removed and fixed in 4% paraformaldehyde for 24 h at 4°C. After several washes in PBS buffer, the mouse brain was then embedded in O.C.T. compound™ (Tissue-Tek®, Sakura) on a metal block cooled on dry ice. Horizontal 15 µm sections of the brain were cut at -20°C using a cryostat (JUNG CM 3000, Leica) and mounted onto Superfrost Plus glass slides (Roth). Sections were washed several times with PBS and permeabilized with 0.1% Triton X-100in PBS for 15 min at RT. After blocking with 5 % horse serum in PBS for 2 h at RT, sections were incubated with anti-PDZ10 antibody diluted to 1:50 in blocking solution for 72 h at 4°C. At the end of incubation, the sections were washed three times with PBS, and then the sections were incubated with Cy3-conjugated goat anti-rbIgG secondary antibody in PBS for 2 h at RT. Finally, the sections were then washed three times with PBS before mounted with FlourSave™ reagent and glass coverslip.

2.2.4.3 Microscopy

Visualization and documentation of the fluorescence signals were done with either a Aristoplan Fluorescence microscope (Leitz) in combination with a CCD C4742-95-12NRB digital camera (Hamamatsu) and the OpenLab 2.2.5 software (Improvision) or a confocal laser scanning microscope Leica TCS SP2 (Leica) and the Leica confocal TCS NT version. Protein signal from a Cy3 conjugated secondary antibody were visualized with a N2.1 filter (Leica; Excitation: 515-560 nm, Emission: 580 nm) or a Helium-Neon laser (Excitation: 543 nm, Emission: 570 nm). Signals from Cy2 or Alexa Fluor 488 conjugated secondary antibody or EGFP autofluorescences were visualized with a L5 filter (Leica; Excitation: 480 nm, Emission: 505 nm) or an Argon laser (Excitation: 488 nm, Emission: 510-525 nm). Images were processed using Adobe Photoshop 6.0 (Adobe Photoshop Incorporated).

2.2.5 Biochemical Techniques

2.2.5.1 SDS-Polyacrylamide-Gel-Electrophoresis (SDS-PAGE)

(Laemmli, 1970)

SDS-PAGE gels containing 8-15 % Polyacrylamide in the separation gel and a stacking gel, cast according to the methodology established by Laemmli, were used for protein separation according to their molecular weight. The gel electrophoresis was carried out with the Mini-PROTEAN II System (BioRad). The protein samples were first heat denatured at 95°C for 5 min in 1x Laemmli buffer (10 % (v/v) glycerin, 20 mM DTT, 1.5 % (w/v) SDS, 60 mM Tris/HCl, 0.05 % Coomassie G-250; pH 6.8) and then electrophorezed in SDS running buffer (25 mM Tris, 192 mM glycine, 0.1 % (w/v) SDS) at a constant voltage of 100-180 V. Molecular weight of the proteins were estimated with the protein molecular weight marker (Full Range Rainbow Marker, Amersham Biosciences; Broad Range Prestained, New England Biolabs), which was run alongside with the samples.

2.2.5.2 Coomassie Staining of SDS-PAGE Gel

After gel electrophoresis, the SDS-PAGE gel was stained in Coomassie solution (40 % (v/v) methanol, 10 % (v/v) glacial acetic acid, 0.1 % (w/v) Coomassie G-250) for 20-30 min at RT with shaking. After which, the stained gel was destained with destaining solution (25 % (v/v) methanol, 10 % (v/v) glacial acetic acid) until the bands appeared. Documentation was done using CS1 gel documentation system from Cybertech or scanned with ScanMaker® X12 USL™ (Microtek) and the ScanWizard 5 V5.61 software.

2.2.5.3 Protein Concentration Determination

(Bradford, 1976)

Up to a total volume of 10 µl of neat or diluted protein samples and a serial dilution of bovine serum albumin (BSA) (0.1-5 mg/ml) concentration standard were prepared in a 96 wells microtitre plate. The plate was incubated at 37°C for 20-30 min after the addition of 200 µl of Bradford reagent (Sigma) or BCA (Pierce) for each sample. The protein concentration was then determined via the extinction measurement at 620 nm with an ELISA reader (Titertek Multiskan Plus, Flow Laboratories). For protein samples in which Bradford reagent could not be used for concentration determination, the samples together with BSA concentration standard were first electrophorezed in a SDS-PAGE gel (2.2.4.1) and then Coomassie-stained (2.2.4.2) for visual concentration determination.

2.2.5.4 Western Blot Analyses

After gel electrophoresis, proteins in the gel were electro-transferred and immobilized onto nitrocellulose membrane (PROTRAN, Schleicher & Schuell) in blotting buffer (20 % (v/v) methanol, 192 mM glycine, 25 mM Tris, 0.02 % (w/v) SDS) with Mini-Trans-Blot Apparatus (BioRad) for 1 h at 4°C with a constant voltage of 100 V. The membrane was rinsed once with TBS-T buffer (150 mM NaCl, 50 mM Tris/HCl, 0.2 % Tween-20; pH 7.9) after the transfer before incubated for 1 h at RT with blocking buffer (5 % (w/v) skim milk powder in TBS-T). After which, the blot was incubated with appropriate primary antibody diluted to the working concentration in blocking buffer for either 2 h at RT or overnight at 4°C, with shaking. After incubation, the blot was washed three times with TBS-T with an interval of 10 min, after which, the blot was again incubated with appropriate HRP-conjugated secondary antibody diluted to the working concentration in TBS-T for 1 h at RT with shaking. After this the blot was again washed three times with TBS-T and the luminescence signal generation was done with ECL™ reagent (Enhanced Chemiluminescence, Amersham Biosciences) according to manufacturer's recommendation. The chemiluminescence sign als were detected with a piece of Cronex 5 Medical X-Ray Film (Agfa).

2.2.5.5 Expression and Purification of Fusion Protein

For the generation of glutathione S-transferase (GST) fusion proteins, sequences of interest were cloned in-frame into pGEX-6P-1 or pGEX-4T-1 vector (Amersham Biosciences). One colony of transformed *E. coli* TOP10F' cells with respective plasmid DNA was inoculated into 5 ml of LB/Amp medium (100 µg/ml Ampicillin) overnight at 37°C at 250 rpm. On the following day, the preculture was used to inoculate a 200 ml LB/Amp medium and incubated at 37°C and 250 rpm until the OD_{600} reached 0.6. Expression of the fusion protein was induced with 1 mM IPTG (Isopropyl-β-D-thio-galactopyranoside) for 2 h at 37°C at 250 rpm. The cells were harvested by centrifugation at 8,000 rpm for 10 min at 4°C with Sorvall A6.14 and washed once with STE buffer (150 mM NaCl, 10 mM Tris/HCl, 1 mM EDTA; pH 8.0). The cells were resuspended in lyses buffer (10 ml STE buffer, 100 µl lysozyme (10 mg/ml), Protease inhibitors (10 µg/ml leupeptin, 1 µg/ml pepstatin A, 100 µg/ml bacitracin, 100 µM phenylmethylsulfonyl fluoride (PMSF)) and sonicated 5 times for 5 s on ice at level 4 of the SONIFIER® B-12 (Branson Sonic Power Company). After the sonication, 2 ml of 10 % (v/v) Triton X-100 was added into the cell lysis suspension, and it was incubated on ice for another 20 min. Cell debris was pelleted by centrifugation at 15,000 rpm at 4°C for 25 min with

Sorvall A8.24 and the supernatant was incubated with 1 ml of Gluthatione Sepharose™ 4 Fast Flow (Amersham Biosciences) at 4°C on a rotator for 1 h. The sepharose was then washed three times with ice-cold STE buffer before 1 ml of elution buffer (10 mM Glutathione, 50 mM Tris/HCl; pH 8.0) was added to the sepharose and incubated at 4°C for 15 min. The quality and quantity of the purified fusion protein was then monitored on SDS-PAGE (2.2.5.1) and stained with Coomassie staining solution (2.2.5.2).

2.2.5.6 Antibody Affinity Purification

Fusion protein (GST-PDZ10) used for the generation of the antisera was first expressed and purified (2.2.4.5). 500-1000 µg of the purified fusion protein was then electrophorezed along the entire length of a SDS-PAGE and transferred onto a nitrocellulose membrane (2.2.4.4). The blot was first stained with 0.2 % Ponceau S (3-hydroxy-4-[2-sulfo-4-(sulfo-phenylazo)phenylazo]-2,7-naphthalene disulfonic acid) in 3 % trichloroacetic acid, 3 % sulfosalicylic acid and later destained with water. The band corresponding to the fusion protein was then excised and blocked with blocking solution (3 % BSA in PBS) for 1 h at RT with shaking. 0.5-1 ml of the heat inactivated antisera was diluted 10 fold in blocking buffer and incubated with the membrane strip for 2 h at RT or 4°C overnight with shaking. There after, the membrane strip was washed twice with 150 mM NaCl for 10 min at RT followed by washing with PBS three times for 5 min. The purified antibody was then eluted with 5 ml of 0.2 M glycine; pH 2.8, 1 mM EGTA for 10 min at RT. The eluted antibody was immediately neutralized with 1 ml of 2 M Tris/HCl; pH 8.0. The quality and quantification of the purified antibody was done with Western blot (2.2.5.4) with either fusion protein or cell lysate or immunocytochemistry (2.2.4.1).

2.2.5.7 Covalent Coupling of Antibody to Protein A/G Agarose

(Harlow & Lane, 1988)

Purified antibody was first incubated with protein A/G Plus agarose at a concentration of 2 mg/ml of agarose at RT for 1 hr with rocking. Agarose was then washed with 10 volumes of 0.2 M sodium borate, pH 9.0, the agarose was collected by centrifugation at 10,000 g for 30 s before resuspension in 10 volumes of the washing buffer. After an equivalent of 10µl of agarose was removed for analyses, powder dimethylpimelimidate was added to a final concentration of 20 mM. The mixture was again incubated at RT for 30 min before another 10µl of agarose was removed for analyses. The coupling reaction was stopped by washing once with 0.2 M ethanolamine, pH 8.0 and then incubated in the same buffer for 2 h at RT.

At the end of incubation, agarose was then washed thrice in PBS and finally resuspended in an equal volume of PBS with 0.05% sodium azide. Antibody coupled Protein A/G agarose was ready for use. Agarose removed before and after coupling were then boiled in sample buffer before analyzed by Western blot for the efficiency of coupling.

2.2.5.8 Precipitation Assays

2.2.5.8.1 Co-immunoprecipitation from Mammalian Cells

Cells 36-48 h after transfection or untransfected wild type cells were lysed in 1 ml of RIPA buffer (50 mM Tris/HCl; pH 8.0, 150 mM NaCl, 1 % (v/v) NP-40, 0.5 % (w/v) Na-deoxycholate, 5 mM EDTA, 0.1 % SDS, 100 µM PMSF, 1 µg/ml pepstatin, 10 µg/ml leupeptin, 100µg/ml bacitracin) per 100 mm culture dish on ice for 15 min. Lysates were centrifuged for 15 min at 14,000 rpm at 4°C to remove the insoluble matter. Either a primary antibody or 35 µl of a T7 antibody-coupled agarose (Novagen) was added to the cell lysates and incubated at 4°C for 2 h on a rotator. If a primary antibody was used initially, 20 µl of Protein A/G PLUS Agarose (Santa Cruz) was added and further incubated at 4°C for 1.5 h to precipitate the immune complex. Agarose with the bound immune complex was then washed 5 times with 1 ml of RIPA buffer at 500 g for 1 min at 4°C and the proteins were denatured in Laemmli buffer at 95°C for 5 min before electrophorezed on a SDS-PAGE (2.2.5.1) and analyzed with Western blot (2.2.5.4).

2.2.5.8.2 Affinity Precipitation with Synthetic Peptide

For affinity precipitation, synthetic peptides of human SSTR3 C-terminal (KSSTMRISYL, Acc. CAG30471), rat SSTR3 C-terminal (KASTLSHL, Acc. CAA45130), rat GKAP/SAPAP (IYIPEAQTRL, Acc. U67987) were obtained from Genemed Synthesis Inc.). 3 mg of the peptide was covalently coupled to 1 ml of NHS-activated Sepharose™ 4 Fast Flow (Amersham Biosciences) in 1 ml of coupling buffer (0.1 M $NaHCO_3$, 0.5 M NaCl; pH 7.5) according to manufacturer's recommendation.

For precipitation from mammalian cells, transfected or untransfected wild type cells were lysed and cleared as described in 2.2.4.7.1. 35 µl of the peptide-coupled sepharose was added to cell lysate and incubated at 4°C on rotator for 2 h before washed five times with 1 ml of RIPA buffer. After denaturation with Laemmli buffer, the precipitates were analyzed with either Western blot (2.2.5.4) or Coomassie (2.2.5.2) stained SDS-PAGE (2.2.5.1) gel.

For precipitation from mouse or rat brain, whole brain lysate was prepared by first homogenized the whole brain in DOC lysis buffer (50 mM Tris/HCl; pH 9.0, 1 % (w/v) Na-deoxycholate, 50 mM Na-flouride, 20 µM ZnCl, 1 mM Na-orthovanadate, 100 µM PMSF, 1 µg/ml pepstatin, 10 µg/ml leupeptin, 100 µg/ml bacitracin) in a homogenizer and then solubilized at 4°C on rotator for 2 h. Insoluble matter was pelleted by centrifugation at 15,000 rpm for 45 min at 4°C and supernatant was transferred to 60 µl of peptide-coupled sepharose for precipitation. After incubation at 4°C for 2 h on a rotator, the sepharose was then washed five times with DOC buffer and the proteins were denatured in Laemmli buffer at 95°C for 5 min. The samples were then analyzed with either Western blot (2.2.5.4) or Coomassie (2.2.5.2) stained SDS-PAGE (2.2.5.1) gel.

2.2.5.9 Mass Spectroscopy

All the mass spectroscopy analyses were done in the analytical laboratory of Institute for Cell Biochemistry and Clinical Neurobiology (University Hospital Eppendorf, Hamburg). Protein bands of interest were excised from Coomassie stained SDS-PAGE gel and in gel trypsin-digested according to Shevchenko *et al*. (1996). After that, the peptides were extracted and purified with ZipTipµ-C18 (Millipore) and concentrated is necessary before analyzed in a ESI-QTOF2 Mass Spectrometer (MicroMass). The resultant data were then analyzed with the program Mascot MS/MS Ion Search from www.MatrixScience.com.

2.2.5.10 Overlay Assays

Proteins were precipitated with peptide-coupled sepharose (2.2.5.7.2) from wild type HEK293, MDCK II or MCF-7 cells and subjected to SDS-PAGE before transferred onto nitrocellulose membrane. The blot was then blocked with 10 % (w/v) skim milk powder in TBS-T overnight at 4°C with shaking to allow renaturation of the proteins. On the following day, the blot was incubated with 5-10 µg of GST fusion protein in the blocking buffer for 2 h at RT, washed three times with TBS-T, and then incubated with rabbit anti-GST antibody for 1 h at RT. After another three washes with TBS-T and further incubation with HRP-conjugated anti-rabbit IgG antibody for 1 h. The blot was washed and the signals were generated with ECL™ reagent (2.2.5.4).

2.2.5.11 Transepithelial Electrical Resistance (TER) Measurement

Transepithelial electrical resistance of the epithelial cells were measured using a Millicell®-ERS (Electrical Resistance System) (Millipore). MDCK II or MCF-7 cells were first seeded into Transwell® Clear inserts at 1x 10^5 cells per 12 mm insert as described in 2.2.3.1. On the following day, the electrode was equilibrated in the culturing medium for 2 h before used. After that the electrode was connected to the measuring meter and tested for the voltage and resistance reading according to manufacturer's manual. The electrode was then sterilized by immersing in 70 % ethanol for 15 min in a laminar flow hood. At the same time, the samples were removed from the incubator in order to equilibrate to RT before the measurement was taken. The sterilized electrode was again placed in a sterile cell culture medium for 15 min and the voltage potentiometer were adjusted to zero before the system was switched to resistance mode. The electrode was then placed as shown in Figure 2.2 in between the insert and the outer well where the insert was resting on and the resistance reading was shown on the meter once the measure button on the meter was pushed. After the measurement, culture medium was changed before the samples were returned to the incubator.

The resistance of the cell monolayer was calculated by subtracting the average resistance measurement of two blank wells (insert without cells) from the average sample wells resistance measurement. Finally the arrived absolute resistance measurement was multiplied with the area of effective membrane diameter on the insert to give the TER reading independent of the membrane size used.

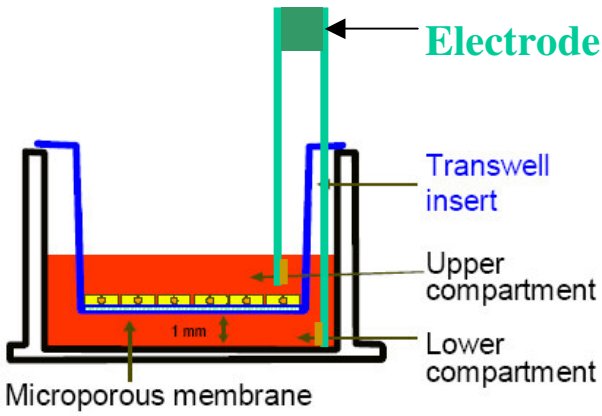

Figure 2.2 The fork-like electrode was placed in the culture plate as shown above. The unequal length of the electrode arms was designed to avoid damage to the cell monolayer while the measurement was taken.

2.2.5.12 Calcium Switch Assays

(González-Mariscal *et al*., 1985)

Confluent monolayer (stable TER reading) on the Transwell insert was rinsed twice with PBS and incubated with low calcium (<5 μM) DMEM (Invitrogen) for 2 h in the 37°C incubator. Resistance of the monolayer was again measured to monitor extend of the tight junction disruption. The low calcium medium of the disrupted cell monolayer was replaced with normal calcium (1.8 mM) medium (DMEM) and the cells were incubated at 37°C until the resistance of the monolayer was measured (2.2.5.10).

2.2.5.13 Statistical Analysis

Data are presented as means ± standard deviation of the mean (S.D.). Statistical analysis was performed, when appropriate, using Student's t-test. A difference of $p < 0.05$ was considered statistically significant.

CHAPTER THREE RESULTS

3.1 Identification of Interaction Partners for Human Somatostatin Receptor 3 with the Yeast Two-Hybrid System

This project was started with the aim of elucidating the function of the human somatostatin receptor subtype 3 (hSSTR3). One method of elucidating a protein function, in this case a receptor, is to identify possible interaction partners.

The Matchmaker yeast two-hybrid system (Clontech) was used in this study to identify the interaction partners for hSSTR3. In brief, a bait is expressed as a fusion protein to a GAL4 DNA-binding domain (DNA-BD) in a haploid yeast reporter strain, while another gene or cDNA library is expressed as a fusion protein to the GAL4 activation domain (AD) in another haploid yeast strain. During the mating of these two haploid yeast strains, the bait and the library fusion proteins are brought together in the same cells. When bait and library fusion proteins interact, the DNA-BD and AD brought into close proximity, which will in turn activate the transcription of four reporter genes (Figure 3.1).

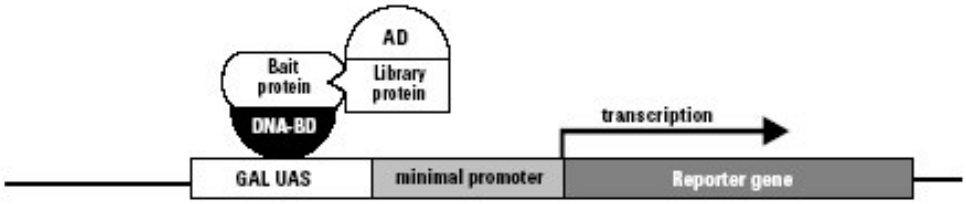

Figure 3.1 Principle of the yeast two-hybrid system
(from Pretransformed MATCHMAKER Libraries User Manual, 2001, Clontech)
When the fusion library-AD protein comes in proximity to the fusion bait-DNA-BD resulting from an interaction between the bait protein and the library protein, activating domain (AD) allows the transcription of the reporter genes [*ADE2* (complement adenine auxotrophic), *HIS3* (complement histidine auxotrophic), *MEL1* (α-galactosidase) and *lacZ* (β-galactosidase)] by binding to the GAL UAS (upstream activating sequence) through the DNA-BD. Following transcription of the reporter genes, the auxotrophic yeast strain is able to grow on selective minimal medium.

The cDNA coding for entire C-terminus of the hSSTR3 (1046-1354 bp; Acc. NM_001051) was amplified from human genomic DNA, cloned in-frame into yeast expression vector pGBKT7 (pGBKT7-hSSTR3-C) and verified by sequencing.

human SSTR3

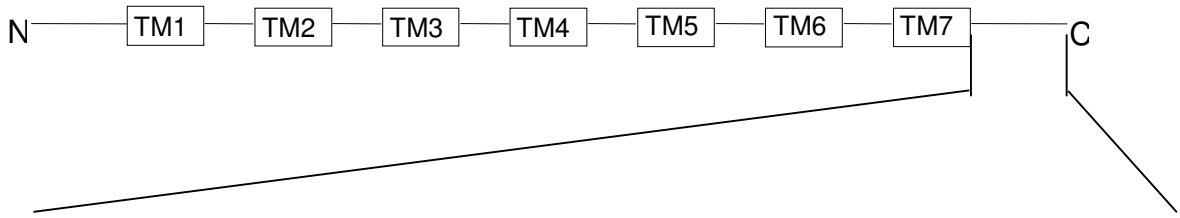

317 SYRFKQGFRRVLLRPSRRVRSQEPTVGPPEKTEEEDEEEEDGEESREGGKGKEMNGRVSQITQPGTSGQERPPS RVASKEQQLLPQEASTGEKSSTMRISYL. **419**

Figure 3.2 Schematic depiction of the human SSTR3
The boxes represent the seven transmembrane (TM) regions of the receptor. The sequence shown (C-terminus of hSSTR3) was used as bait for yeast two-hybrid screening.

The bait plasmid, pGBKT7-hSSTR3-C, was first transformed into yeast strain AH109 and the resulting strain was then mated with the pretransformed human brain cDNA library in yeast strain Y187. A total of 3.6 x 10^7 clones were screened with a mating efficiency of 20%. A total of 51 clones were isolated from both the 3 times dropout (3DO) plates (-Trp/-Leu/-His) and 4 times dropout (4DO) plates (-Trp/-Leu/-His/-Ade). Clones were then restreaked onto both 3DO and 4DO plates for phenotype verification. 13 clones were unable to grow on either of the selection plates and 7 clones were negative for β-galactosidase assay. All 29 β-galactosidase positive clones were grown and their plasmids were isolated and sequenced. 8 of the clones contained cDNA coding for RAN binding protein, which has been shown in our laboratory to be a common false positive of the screen. Sequences of 16 clones were part of the cDNA coding for Multiple PDZ Domain Protein 1 (MUPP1/MPDZ; Acc. NM_003829; Ullmer *et al*., 1998), 3 clones coded for PDZ Domain Protein Interacting Specifically with TC10 (PIST; Acc. NM_020399; Neudauer *et al*., 2001) and 2 clones were coding for Brain Angiogenesis Inhibitor-Associated Protein 1 (BAIAP1/BAP1; Acc. NM_004742 ; Shiratsuchi *et al*., 1998).

As the name implies, MUPP1 is a protein containing, 13 PDZ (PSD-95/disc-large/ZO-1 homology) domains and one MRE (MAGUK recruitment domain) for protein-protein interactions. PIST has one PDZ domain, two coiled-coil domain and a leucine zipper, while BAIAP1 has 6 PDZ domains, 2 WW (Trp-Trp) domains and a GK (guanylate kinase) domain, all of which are potential protein-protein interaction modules (Figure 3.3). These three proteins identified seem to be authentic interaction partners of hSSTR3 since it contains a type I PDZ binding motif at the extreme C-terminus which was used as the bait for the screen.

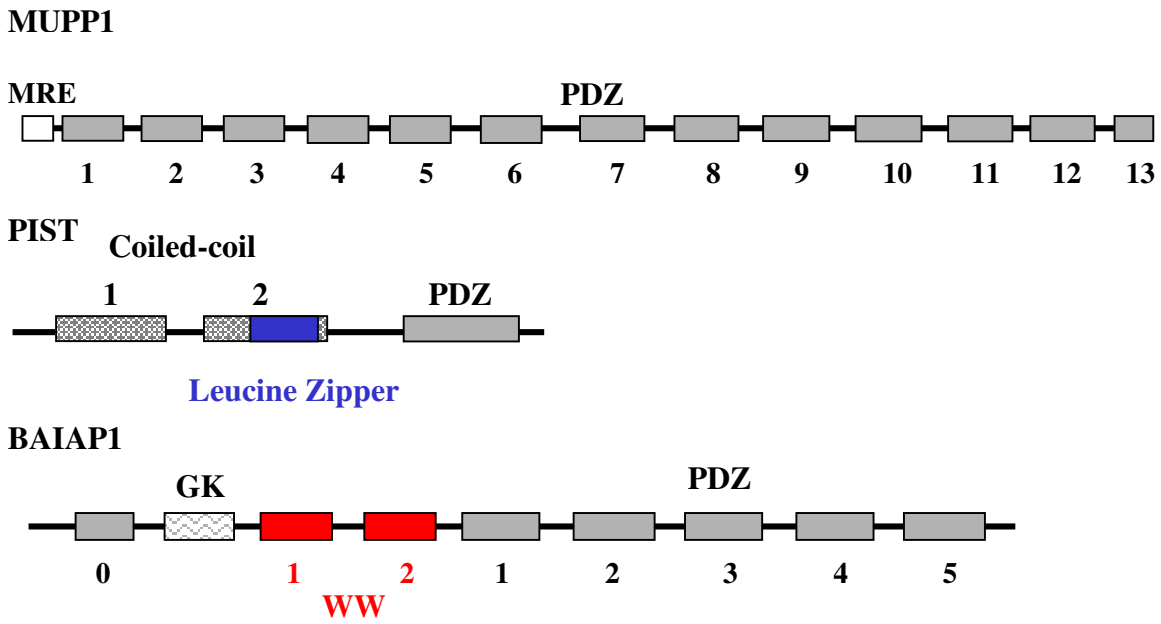

Figure 3.3 Schematic depictions of the potential interaction partners of hSSTR3
All the above proteins contain one or more PDZ domains, which have been shown to be one of the most abundant protein interaction modules present in the mammalian genome. GK-Guanylate kinase; MRE-MAGUK recruitment domain; PDZ-PSD-95/disc-large/ZO-1 homology; WW-Trp-Trp.

Sequence analysis of all the clones coding for MUPP1 revealed that all of the cDNA essentially encoded the last 5-6 PDZ domains of the protein (Figure 3.4) as well as the complete 3' UTR (untranslated region). For the PIST protein, three identical clones coding for almost a full-length protein (start 5' to the coiled-coil domain) were isolated and two identical BAIAP1 clones (start in the middle of GK domain) were found.

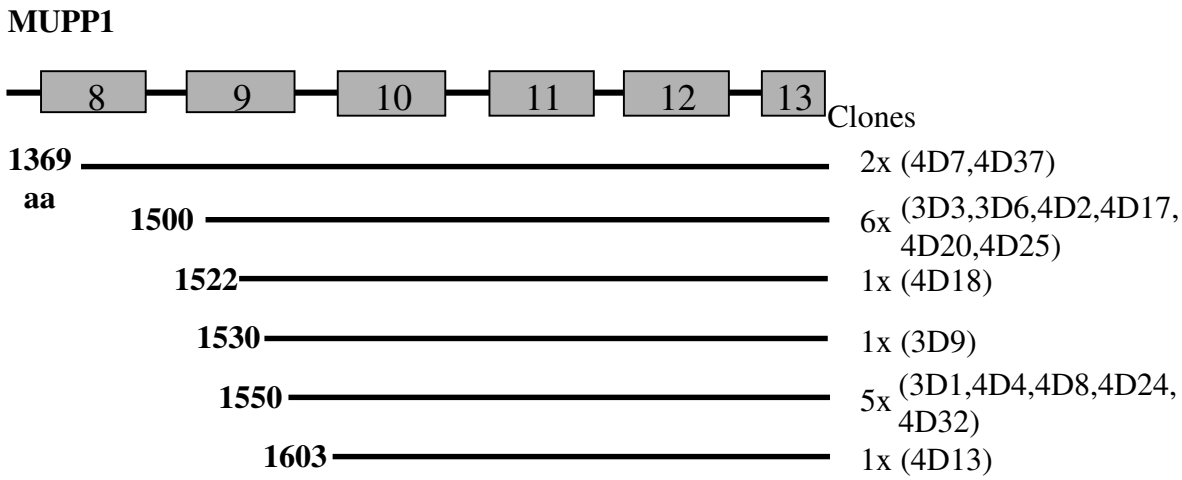

Figure 3.4 cDNA clones from yeast two-hybrid screen coding for MUPP1
MUPP1 was found to be the main interaction partner for hSSTR3 in this yeast two-hybrid screen. 16 clones were isolated and sequenced. Domains or regions between domains 10-13 were expected to mediate the interaction to hSSTR3.

In order to confirm the interaction of the bait with the interaction partners found from the yeast two-hybrid screen, the bait (pGBKT7-hSSTR3-C), a control bait (pAS-hSSTR5-C; somatostatin receptor 5; Wente, 2004) or the corresponding empty vectors were co-transformed into the yeast AH109 together with the 'fished' clones and deletion constructs of MUPP1, BAIAP1 or PIST (Hassel *et al.*, 2003). Transformants were selected on both the 3DO and 4DO plates. The results of the retransformation (Table 3.1) clearly show that the interactions of the 'fished' proteins and the bait are reproducible and that the PDZ domain is the module mediating the interaction. For the protein MUPP1, PDZ domain 10 is the interacting domain to hSSTR3. The PDZ domain of PIST and one or more of the PDZ domains of BAP1 are involved in the interaction with the receptor. PIST was also found to interact with SSTR5 receptor but not the other receptor subtypes (Wente, 2004).

One interesting observation was that the rat homolog of SSTR3 (rSSTR3) did not seem to interact with the MUPP1, PIST as well as BAP1 proteins in the yeast system. This might be due to differences in the amino acid sequence of the C-terminus (Figure 3.5), which contains the PDZ binding motif (see discussion). Deleting the last 8 amino acids abolishes the interaction of hSSTR3 and the putative interaction partners, demonstrating that the interaction of hSSTR3 with the interaction partners is indeed mediated by the extreme C-terminal PDZ binding motif.

```
SSTR3-Mouse      KASTL--SHL 428
SSTR3-Rat        KASTL--SHL 428
SSTR3-Human      KSSTMRISYL 418
                 *:**:  *:*
```

Figure 3.5 Sequence alignment of the extreme C-terminus of human and rodent SSTR3
Differences in the amino acids of the SSTR3 C-terminus could dictate the binding specificity and affinity to the interaction proteins. "*": identical residues; "**:**": conserved substitutions.

pACT2-constructs	pAS2-constructs		pGBKT7-constructs			
	empty	hSSTR5-C	empty	hSSTR3-C	hSSTR3-8C	rSSTR3-C
empty	ND	ND	-	-	ND	ND
3D1(MUPP1)	-	-	-	+++	-	-
3D6(MUPP1)	ND	ND	ND	+++	ND	ND
PDZ-10-13	ND	ND	ND	+++	ND	-
PDZ-11-13	ND	ND	ND	-	ND	ND
PDZ-12-13	ND	ND	ND	-	ND	ND
PDZ-13	ND	ND	ND	-	ND	ND
PDZ-10	ND	ND	ND	+++	ND	ND
3D7(BAIAP1)	ND	ND	-	+++	-	-
BAIAP1 (PDZ1-5)	ND	ND	ND	+++	ND	ND
BAIAP1 (GK-WW)	ND	ND	ND	-	ND	ND
PIST	-	+++	-	+++	-	-
PIST (PDZ)	-	+++	ND	+++	ND	-
PIST (-PDZ)	-	-	ND	-	ND	-

Table 3.1 Results of the yeast two-hybrid retransformations.
Putative interaction partners of hSSTR3 isolated from the yeast two-hybrid screen were co-transformed into yeast strain AH109 with the appropriate control vectors and deletion constructs. Transformants were selected on 3DO and 4DO plates until the colonies appeared. +++ (strong interaction); - (no interaction) and ND (not determined).

3.2 Identification of Novel Splice Variants for MUPP1

A multiple sequence alignment of all the sequenced MUPP1 clones isolated from the yeast two-hybrid screen with the published human MUPP1 mRNA sequence (Acc. NM_003829) allowed the identification of multiple novel splice variants present in the isolated clones.

MUPP1 protein is encoded by a 6129 bp mRNA comprising at least 46 exons. Analysis of all the yeast two-hybrid clones revealed 4 novel splice variants resulting from alternative usage of splice acceptors, splice donors or exons. All of the alternative splicing events found are located between exon 35-40 which encodes PDZ domain 10.

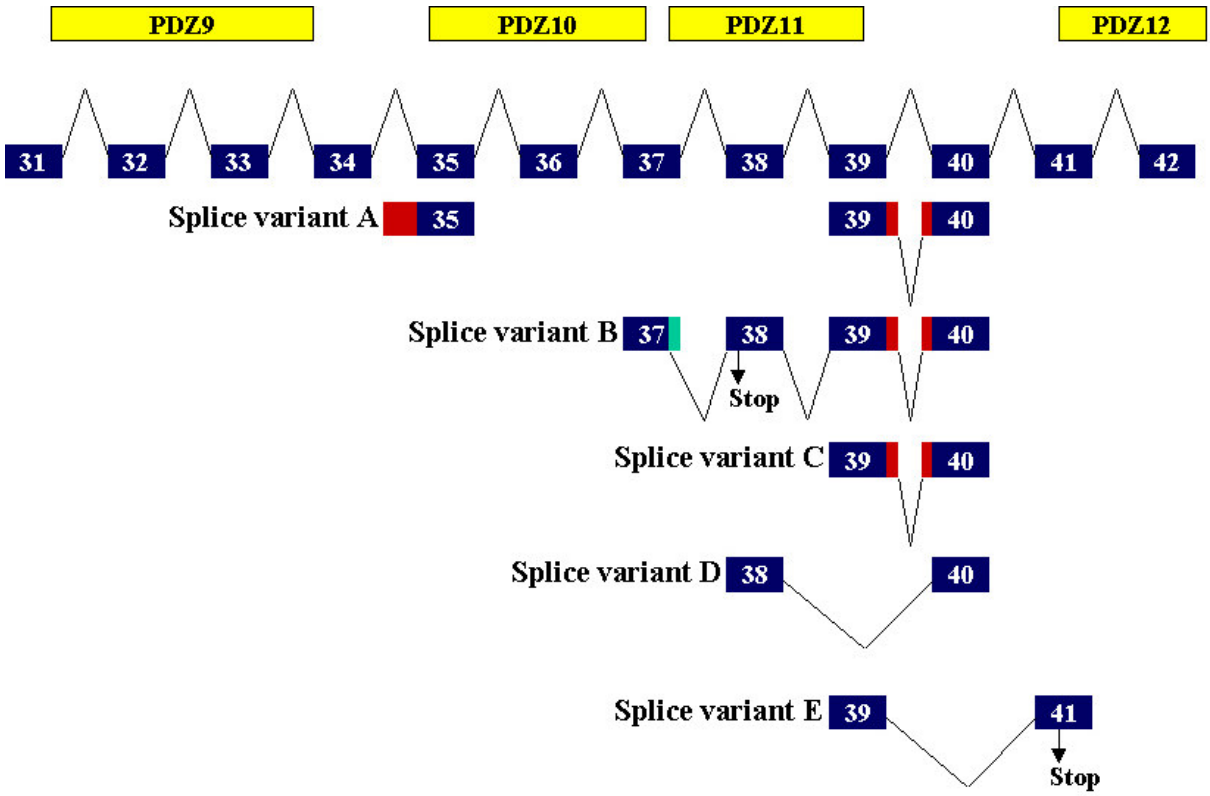

Figure 3.6 Novel splice variants identified in the MUPP1 yeast two-hybrid clones and PCR amplification
All 16 clones of MUPP1 isolated from yeast two-hybrid screen were sequenced and analyzed. Four novel splice variants (A, B, C, D) were found, all have an alternative splice donor or splice acceptor site after the coding sequence of PDZ10 domain. Splice variant E was found during the course of PCR tissue distribution analysis of the other splice variants (see below).

Splice variant A (clone 4D13), which has an alternative splice acceptor site in the intron between exon 34 and exon 35 leads to the insertion of 35 residues N-terminal to PDZ domain 10, which remains unaffected despite the alternative splicing. Attempts to find the joining exon 5' to the alternatively splice exon 35 were unsuccessful so far but evidence from public databases shows that it is an alternative exon other than exon 34. Three expressed sequence tags (EST; # R70610, AL695160, BX492831) were identified in the NCBI EST database, which provided support for the authenticity of this clone.

Splice variant B (clones 3D1, 4D4, 4D8, 4D24, 4D32) arises from two alternative splicing events. Alternative usage of a splice donor site on exon 37 results in a 16 bp deletion of the exon, which in turn causes a frame-shift truncation of the MUPP1 protein around the PDZ domain 11.

Splice variant C (clones 3D3, 3D6, 3D9, 4D2, 4D13, 4D17, 4D18, 4D20, 4D25) is a product of alternative usage of splice donor and splice acceptor sites which result in an 84 bp

extension of the mRNA. This results in the addition of 27 amino acid residues to MUPP1, without changing existing domains or creating any known functional domain. This splicing event is also observed in variant B, but has no influence on the coding sequence.

The fourth splice variant (clones 4D7, 4D37) omits the exon 39 by using the alternative splice acceptor site of exon 40 as in the case of splice variant C. The product of this splice variant has a truncated PDZ domain 11. The implication of this truncation remains to be determined.

In order to ascertain the existence of these splice variants *in vivo*, a human Multiple Tissue cDNA (MTC™) panel (Clontech) was obtained and various selective PCR-primers for individual splice variants were designed and synthesized. The amount of a housekeeping gene cDNA, glyceraldehyde-3-phosphate dehydrogenase (G3PDH) was determined to verify that similar amounts of cDNA were present in different tissues in the panel. In all the PCR reactions, H_20 was included as negative control.

All the PCR products were cloned into pCR®II-TOPO® vector whenever possible and for each product several clones were sequenced. Surprisingly, not only all the splice variants identified in the yeast two-hybrid were found in the MTC™ panel, but one more new splice variant, E, was also discovered (Figure 3.6).

As shown in Figure 3.7(A), the primer pair of hMUSV2-F(n) and hMUSV2-R(n) gave rise to two distinct bands in all the tissues included in the panel. The higher and more intense band corresponded to splice variant C based on the PCR products cloned and sequenced. Sequencing of the clones from the lower PCR band confirmed the presence of splice variants D, and E a new splice variant, E, which gives rise to a truncated MUPP1 protein. However, the splice variant based on the published Genbank (GB) sequence and splice variant B were not found.

In view of this, a primer to specifically amplify the GB splice variant was designed [hMUSV2-R2(n)]. From the result shown in Figure 3.7(B), the GB splice variant was indeed present in all the tissues tested with a slightly lower expression level in pancreas.

A pair of primers (hMUSV2-F3 and hMUSV2-R3) was also designed to amplify splice variant B specifically. Only brain, lung, liver and pancreas were found to express this splice variant, with the highest expression level found in both brain and lung (Figure 3.7C). This might be the reason that this splice variant was identified in the yeast two-hybrid screen against the human brain cDNA library even though its expression is rather low.

(A)

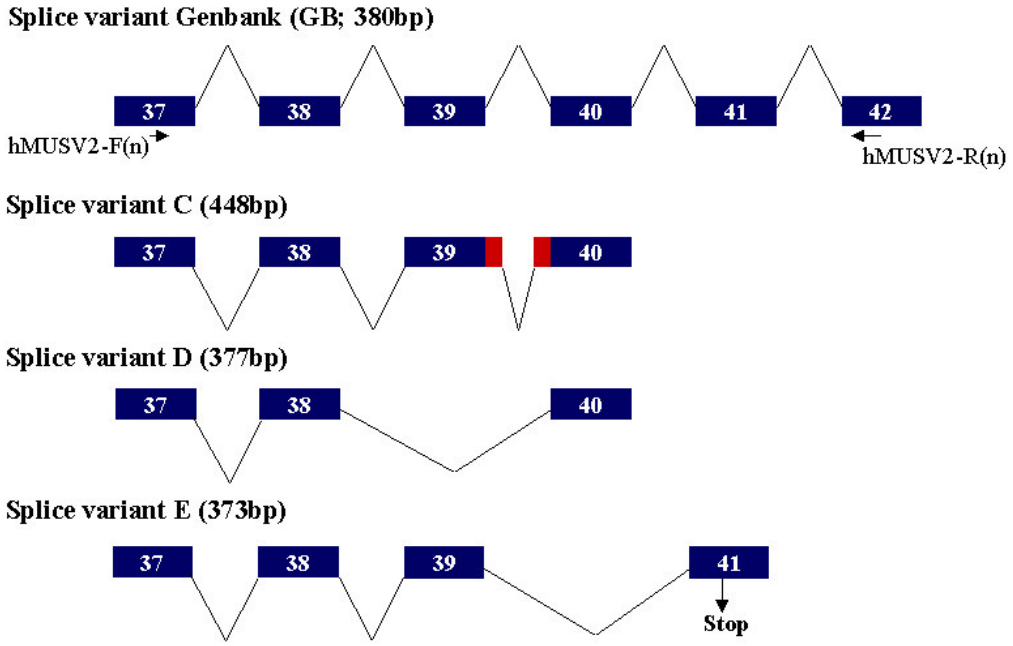
Splice variant Genbank (GB; 380bp)
37
38
39
40
41
42
hMUSV2-F(n)
hMUSV2-R(n)
Splice variant C (448bp)
37
38
39
40
Splice variant D (377bp)
37
38
40
Splice variant E (373bp)
37
38
39
41
Stop

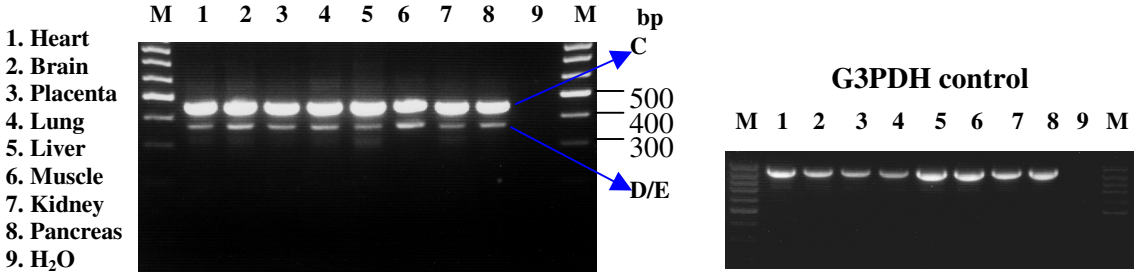
1. Heart
2. Brain
3. Placenta
4. Lung
5. Liver
6. Muscle
7. Kidney
8. Pancreas
9. H2O
M 1 2 3 4 5 6 7 8 9 M
bp
C
500
400
300
D/E
G3PDH control
M 1 2 3 4 5 6 7 8 9 M

(B)

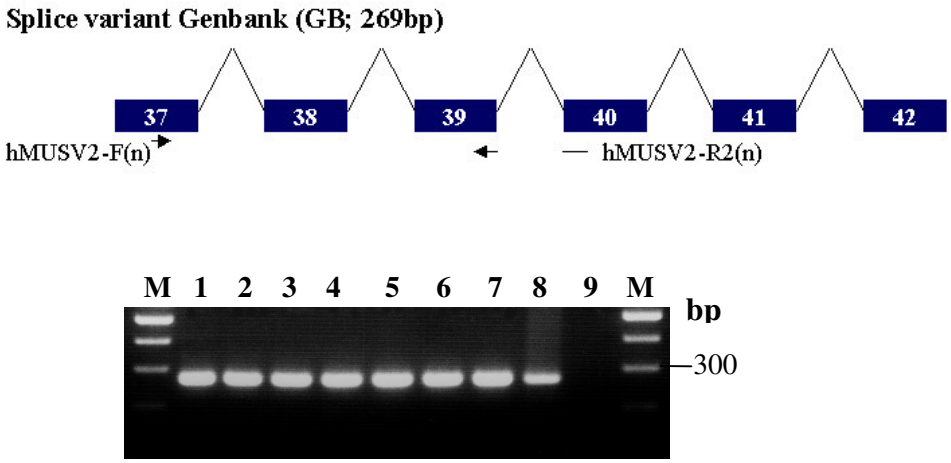
Splice variant Genbank (GB; 269bp)
37
38
39
40
41
42
hMUSV2-F(n)
hMUSV2-R2(n)
M 1 2 3 4 5 6 7 8 9 M
bp
300

(C) **Splice variant B (430bp)**

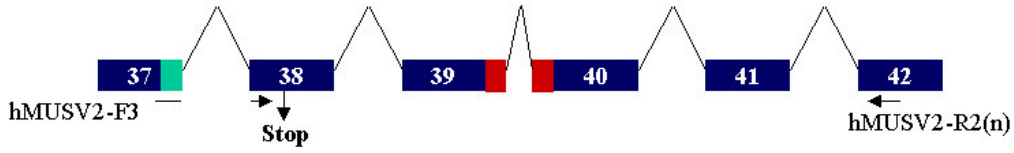

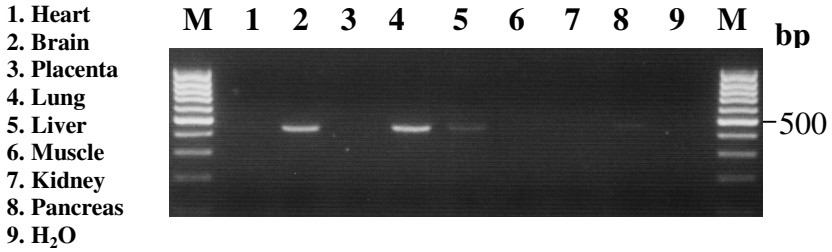

Figure 3.7 MUPP1 splice variants expression level study in human MTC™ panel.
Expression levels of different splice variants were investigated with selective PCR-primers. The amount of a housekeeping gene cDNA, glyceraldehyde-3-phosphate dehydrogenase (G3PDH) was determined to verify that similar amounts of cDNA were present in different tissues in the panel. In all the PCR reactions, H_20 was included as negative control.

Results from the PCR analysis on the distribution of splice variants in different human tissues showed that MUPP1 is ubiquitously expressed in all the tissues examined. This suggests that MUPP1 is most probably co-express with any tissue that expresses the receptor.

3.3 Interaction of hSSTR3 with MUPP1 In Immunoprecipitation Assay

3.3.1 Co-Immunoprecipitation from Overexpressed Cells

The interactions of hSSTR3 and its interaction partners have been clearly shown in the yeast two-hybrid system. However, any protein-protein interaction undoubtedly has to be confirmed in a eukaryotic expression assay. One way to confirm an interaction in mammalian cells is co-immunoprecipitation (CoIP) assay, where the proteins of interest are expressed in a cell line. One of the proteins is then precipitated with an antibody and the interaction partner should be should detected in the precipitate.

In order to perform this experiment, cDNA of hSSTR3 and rSSTR3 were first amplified by PCR from human genomic DNA and rat brain cDNA library and subsequently cloned into a eukaryotic expression vector, pCDNA3-T7-Ntag, which leads to the addition of the T7 epitope to the N-terminus of the receptor. On the other hand, the putative interacting domain of MUPP1, PDZ domain 10 (PDZ10), was cloned from the yeast two-hybrid clone pACT2-3D1 (including partial PDZ9 and PDZ11) into the expression vector pCMV-Tag-2C where a

flag epitope tag is fused with the PDZ10 domain protein. Besides this, a full-length rMUPP1 cDNA in pXMD1 vector was obtained from Dr. Ullmer (Bécamel *et al.*, 2001) for the CoIP experiment. Equal amounts of the plasmid DNAs coding for hSSTR3 or rSSTR3 and rMUPP1 or PDZ10 were transfected into COS-7 cells with transfection reagent Polyfect. Transfected cells were lysed 36 h after transfection, clarified by centrifugation and the receptors were precipitated with T7 antibody-coupled agarose. Precipitated proteins were then separated and detected on Western blots with either T7 antibody for the receptor, anti-flag antibody for the PDZ10 domain or anti-MUPP1 antibody for the full-length MUPP1 protein.

Results shown in Figure 3.8 clearly demonstrated that the (A) PDZ10 or (B) MUPP1 protein interacts with the hSSTR3 receptor in transfected cells. Both proteins co-precipitated with SSTR3 when the receptors were precipitated with an anti-T7 agarose. The strong smearing signals of the receptor detected with the T7 agarose was presumably due to post-translational glycosylation and phosphorylation modification of SSTR3 in the cells. Unmodified receptor migrates at around 40 kDa (arrow) as shown in Figure 3.8 (A). Unlike in the yeast two-hybrid system, the MUPP1 protein was found to co-precipitate with the rat SSTR3 as well. This is most probably due to the over-expression of both proteins in the cells in which even a low affinity interaction could occur under a saturating environment.

Due to the overwhelming number of yeast two-hybrid clones isolated, further work was concentrated on MUPP1. However, the interaction of the hSSTR3 with BAIAP1 and PIST were also confirmed by CoIP in COS7 cells (data not shown).

(A)

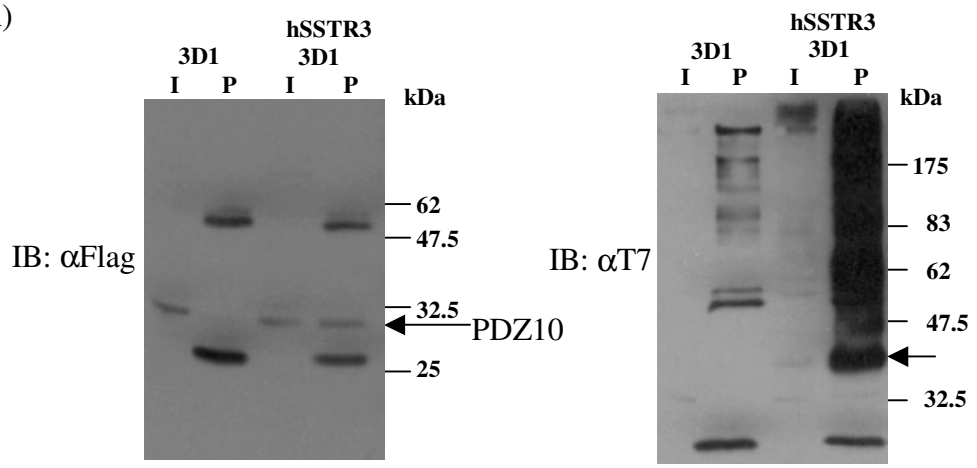

IP: αT7 agarose

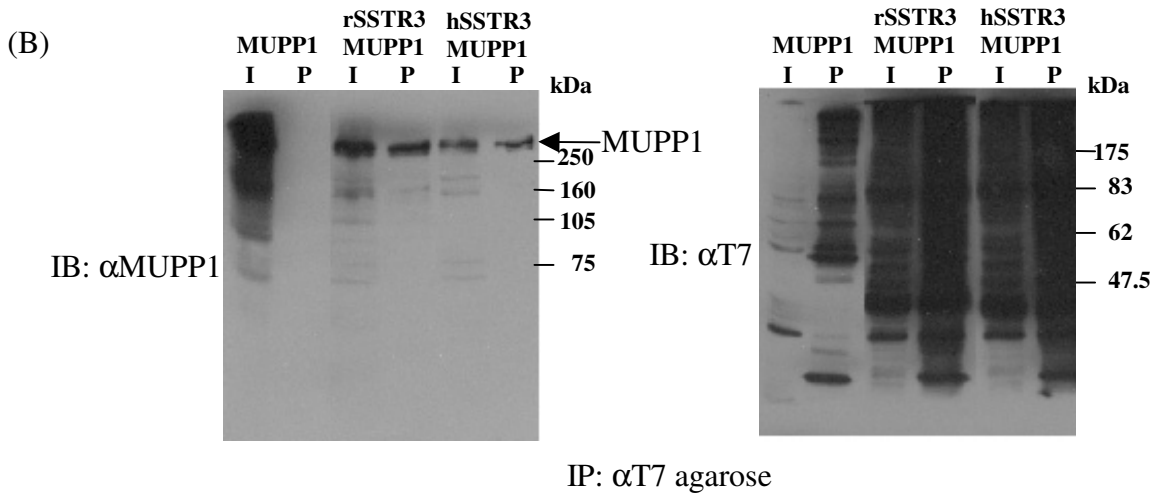

Figure 3.8 Co-immunoprecipitation of SSTR3 with PDZ10 or MUPP1 in transfected cells
Cells transfected with the expression constructs indicated on top of each blot were lysed in RIPA buffer and clarified. T7-tagged receptor was immunoprecipitated (IP) by incubating the cell lysate (I) with T7 agarose. Proteins in the lysate (I) and precipitate (P) were then detected (IB) with antibodies indicated beside the blot.

3.3.2 Generation and Purification of Anti-PDZ10 Antibody

However, the CoIP assay was done under conditions where both proteins of interest were over-expressed. In order to verify the intracellular interaction of endogenous hSSTR3 with MUPP1, an antibody against MUPP1 was required. In order to raise an antibody against the MUPP1 protein, an antigen comprised of the PDZ domain 10 was generated. The PDZ10 domain was amplified, cloned in-frame into pGEX-4T-1, expressed in *E. coli* strain TOP10F', purified as GST-PDZ10 fusion protein and used for immunization in rabbit. Anti-PDZ10 antibody from the immunized serum was purified by incubating with GST-PDZ10 fusion protein immobilized on a nitrocellulose membrane before elution. The quality of the purified anti-PDZ10 antibody was evaluated by both Western blot and immunocytochemistry on confluent Madin-Darby canine kidney (MDCK) cells.

3.3.3 Co-Immunoprecipitation from Non-overexpressed Cells

With the purified anti-PDZ10 antibody described above, the interaction of the receptor and MUPP1 could now be confirmed in a non-overexpressed cell system. In this case, the human breast adenocarcinoma cell line, MCF-7 was used for non-overexpressed CoIP. It has been indirectly shown previously that MCF-7 cells express endogenous SSTR3 receptor (Sharma and Srikant, 1998) and due to their epithelial origin, MUPP1 was expected to be expressed endogenously, which I confirmed by both Western blot and immunocytochemistry.

Rabbit IgG from pre-immune rabbit serum of anti-PDZ10, purified anti-PDZ10 antibody and purified anti-shank antibody were first covalently coupled to protein A/G Plus agarose before being used for non-overexpressed CoIP experiments. The coupled antibody-agarose complexes were added to cleared confluent MCF-7 cell lysates in RIPA buffer and then incubated at 4°C for 2 h. In one of the reactions where anti-PDZ10 coupled agarose was added, 1 mg/ml of the hSSTR3 (hS3 in Figure 3.12A) C-terminal peptide was added to the cell lysate mixture, which would serve as an additional control as a post lysis interaction between the receptor and MUPP1 would be prevented by the hSSTR3 peptide. Following incubation, the agarose pellets were extensively washed in ice-cold RIPA buffer and analyzed by Western blotting with anti-hSSTR3 and anti-PDZ10 antibodies.

Results shown in Figure 3.9 clearly demonstrate that the SSTR3 receptor and the MUPP1 protein indeed interact in MCF-7 cells since the receptors were co-precipitated with MUPP1 when the anti-PDZ10 antibody was used with or without the presence of the hSSTR3 C-terminal peptide. Arrows indicated on the left panel showed various post-translationally modified forms of the receptor in the MCF-7 cells.

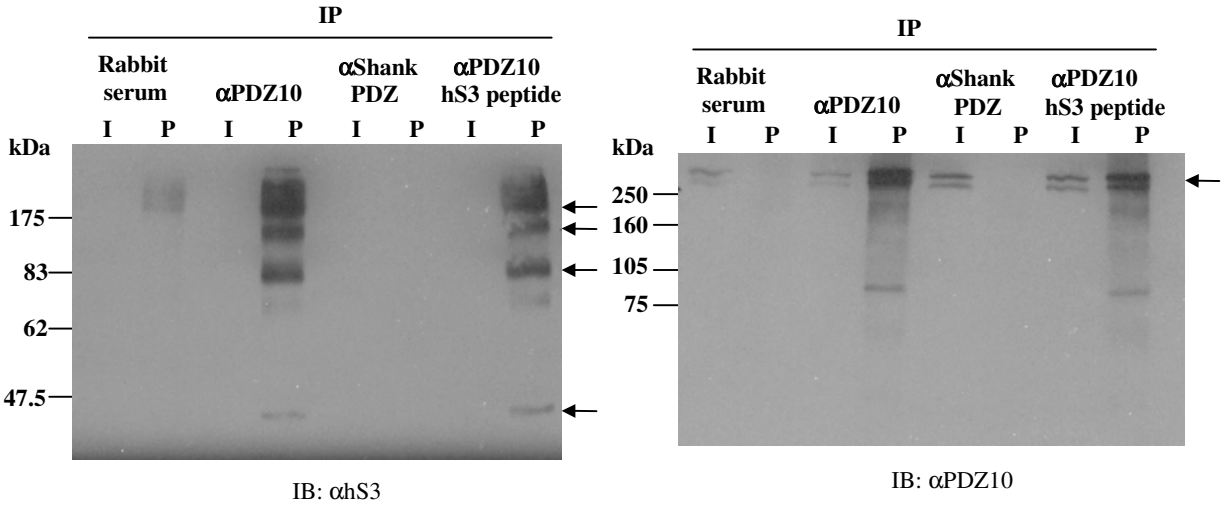

Figure 3.9 CoIP of hSSTR3 and MUPP1 in MCF-7 cells
Confluent MCF-7 cells were lysed in RIPA buffer and clarified. Cell lysates (I) were immunoprecipitated (IP) with the antibody-coupled agarose as indicated on top of each blot. Proteins present in both the lysate (I) and precipitate (P) were detected (IB) with antibodies indicated. Pre-immune rabbit serum and anti-shank PDZ antibody were used as negative control whereas hSSTR3 peptide was added into the cell lysate during the immunoprecipitation to prevent post lysis interaction between the receptor and MUPP1.

3.4 Localization of MUPP1 in Epithelial Cell Lines and Choroid Plexus

In order to investigate the localization of MUPP1 in epithelial cell lines as well as in tissue, the affinity and the specificity of the antibody needed to be determined. Confluent filter-grown MDCK cells were fixed and stained with purified anti-PDZ10 and anti-MUPP1 (Upstate) antibodies for comparison. The pre-immune rabbit serum was used as negative control. Results of the immunostaining (Figure 3.10) showed that the purified anti-PDZ10 antibody specifically labeled a very thin layer of the MDCK cell junction because it was out of focus easily under the microscope (middle; upper right corner). This result is consistent with the tight junction localization of MUPP1 as reported previously (Hamazaki *et al*., 2002). When the staining patterns of the anti-PDZ10 antibody and anti-MUPP1 antibody were compared, it was evident that the anti-PDZ10 antibody has higher specificity and produces less background compared to the anti-MUPP1 antibody.

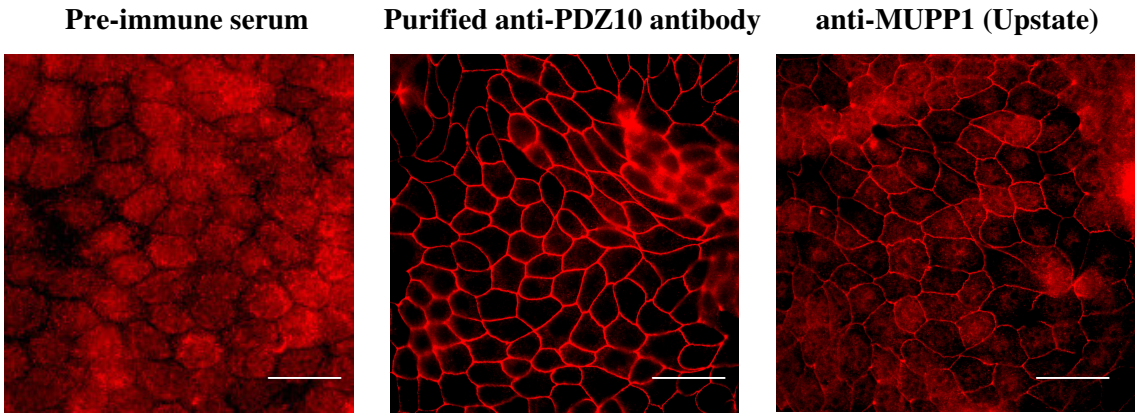

Figure 3.10 Specificity of the purified anti-PDZ10 antibody
Confluent MDCK cells grown on transwell filter were fixed and immunostained with pre-immune rabbit antisera, the purified anti-PDZ10 antibody or the anti-MUPP1 antibody from Upstate Biotechnology. Images were taken with the fluorescence microscope and processed in Adobe Photoshop. Scale bar, 20 µm.

After confirmation of the specificity of the purified anti-PDZ10 antibody, the localization of MUPP1 proteins was investigated in various epithelial cell lines, as well as at the mouse brain. As shown in Figure 3.11, MUPP1 is expressed in MDCK, MCF-7 and HEK293 (Human Embryonic Kidney) cells and concentrated at the cell-cell contact sites. Localization of the MUPP1 at cell junction depends on the availability of the cell-cell contact, which was shown clearly in the case for MDCK cells (Figure 3.11A). However, the staining of MUPP1 in MCF-7 cells was found consistently more diffuse compared to the MDCK cells. In HEK293 cells, MUPP1 was concentrated only at some of the cell-cell contact sites.

In the mouse brain, MUPP1 immunostaining signals were found mainly at the choroid plexus epithelium, which forms the blood-cerebrospinal fluid (CSF) barrier. In collaboration with Michaela Schweizer (ZMNH, Hamburg), MUPP1 was also found in a subpopulation of calretinin positive GABAergic interneurons in the cortex, hippocampus and glomeruli of olfactory bulb using the purified α-PDZ10 antibody

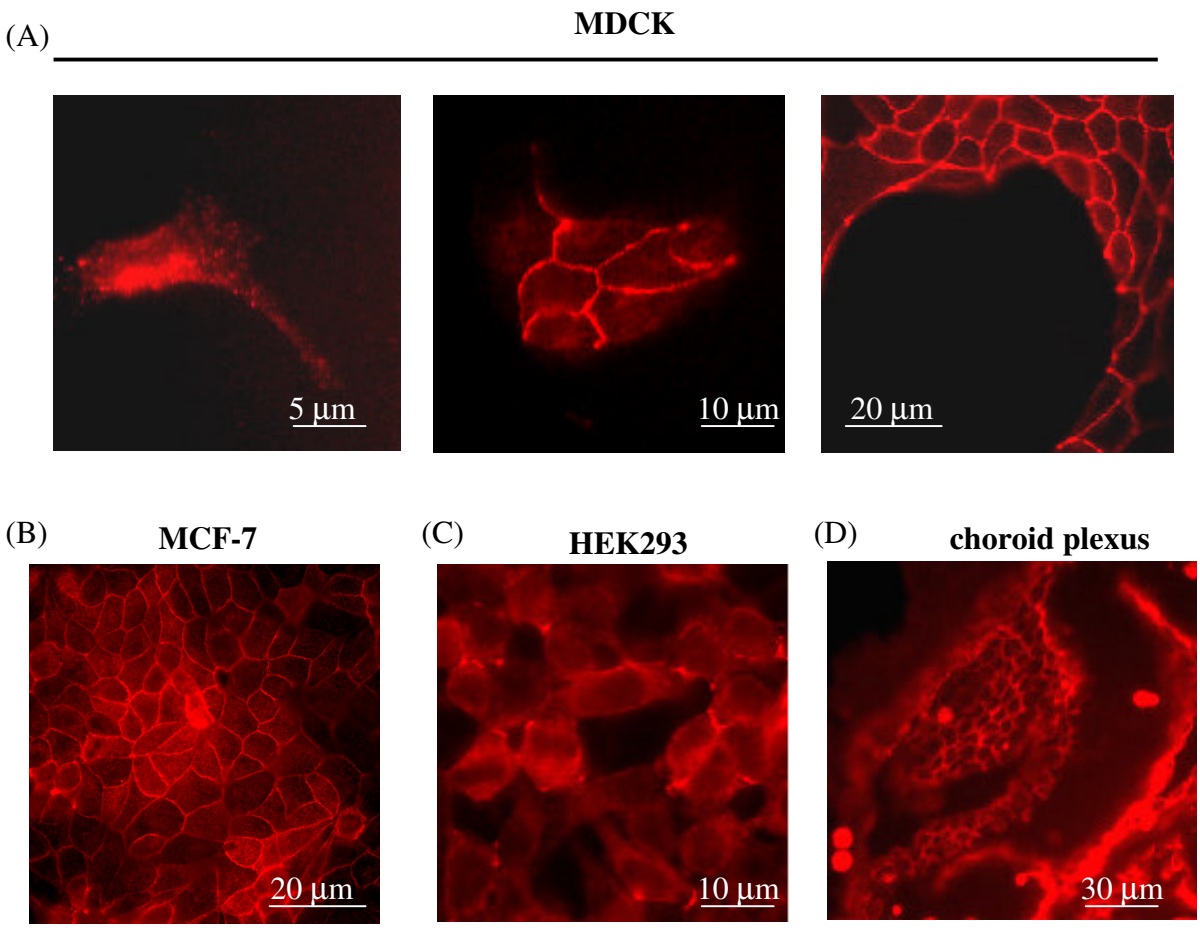

Figure 3.11 Localization of MUPP1 in epithelial cell lines and choroid plexus
(A) MDCK cells at various stages of confluency, (B) Confluent MCF-7 cells grown on coverslip, (C) HEK293 cells and (D) mouse brain sections were fixed and stained for MUPP1 with anti-PDZ10 antibody. Images were taken with fluorescence microscopy and processed in Photoshop.

3.5 Affinity Purification of MUPP1 Associated Macromolecular Complexes

3.5.1 Affinity purification with hSSTR3 Peptide Coupled NHS-Sepharose

Due to the conflicting results on the binding of rSSTR3 to MUPP1 obtained from the CoIP and the yeast transformation experiments, a more stringent and competitive assay was developed to clarify this discrepancy. Essentially, affinity purification using the corresponding receptor peptides was done with tissue or cell lines expressing endogenous MUPP1. In brief, the peptides corresponding to the last eight and ten amino acids of the rat

and human SSTR3 receptor respectively, as well as the C-terminus of GKAP /SAPAP (Acc. U67987; Figure 3.12A) were synthesized and coupled to NHS-sepharose for affinity pull-down experiments. Rat brains were homogenized and solubilized in DOC lysis buffer, clarified by centrifugation and incubated with the coupled peptides. The proteins precipitated were first denatured in sample buffer and then analyzed on Western blot.

As shown in Figure 3.12(B), hSSTR3 peptide precipitated much more MUPP1 than the rSSTR3 peptide, suggesting that MUPP1 has a much higher affinity for the human than the rat receptors.

(A)

GKAP peptide:
IYIPEAQTRL*

rSSTR3 peptide:
KASTLSHL*

hSSTR3 peptide:
KSSTMRISYL*

(B)

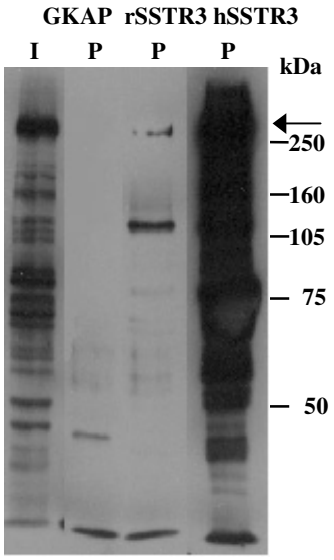

IB: α MUPP1

Figure 3.12 Affinity purification from brain lysate with NHS-coupled peptides
(A) Sequences of peptides used in the affinity pull-down experiments. All peptides were coupled to NHS sepharose through the primary amino group found on the first amino acid (I or K). (B) Rat brains were homogenized in DOC buffer and clarified. Brain lysate (I) was affinity precipitated with the peptides indicated on top of the blot. Proteins of the precipitate (P) were detected with anti-MUPP1 antibody.

3.5.2 Identification of MUPP1 Macromolecular Complexes

This high affinity interaction of hSSTR3 with MUPP1 suggested an opportunity to identify and isolate proteins associated with MUPP1, since many of the PDZ domain-containing proteins have been shown to function as scaffolding proteins.

Attempts to isolate MUPP1 macromolecular complexes were made possible by the high binding affinity of hSSTR3 to MUPP1 protein. Mouse brain, HEK cells, and MCF-7 cells lysates were incubated with the NHS-sepharose coupled peptides. Precipitated proteins were denatured and separated on SDS-PAGE followed by staining with Coomassie dye. The

prominent bands were excised, digested with trypsin and then analyzed by mass spectrometry.

Protein profiles identified from either mouse brain or cell lines were strikingly similar even though the relative abundance of some proteins purified varied from one sample to another (Figure 3.13A). Nonetheless, most of the proteins identified were known TJ proteins, for examples ZO-1, MAGI-1, MAGI-3, ZO-2 and Pals1 (González-Mariscal *et al*., 2003).

MUPP1, BAIAP1 and PIST have been previously identified as hSSTR3 interaction partners, but how were the other co-purified proteins connected to hSSTR3? Are they connected to hSSTR3 directly or indirectly through MUPP1? Since many of the PDZ domain containing proteins were identified in the affinity purification, which ones were potentially interacting with the PDZ binding motif of the hSSTR3?

In order to address this question, an overlay assay was performed on the precipitates of hSSTR3 peptide with the GST-hSSTR3 fusion proteins. In the overlay assay, direct or indirect interaction of two proteins could be clearly distinguished by the direct binding of the fusion proteins to their interaction partners immobilized on the nitrocellulose membrane.

For this purpose, the last 50 amino acids of the hSSTR3 C-terminus were cloned in-frame into pGEX-6P-1. GST-hSSTR3-50C fusion protein and GST protein as negative control were expressed in *E. coli*, purified and quantified.

Then, protein complexes were precipitated with the NHS-sepharose coupled hSSTR3 peptide and GKAP peptide, as a negative control, from mouse brain lysate, HEK293 and MCF-7 cells lysates. The complexes were separated on SDS-PAGE and transferred onto a nitrocellulose membrane. The blots were then blocked with 10% blocking buffer at 4°C overnight, this would allow the proteins to refold on the blot. On the following day, blots were incubated with either 10 µg of GST-hSSTR3-50C or GST protein, and the fusion proteins were detected with anti-GST antibodies.

Results in Figure 3.13 (B) showed the specific binding of GST-hSSTR3-50C fusion protein to MUPP1 precipitated from the mouse brain as well as MCF-7 and HEK293 cell lysates. The GST-hSSTR3-50C fusion protein was also bound to bands corresponding in size to BAIAP and PIST, which are the interaction partners of hSSTR3 identified earlier in this study. In MCF-7 and HEK293 cell lysates the GST protein as negative control (Figure 3.13C) clearly showed the specificity of the results obtained with the GST-hSSTR3-50C fusion protein.

(A)

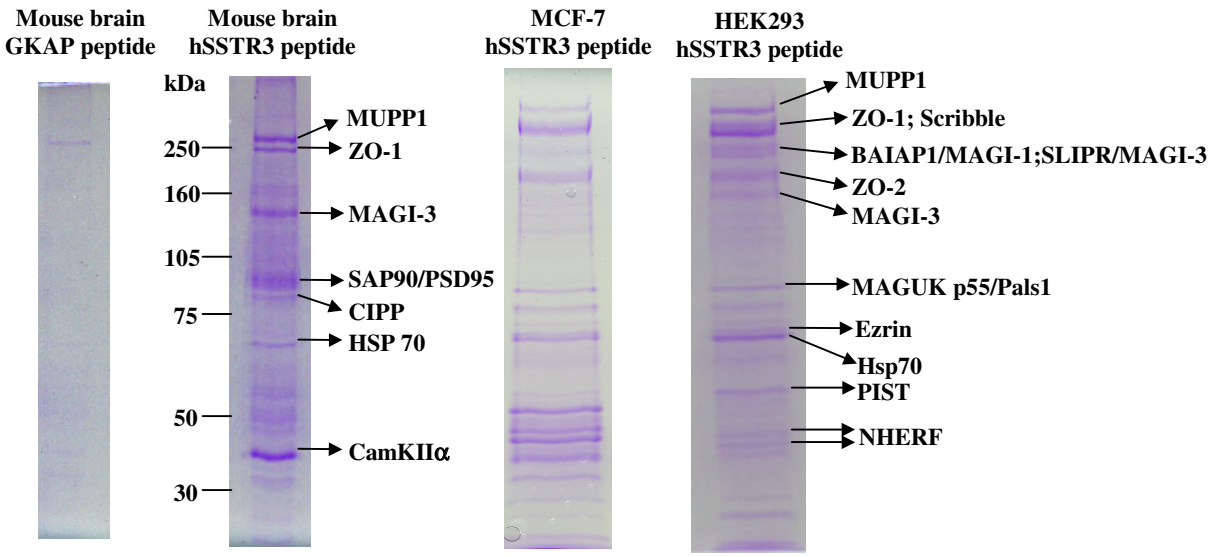
Mouse brain
GKAP peptide
Mouse brain
hSSTR3 peptide
MCF-7
hSSTR3 peptide
HEK293
hSSTR3 peptide
kDa
250
160
105
75
50
30
MUPP1
ZO-1
MAGI-3
SAP90/PSD95
CIPP
HSP 70
CamKIIα
MUPP1
ZO-1; Scribble
BAIAP1/MAGI-1;SLIPR/MAGI-3
ZO-2
MAGI-3
MAGUK p55/Pals1
Ezrin
Hsp70
PIST
NHERF

(B)

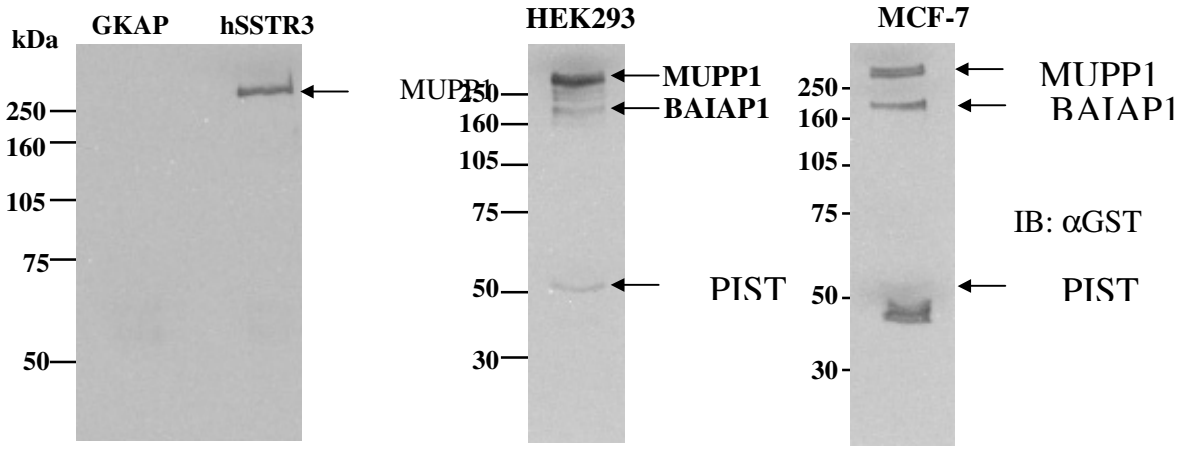
kDa
GKAP
hSSTR3
250
160
105
75
50
HEK293
MUPP1
BAIAP1
PIST
MCF-7
MUPP1
BAIAP1
IB: αGST
PIST
Overlay: GST-hSSTR3-50C

(C)

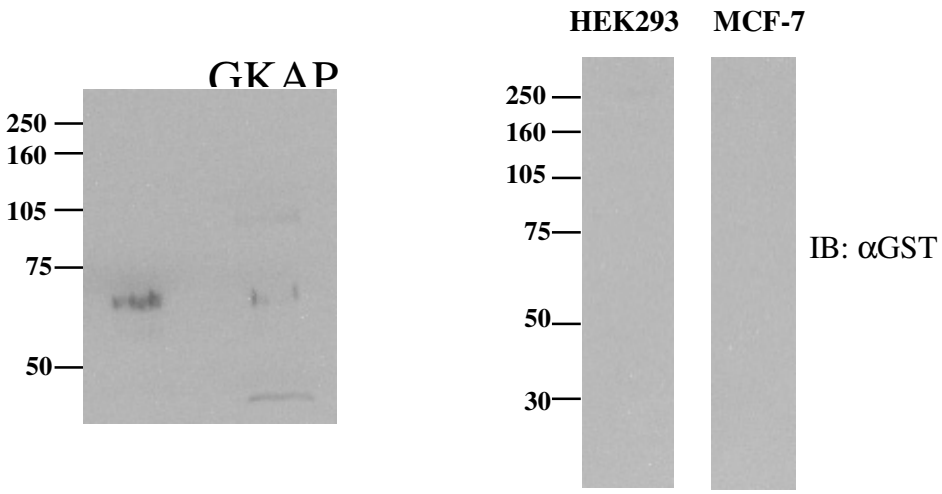
GKAP
250
160
105
75
50
HEK293
MCF-7
IB: αGST
Overlay: GST

Figure 3.13 Identification and verification of MUPP1 protein complexes in mouse brain and cell lines

(A) Mouse brains, or MCF-7 and HEK293 cells were lysed in DOC or RIPA buffer respectively. Clarified lysates were precipitated with either sepharose coupled GKAP peptide as negative control or sepharose coupled hSSTR3 peptide. Precipitates were separated on SDS-PAGE and Coomassie stained. Prominent bands were excised, digested with trypsin and then analyzed by mass spectrometry.

(B) Proteins were precipitated with either GKAP or hSSTR3 peptides from mouse brain or cell (MCF-7 and HEK293) lysates. After separation on SDS-PAGE, the precipitates were blotted onto nitrocellulose membrane and incubated with the GST-hSSTR3-50C fusion protein. The fusion protein was detected with anti-GST antibody.

(C) GST protein was used to overlay on the GKAP and hSSTR3 peptide precipitates as negative control. GST protein was detected with anti-GST antibody.

Results from the overlay assay clearly showed that only 3 proteins, namely MUPP1, BAIAP1 and PIST, bind to hSSTR3 directly. The question now is whether the rest of the pulled-down proteins interact with MUPP1? In order to address this question, some of the proteins identified were cloned into expression vector for CoIP experiments.

cDNA coding for rPSD-95 was cloned in-frame into the pEGFP vector and expressed in COS7 cells with either cDNA expression construct of rSSTR3 or hSSTR3. Anti-T7 agarose was used to immunoprecipitate the receptor and the presence of GFP-rPSD95 was detected on Western blots with an anti-GFP antibody. As shown in Figure 3.14 (A; left), neither hSSTR3 nor rSSTR3 was able to co-precipitate the GFP-rPSD95. However, when the αMUPP1 antibody was used for immunoprecipitation from COS7 cells co-expressing PSD95 and MUPP1, GFP-rPSD95 was consistently found to co-immunoprecipitate with MUPP1 protein (Figure 3.14A; right). From this result, we could conclude that PSD95 was precipitated by hSSTR3 peptide through MUPP1.

Another protein, channel-interacting PDZ domain protein (CIPP; Kurschner *et al*., 1998), was also cloned and expressed as a flag-epitope tagged protein (CMV-26-mCIPP) in COS7 cells with either rSSTR3 or hSSTR3 and MUPP1 protein. Figure 3.14 (B; top left) shows that co-immunoprecipitation of CIPP was only possible when MUPP1 was also co-expressed. This again shows that CIPP is connected to the hSSTR3 receptor through their common interaction partner, MUPP1.

Besides the above described CoIP of over-expressed proteins, the interaction of MUPP1 and scribble was also confirmed by CoIP from cell lines with an anti-scribble antibody. In brief, HEK293 or MCF-7 cells lysate was first clarified by centrifugation, then incubated with goat anti-scribble antibody or goat serum as negative control before protein A/G Plus agarose was added to precipitate the scribble bound protein complex. Analysis by Western blotting with

anti-scribble or anti-PDZ10 antibodies showed that MUPP1 consistently co-immunoprecipitated with scribble protein in both HEK293 and MCF-7 cells (Figure 3.14C). Once again, these results suggested that most of the proteins, which were precipitated by the hSSTR3 peptide, were connected through MUPP1 as a scaffolding molecule to the receptor.

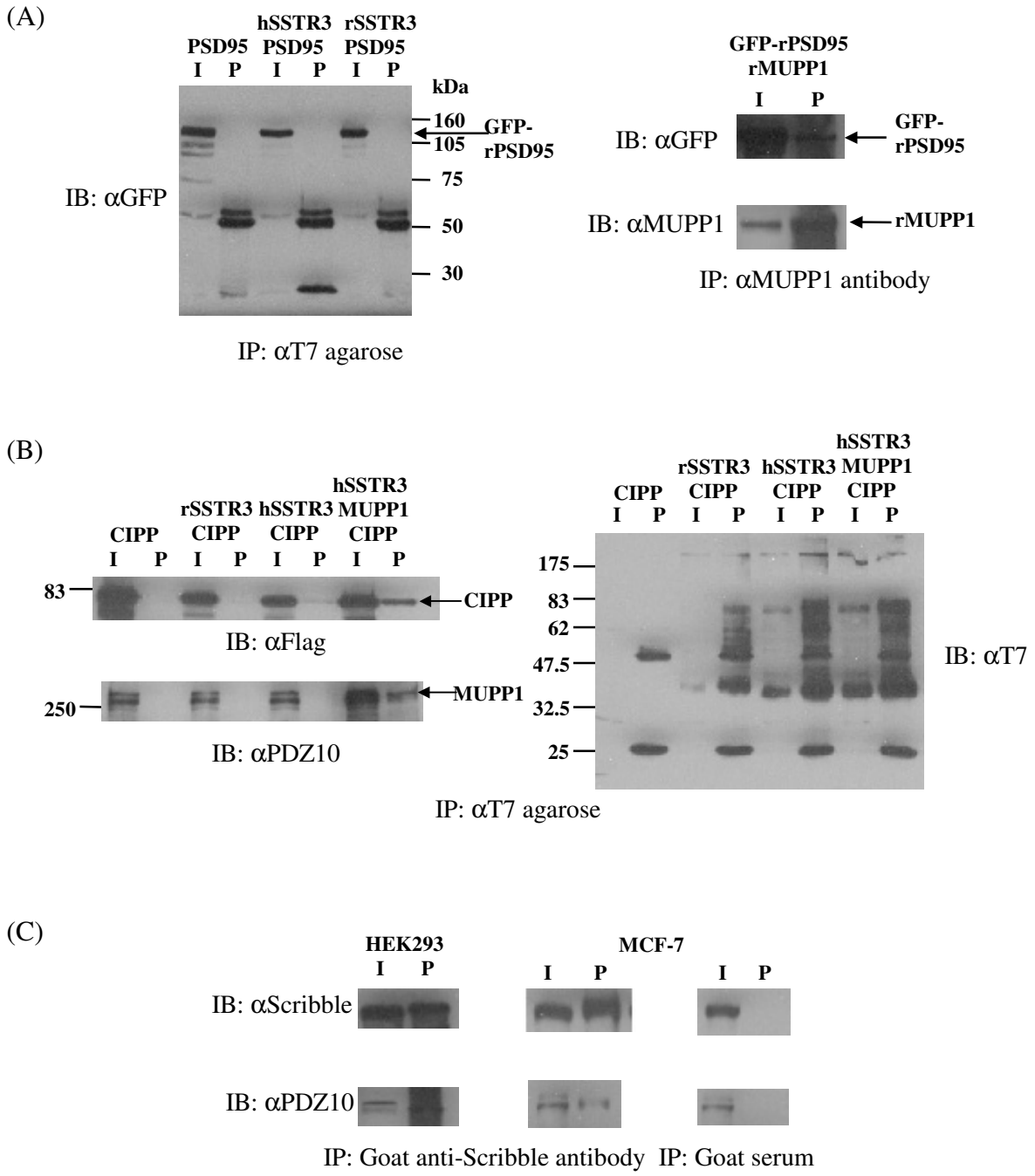

Figure 3.14 Co-immunoprecipitation assays demonstrating MUPP1 as part of a macromolecular complex

(A) Cells transfected with the expression constructs indicated on top of each blot were lysed in RIPA buffer and clarified. (Left) T7-tagged receptor was immunoprecipitated (IP) by incubating the cell lysate (I) with T7 agarose. (Right) MUPP1 was precipitated (IP) with anti-MUPP1 antibody. Proteins in the lysate (I) and precipitate (P) were then detected (IB) with antibodies indicated beside the blot.

(B) Cell lysates transfected with the constructs indicated were prepared as described in (A). T7-tagged receptor was precipitated with T7 agarose. Proteins in the lysate (I) and precipitate (P) were then detected (IB) with antibodies indicated.
(C) HEK293 and MCF-7 cell were lysed in RIPA buffer and clarified. Scribble was precipitated with anti-scribble antibody and goat serum was used as negative control. The lysate and precipitated proteins were detected by the antibodies indicated.

Taken together, these results clearly support the suggestion that MUPP1 functions as a scaffolding protein at cell-cell junction, as most of the proteins were co-precipitated by hSSTR3 peptide were due to their indirect interaction with MUPP1.

3.6 Differential Binding Affinity of SSTR3 Homolog Dictated by Amino Acid Composition of the PDZ Binding Domain at the C-terminus

Up to this point, the binding ability of the rSSTR3 to MUPP1 was still unclear based on yeast two-hybrid assay and *in vitro* CoIP in which contradicting results were obtained. In order to investigate this issue further, the last 50 amino acids of the rSSTR3 receptor were cloned into the pGEX-6p-1 vector, and GST-rSSTR3-50C fusion protein was expressed and purified. The fusion protein was then used for an overlay assay where the precipitate of the HEK293 and MDCK II cell lysates were immobilized on the blot. The result obtained showed that the rat homolog of SSTR3 did not interact with the MUPP1 protein (Figure 3.15C). This could be due to differences in the PDZ binding motifs at the C-termini. So, the question now was whether the hSSTR3 PDZ binding motif is an exception since both rodent counterparts differ from the human sequence? In order to answer this question, we need to find out the sequences of SSTR3 from other organisms. With the on-going dog (*Canis familiaris*) genome project, I managed to clone out the SSTR3 from canine first virtually by aligning multiple trace sequences download from Genbank and then by PCR from the genomic DNA of MDCK II cells. The sequence of the cSSTR3 was verified by sequencing and then deposited into the Genbank (AY643737). At the same time, we managed to find the sequence of the chimpanzee (*Pan troglodytes*) SSTR3 (AY400333) from the Genbank database. As shown in Figure 3.15 (A), the human, chimp and the dog have exactly the same last four amino acids of the C-terminal PDZ binding motif.

So, in order to show that the amino acid sequence of the PDZ binding motifs found at the SSTR3 does contribute to the differential binding affinity towards MUPP1, the last fifty amino acids of the canine SSTR3 C-terminus were cloned into the pGEX-6P-1 vector, expressed and purified. The purified fusion protein, GST-cSSTR3-50C, was then used for

overlay assays on precipitates from HEK293 and MDCK II cells. As shown in Figure 3.15 (B), the GST fusion protein of the canine SSTR3 binds to MUPP1, BAIAP1 and PIST with similar affinity as the GST fusion protein of hSSTR3. The human, rodent and canine SSTR3 in particular differ in the amino acid at position P-1: Y (Tyr) vs. H (His) and P-3 and P-4. Could this be the determining factor for the binding ability to MUPP1?

In order to answer to this question, two constructs were constructed where the rSSTR3 C-terminal PDZ binding motif was mutated. Two amino acids R and I (Arg.Ile), were added to rSSTR3 before the position P-2 for one of the constructs. This artificial C-terminus replaced the amino acids that are not present in the rodent receptors as shown in Figure 3.15(A), whereas the second construct simply replaced the His at P-1 with Tyr. GST fusion proteins of the respective artificial receptor C-termini were expressed and purified. 10 µg each of the GST fusion protein of hSSTR3-50C, rSSTR3-50C, rSSTR3-50C-RI and rSSTR3-50C-Y were used for overlay assays on precipitates from HEK293 cells immobilized on nitrocellulose membrane. As shown in Figure 3.15(C), both artificial rSSTR3-50C-RI and rSSTR3-50CY showed improved binding affinity to MUPP1 protein by 4 and 6 times respectively compared to the wild type rSSTR3. However, different amino acid composition of the C-terminus did not seem to significantly affect the binding affinity of SSTR3 to BAIAP1. rSSTR3-50C-Y showed improved binding affinity to PIST and rSSTR3-50C-RI was shown to be a much better PDZ binding motif for PIST compared to the wild type hSSTR3. Interestingly, the artificial PDZ binding motifs also showed increased non-specific binding as seen on the signals marked with asterisks.

(A)

```
SSTR3-Human        KSSTMRISYL 418
SSTR3-Chimpanzee   KSSTMRISYL 419
SSTR3-Dog          KPGALHISYL 425
SSTR3-Mouse        KASTL--SHL 428
SSTR3-Rat          KASTL--SHL 428
                   *.::  *:*
```

(B)

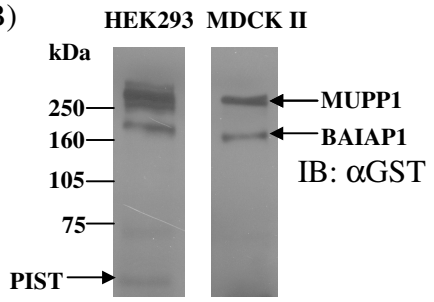

Overlay: GST-cSSTR3-50C

(C)

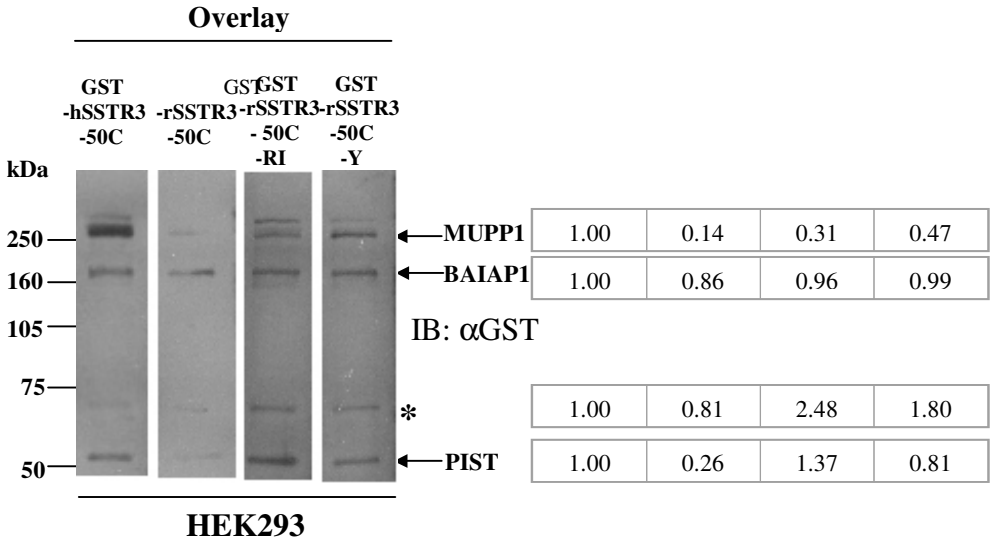

1.00	0.14	0.31	0.47
1.00	0.86	0.96	0.99
1.00	0.81	2.48	1.80
1.00	0.26	1.37	0.81

Figure 3.15 Determination of rSSTR3 binding affinity to MUPP1 by overlay assays
(A) Sequence alignment of the last eight to ten amino acids of SSTR3 from human, chimpanzee, dog, mouse and rat. "*": identical residues; " **:**": conserved substitutions; "**.**" : semi-conserved substitutions.
(B) Overlay assay of GST-cSSTR3-50C fusion protein on HEK293 and MDCKII cell precipitates purified as described in Figure 3.13B.
(C) Precipitatea from HEK cells were immobilized on nitrocellulose membrane and overlay with GST fusion protein as indicated on top of the blot. The fusion proteins were detected with anti-GST antibody. The ratios of the Western blot signals were determined by Image J software (NIH) where the signal intensity of the GST-hSSTR3 fusion protein was arbitrarily set as 1.

3.7 Localization of hSSTR3 in Stably Transfected Epithelial Cell Lines

3.7.1 Mapping of Regions Responsible for Apoptotic Effects of hSSTR3

In order to study the functional relevance of the interaction between hSSTR3 and the TJ protein, MUPP1, a cell system expressing both the receptor and the MUPP1 protein preferably an epithelial cell line was required. Since the rodent homolog of the SSTR3 was found not to interact with MUPP1, this excludes the use of a rodent model in this study. In this case, MCF-7, a human adenocarcinoma epithelial cell line, which was found to endogenously express both the receptor and MUPP1 by Western blot would seem to be the perfect cell model for this functional study. Unfortunately, the presence of the receptor in the cells could not be varifies by our immunofluorescence techniques. This could well due to the low endogenous expression level of the receptor or the quality of the antibody used. However, there was no alternative human SSTR3 antibody available to us. One solution to this problem would be establishing a stable epithelial cell line expressing the hSSTR3

receptor in which the expression level would be higher than endogenous expression, and would allow for the use of an epitope-tagged receptor. Fortunately, another standard epithelial cell line, MDCK, would also be suitable as the cell model for the functional study because information regarding the regulation of tight junction by G-proteins is available (Balda *et al*., 1991; Denker *et al*., 1996; Saha *et al*., 1998) and the functional study could be done in a background free cell line unlike the MCF-7, which expresses endogenous receptor. Furthermore, thus far, there are only limited studies on the regulation of tight junction have been done on the MCF-7 cell lines.

However, attempts to establish the hSSTR3-overexpressing stable cell lines in MDCK background proved to be difficult. This could be due to the apoptotic effect of the activated hSSTR3, as has been reported in previous publications (Sharma *et al*., 1996 and Sharma & Srikant, 1998). Over-expression of hSSTR3 might lead to a substantial amount of spontaneously active receptors, which might contribute to the difficulty in establishing the stable cell lines.

So, various deletion and domain switching hSSTR3 constructs were made to determine the region(s) responsible for these apoptotic effects. Deletion constructions of hSSTR3 were made where the PDZ binding motif (pCDNA3-T7-hSSTR3-8C) and the entire cytoplasmic terminal (pCDNA3-T7-hSSTR3 without C-terminus) were deleted or only the C-terminal of the hSSTR3 (pCDNA3-T7-hSSTR3-C terminal) was expressed. The constructs were transiently transfected in HEK293 cells and the apoptotic effects were monitored. Results in Table 3.2 show that the entire C-terminus of the hSSTR3 was not required for the apoptotic effect.

Since somatostatin receptor signaling is mediated by activation of heterotrimeric G-proteins associated with the third intracellular loop (IC3), the possibility of the involvement of G-protein was tested by exchanging the IC3 of hSSTR3 with the IC3 of mouse SSTR5 (pCDNA3-T7-hSSTR3-mSSTR5-IC3) which has been shown not to have any adverse effect on cells (Wente, 2004). However, this construct also has the apoptotic effect.

In order to overcome the difficulty in establishing an hSSTR3 stable cell line, a fusion receptor was constructed by fusing the entire C-terminal of hSSTR3 to mSSTR5 right after the last transmembrane domain of the receptor (pCDNA3-T7-mSSTR5-hSSTR3-C). This fusion receptor would be suitable for establishing stable cell lines since the interaction with MUPP1 is still possible through the hSSTR3 C-terminus without causing any adverse effects on the cells.

Another fusion receptor was constructed where both of the N- and C-terminal ends of the mSSTR5 receptor were exchanged with the N-and C-termini of hSSTR3 (pCDNA3-T7-mSSTR5-hSSTR3-N-C) to investigate the involvement of the hSSTR3 N-terminus in the apoptotic effects.

From all the deletion and fusion constructs studied so far, it is clear that the apoptotic effects caused by hSSTR3 are not mediated by their N- and C-terminal as well as the third intracellular loop.

Constructs	**Apoptotic Effect**
pCDNA3-T7-hSSTR3	Yes
pCDNA3-T7-hSSTR3-8C	Yes
pCDNA3-T7-hSSTR3-C terminal	No
pCDNA3-T7-hSSTR3 without C-terminus (R3)	Yes
pCDNA3-T7-hSSTR3-mSSTR5-IC3	Yes
pCDNA3-T7-mSSTR5 without C-terminus	No
pCDNA3-T7-mSSTR5-hSSTR3-C	No
pCDNA3-T7-mSSTR5-hSSTR3-N-C	No

Table 3.2 Deletion and fusion constructs used for the study of hSSTR3 apoptotic effects
All constructs were expressed in HEK293 cells, expression of the receptors were verified by T7 antibody under the microscope and classified for cell death.

3.7.2 Localization of hSSTR3 in MCF-7 Cells

Expression construct pCDNA3-T7-hSSTR3 was transfected into wild type MCF-7 cells and the transfected cells were placed under G418 (400 μg/ml) selection until colonies appeared (for MCF-7 cells this could take up to 3 weeks). Colonies were picked and expanded before screening by immunofluorescence with anti-T7 and anti-PDZ10 antibodies. After two rounds of sub-cloning, clones in which 90% of the cells were expressing T7-hSSTR3 were isolated.

One selected clone, MCF7-hSSTR3-0.5B4, was then grown on a transwell filter for immunofluorescence study. The use of Transwell filters to culture the epithelial cells allow them to fully polarize in contrast to the coverslips. Results of the immunostaining with anti-T7 antibody against the epitope-tagged hSSTR3 receptor and anti-PDZ10 antibody against the endogenous MUPP1 protein are shown in Figure 3.16. As mentioned previously, endogenous MUPP1 staining in MCF-7 cells is always more diffuse compared to the MDCK

cells. As seen in the merged image, hSSTR3 co-localized to a large extent with endogenous MUPP1 protein.

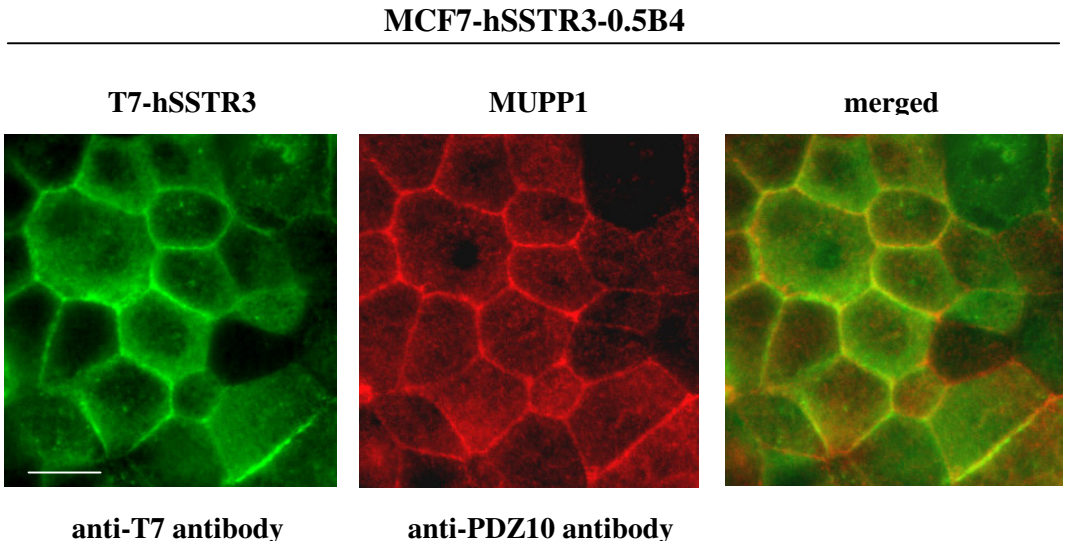

Figure 3.16 Localization of the T7 epitope-tagged hSSTR3 in MCF7 stable cell line
The hSSTR3 stably expressing MCF7 cell line, grown to confluency on polyester filter was fixed and stained with anti-T7 antibody and anti-PDZ10 antibody for the T7-tagged receptor and the endogenous MUPP1, respectively. Images were obtained with fluorescence microscopy and processed in Adobe Photoshop. Scale bar, 10µm.

3.7.3 Localization of hSSTR3 and the Fusion Receptor in MDCK II Cells

Even though the MCF-7 stably expressing T7-hSSTR3 cell line was established, it was still critical to establish the hSSTR3 stable MDCK cell line as MCF-7 is not the standard epithelial cell for the study of TJs. Unfortunately, the task to make the stable hSSTR3 stable cell line in MDCK cells was found to be extremely difficult where even a low expression of the receptor caused apoptosis in some strains of the MDCK cells. Attempts to make the stable cell line were first carried out in the MDCK I cell line; but, none of the selected clones could maintain receptor expression beyond the second passage. In view of this, the next approach was to use a regulated expression system, for example the Tet- On (Gossen *et al*., 1995) or Tet-Off system (Gossen & Bujard, 1992). So, the MDCK II Tet-Off cell line was obtained and the receptor (pTRE2-hyg-T7-hSSTR3) was transfected into the cells with Effectene transfection reagent and then selected with hygromycin (400 µg/ml) and 1 µg/ml of doxycycline to suppress the expression of the receptor. After 10-14 days of selection, clones were picked and screened by immunocytochemistry with anti-T7 and anti-PDZ10 antibodies. The expression of the receptor was induced by culturing the clones in Tet-free medium for

different lengths of time before the cells were fixed and the expression was verified. Unfortunately, even under this regulated expression system, the receptor still could not be maintained stably in the cells. In most circumstances, the cells would lose the receptor expression after two to three passages. This was most probably due to the basal leaky expression of the receptor even under the doxycycline suppression. At the same time, I learned that different strains of MDCK cells (I or II) could be rather different from each other. A strain of MDCK II cells was obtained and the plasmid vector, pCDNA3-T7-hSSTR3, was transfected into the cells with FuGENE 6 transfection reagent and clones were selected with 600 μg/ml of G418 until the colonies appeared (about 10-12 days). Clones were picked and expanded before screening with immunocytochemistry. Surprisingly, several clones were found to contain 30-40 % cells expressing the receptor. One clone (T7-hSSTR3-12) was selected for further sub-cloning by selecting the cells at very low density. After several days in culture, clones were again picked and expanded before screening with immunofluorescence. One clone (T7-hSSTR3-12-16) was found to have about 50% MDCK II cells transformed with the T7-hSSTR3 receptor (Figure 3.17). A detailed immunofluorescence study of this line showed that cytotoxicity of this receptor continued to kill certain number of cells in every passage of the clone; also, different cells expressed a varying amount of the receptor. Nonetheless, the hSSTR3 receptor was detected at the cell-cell junction and overlapped with the MUPP1 immunofluorescence signals (merged; Figure 3.17).

At the same time, the fusion receptor construct, pCDNA3-T7-mSSTR5-hSSTR3-C, was also transfected into the MDCK II cells since this receptor was not apoptotic in HEK293 cells. After 10 days in selection medium, clones were picked and screened. Several clones were found to have a rather high percentage of cells expressing the fusion receptor. A clone, T7-mSSTR5-hSSTR3-C-15, with 90-95 % of cells expressing the fusion receptor was selected for further functional and immunofluorescence studies. Results from the serial XY sections and the XZ section with confocal microscopy showed that the fusion receptor co-localized with the tight junction protein, MUPP1 at the tight junction, as shown in the XZ section of confocal images (Figure 3.18).

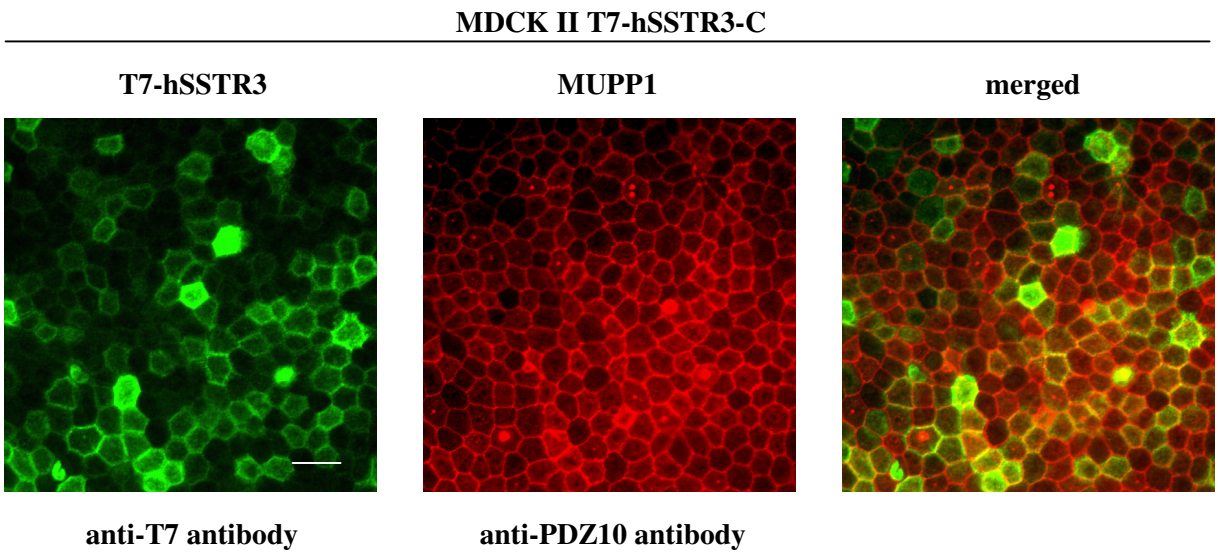

Figure 3.17 Localization of hSSTR3 and MUPP1 in MDCK II stable cell line
Polycarbonate filter-grown hSSTR3 expressing stable MDCK II cells were fixed and stained with anti-T7 and anti-PDZ10 antibodies for the receptor and the MUPP1 respectively. Images were obtained with fluorescence microscopy and processed in Adobe Photoshop. Scale bar, 20µm.

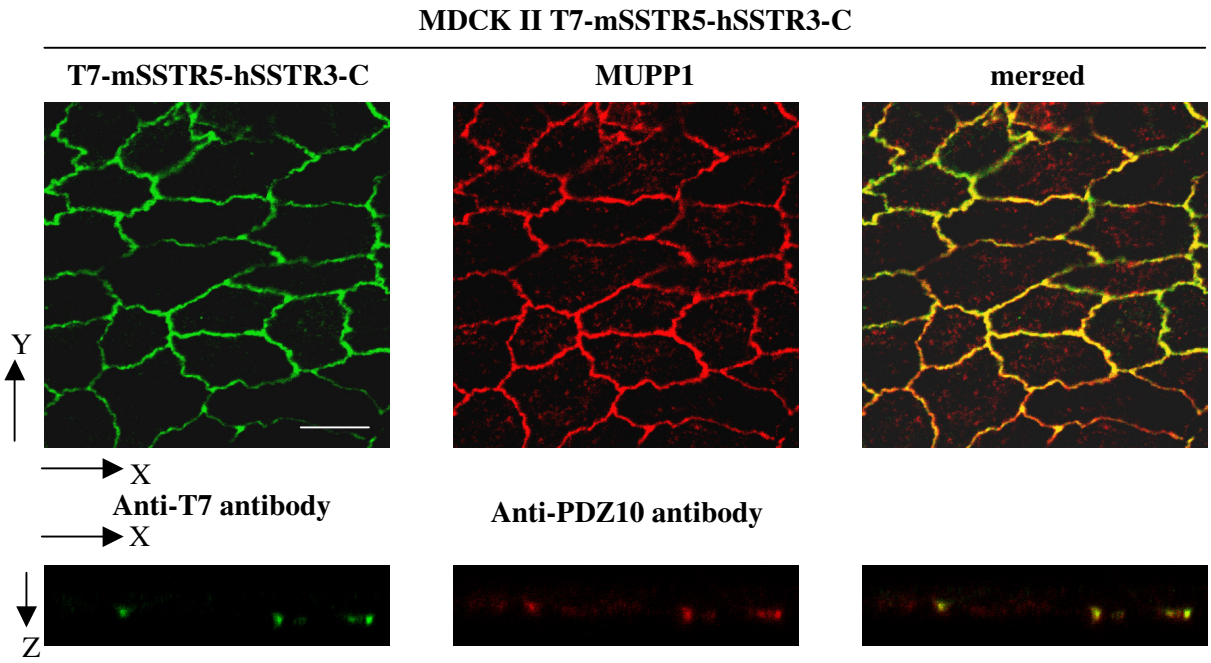

Figure 3.18 Localization of T7-mSSTR5-hSSTR3-C fusion receptor in MDCK II stable cell line
The MDCK II fusion receptor (T7-mSSTR5-hSSTR3-C) stable cell line was grown on polycarbonate transwell filters, fixed, and stained with anti-T7 and anti-PDZ10 antibodies for the fusion receptor and the endogenous MUPP1 protein, respectively. Serial XY sections and XZ section were obtained with confocal microscopy and processed with Photoshop. A representation of the corresponding XY sections are shown. Scale bar, 10 µm.

In addition, fusion receptor expressing cells were also fixed and stained at different stages of confluency to investigate the localization of both the fusion receptor and MUPP1 during the tight junction formation. The results in Figure 3.19 show that the fusion receptor co-localized with MUPP1 in cells with readily formed tight junction. However, at the leading edge of the monolayer, localization of MUPP1 to tight junction seems to precede the receptor (arrows).

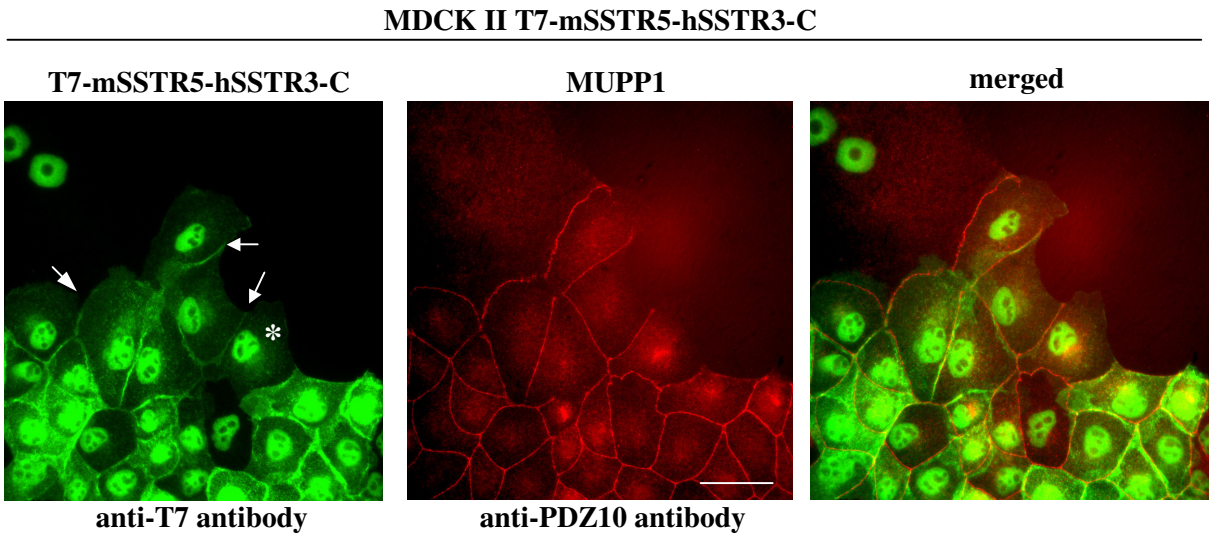

Figure 3.19 Localization of fusion receptor in MDCK II cells forming the TJs
Polyester filter-grown fusion receptor expressing cells were fixed and stained with anti-T7 and anti-PDZ10 antibody at different stages of confluency to investigate the localization of the fusion receptor and MUPP1 during the process of tight junction formation. Localization of MUPP1 to tight junction seems to precede the receptor (arrows). '*' indicated the nucleus stained by the T7 antibody. Scale bar, 10 µm.

From the results presented so far, I demonstrated that the hSSTR3 receptor and the fusion receptor are associated with MUPP1 at tight junction. In order to investigate if the ability of tight junction targeting of the receptor is due to PDZ binding motif, a construct, pCDNA3-T7-mSSTR5-hSSTR3-8C, where the PDZ binding motif was deleted, was constructed and the stable cell line of this mutant fusion receptor was made in MDCK II cells as described previously. As shown in Figure 3.20, immunofluorescence results of this stable cell line demonstrated that the truncated fusion receptor is not present at the tight junction. This result suggests that localization of the hSSTR3 receptor depends on the interaction with the MUPP1 protein through its C-terminal PDZ binding motif.

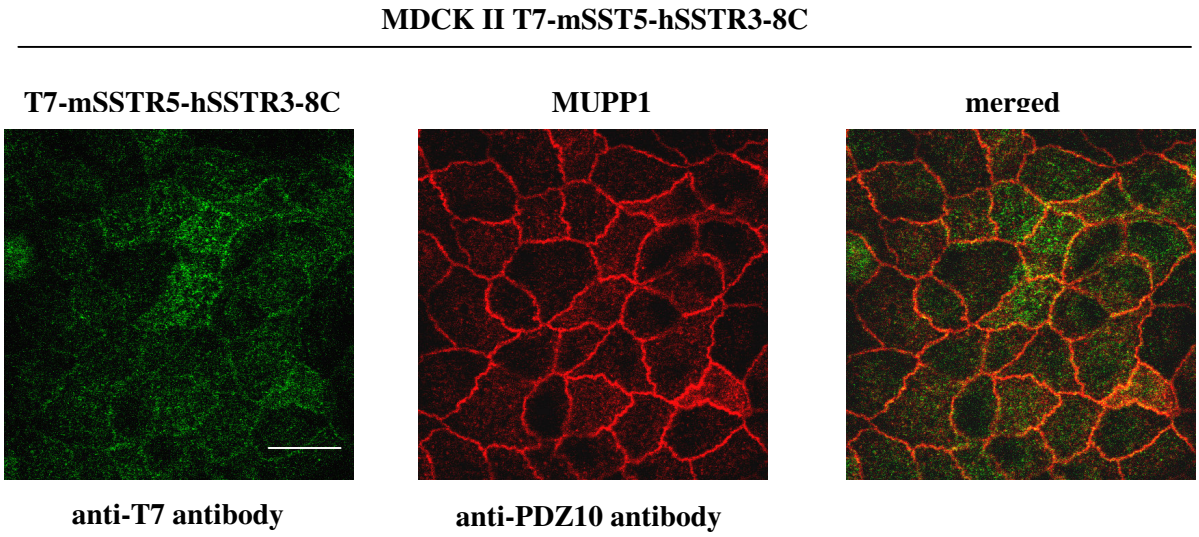

Figure 3.20 Localization of the truncated fusion receptor in MDCK II stable cell line
Polycarbonate filter-grown cells expressing the truncated fusion receptor were fixed and stained with anti-T7 and anti-PDZ10 antibodies. Serial XY sections were obtained with confocal microscope and processed with Photoshop. Representative of the corresponding XY sections were shown. Scale bar, 10 µm.

3.8 Functional Relevance of the Interaction between the Receptor and the TJ Protein, MUPP1

3.8.1 Regulation of the TJ Integrity in the MCF7-hSSTR3 Stable Cell Line

From the results gathered so far, we know that the receptor is targeted to the TJ by interaction with MUPP1 protein in MCF-7 and MDCK II epithelial cells. What could be the function of the receptor at the tight junction of epithelial cells? Several heterotrimeric G proteins such as Gαi2, Gαo and Gαs are localized at the tight junction of MDCK cells (De Almeida et al., 1994; Denker et al., 1996; Dodane & Kachar, 1996; Hamilton & Nathanson, 1997). Regulation of the junctional complex by heterotrimeric G proteins was suggested in early pharmacological experiments (Balda *et al*., 1991), and subsequent studies have demonstrated that pertussis toxin-sensitive G proteins affect the tight junction assembly and the baseline properties (Denker *et al*., 1996; Saha *et al*., 1998).

In order to investigate the potential function of the receptor at the tight junction, the receptor stable cell line, MCF7-hSSTR3-0.5B4, as well as the wild type MCF-7 cells were grown on transwell filters over a period of time to allow the cells to become fully polarized. 1 x 10^5 cells were first seeded onto each pre-equilibrated 12 mm filter with a pore size of 0.4 µm, and the growth as well as the confluency of cells were monitored daily by measuring the

transepithelial electric resistance (TER). As shown in Figure 3.20, the extent of monolayer formation of the wild type and transformed MCF7 cells was monitored by measuring the TER of the monolayer on the transwell filter. Typically, the TER of the monolayer rose steadily over several days after the cells were seeded, the increasing TER reflects the growing and spreading of the cells as well as the formation of the TJ. Normally the resistance of the cells stabilized after about one week in culture. The stably formed monolayer could then be used for agonist or inhibitor treatment.

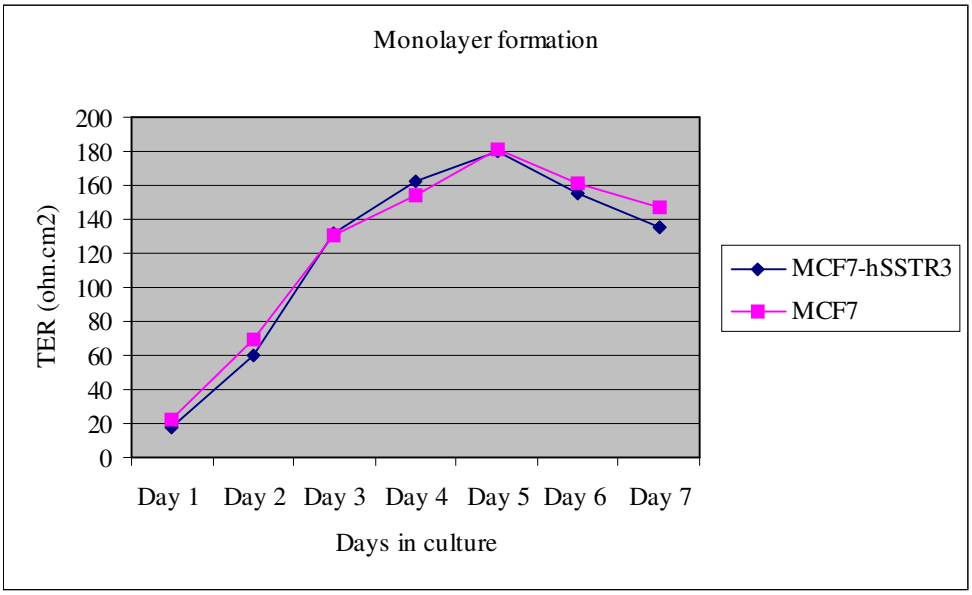

Figure 3.20 Growth curves of the wild type and transformed MCF7 cells
Wild type and stably transfected cells were grown on transwell filters. Extent of the monolayer formation was monitored by the level of the electrical resistance (TER), which directly reflects the extent of TJ formation between cell-cell contact sites.

After the monolayers of the wild type and the hSSTR3 transfected MCF7 cells were formed and stabilized, the hSSTR3 receptor was activated by addition of 1 µM of SST14 agonist and incubated at 37°C for 30 min. The treated as well as untreated samples were measured for their electrical resistance across the cell monolayer. Results obtained from two independent experiments in triplicate of corresponding samples were averaged and plotted in Figure 3.21. The transepithelial electrical resistance of the MCF7-hSSTR3-0.5B4 cell monolayer was reduced by 27.2% after treatment with receptor agonist, SST14 (Figure 3.21A). This reduction of TER was highly significant compared to the untreated paired samples of the same cell line. A significant reduction of the TER of the wild type MCF-7 was also observed after a 30 min treatment of the monolayer with SST14 agonist, which was probably due to the

endogenous hSSTR3 receptor in wild type MCF-7 cells. The agonist effect on the MCF7-hSSTR3-0.5B4 monolayer was completely abolished by overnight pre-incubation of the cell monolayer with 500 ng/ml of pertussis toxin (PTX), an inhibitor of Gαi and Gαo (Figure 3.21B).

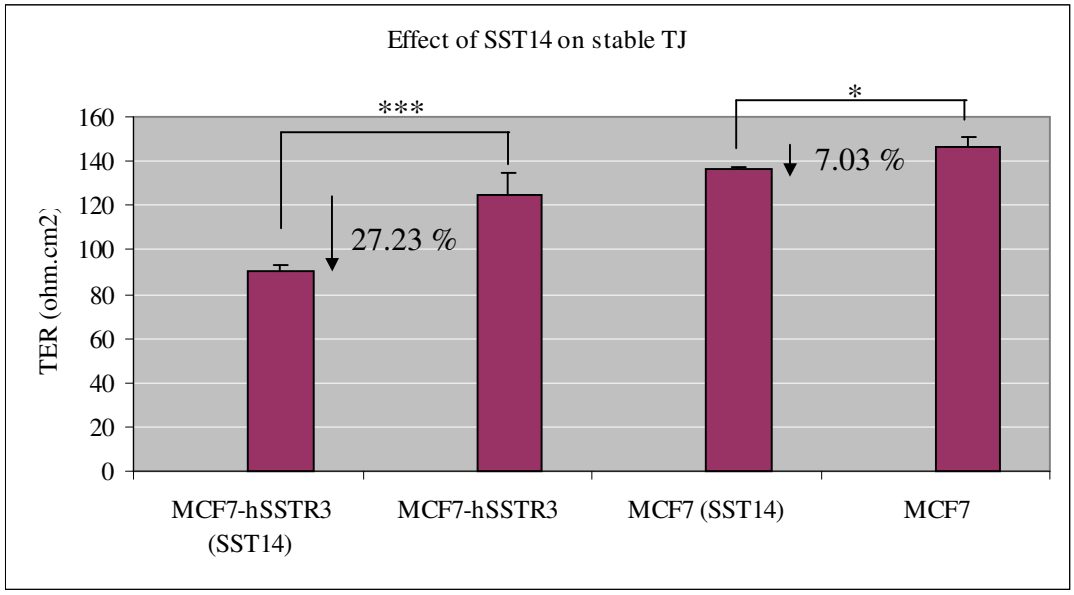

(A)

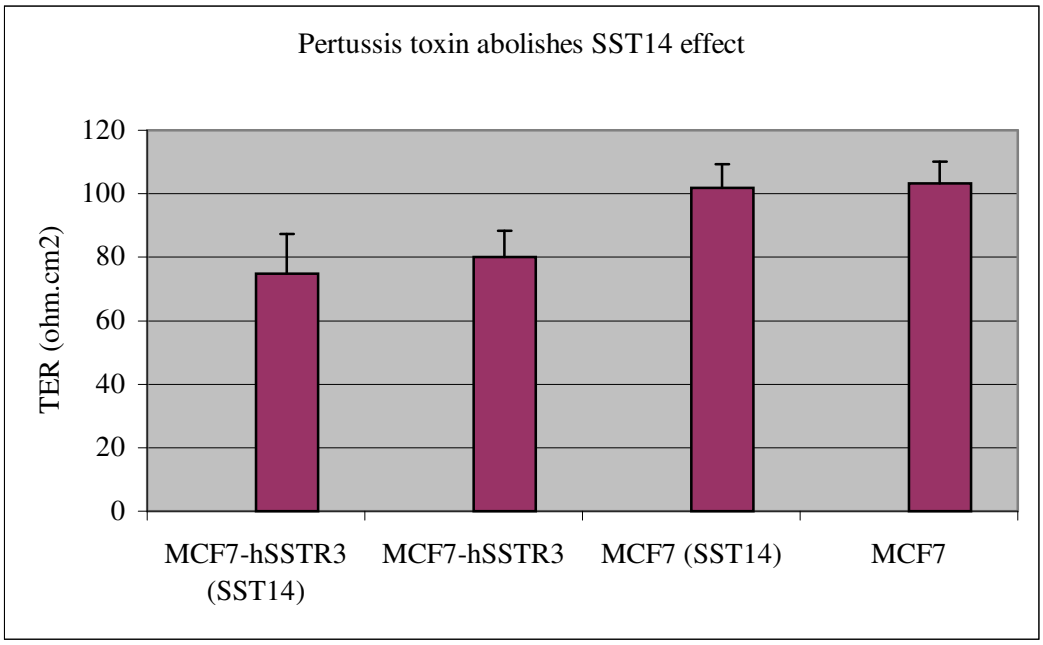

(B)

Figure 3.21 Effect of SST14, on both wild type and stably transfected MCF7 cells

(A) Cells were grown on transwell filters as in 3.20; the TER was measured after 30 min treatment of the cells with 1μM of SST14. The data presented are the mean ± S.D. n = 6. *, $p < 0.05$; ***, $p < 0.001$.
(B) The cells were grown and treated as in (A), but PTX (500 ng/ml) was added 16-18 hour prior to measurement. The values presented are mean ± S.D. n = 6.

The results indicated that activation of the hSSTR3 receptor in MCF-7 cells affects the integrity of the tight junction. Could activation of the receptor also negatively regulate TJ biogenesis? In order to find this out, the agonist was introduced into the growth medium during the establishment of the cell monolayer. The agonist was added to the medium one day after the cells were seeded onto the transwell membrane, and fresh agonist was added daily into the growth medium. The tight junction formation was monitored everyday by measuring the transepithelial electrical resistance of the monolayer. Results in Figure 3.22A show that the tight junction formation of wild type MCF-7 was relatively unaffected by the presence of SST14 in the growth medium. However, the tight junction formation of the MCF7-hSSTR3 stable cell line was significantly slower compared to the untreated counterparts (Figure 3.22B).

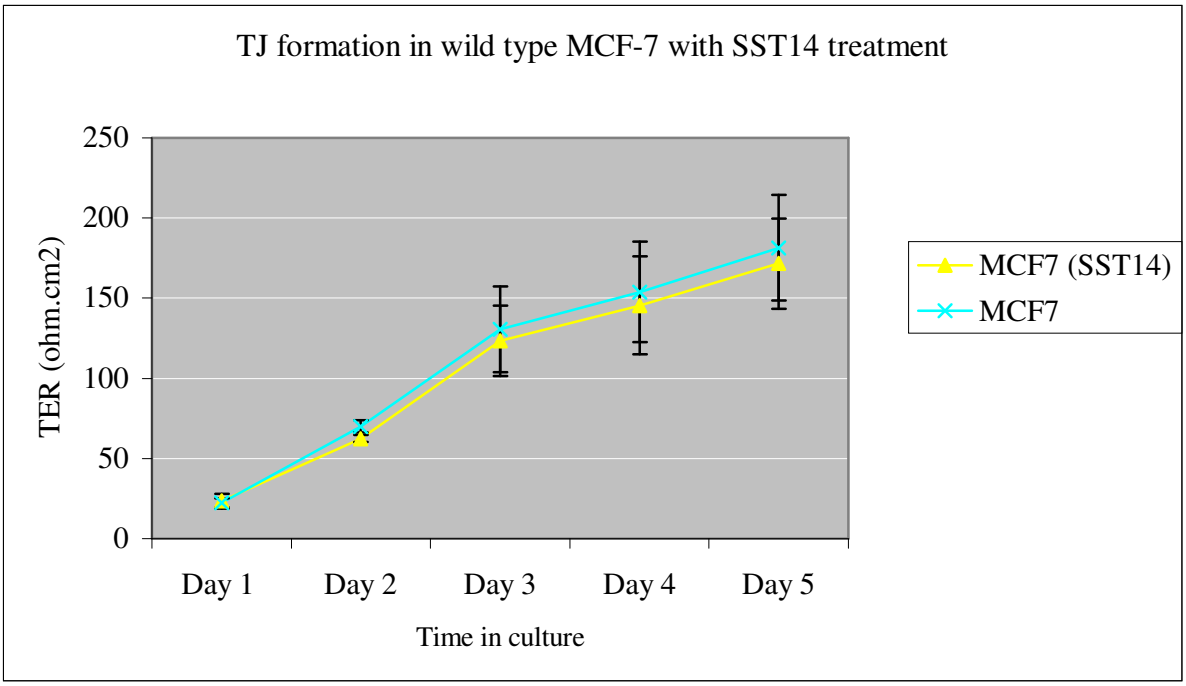

(A)

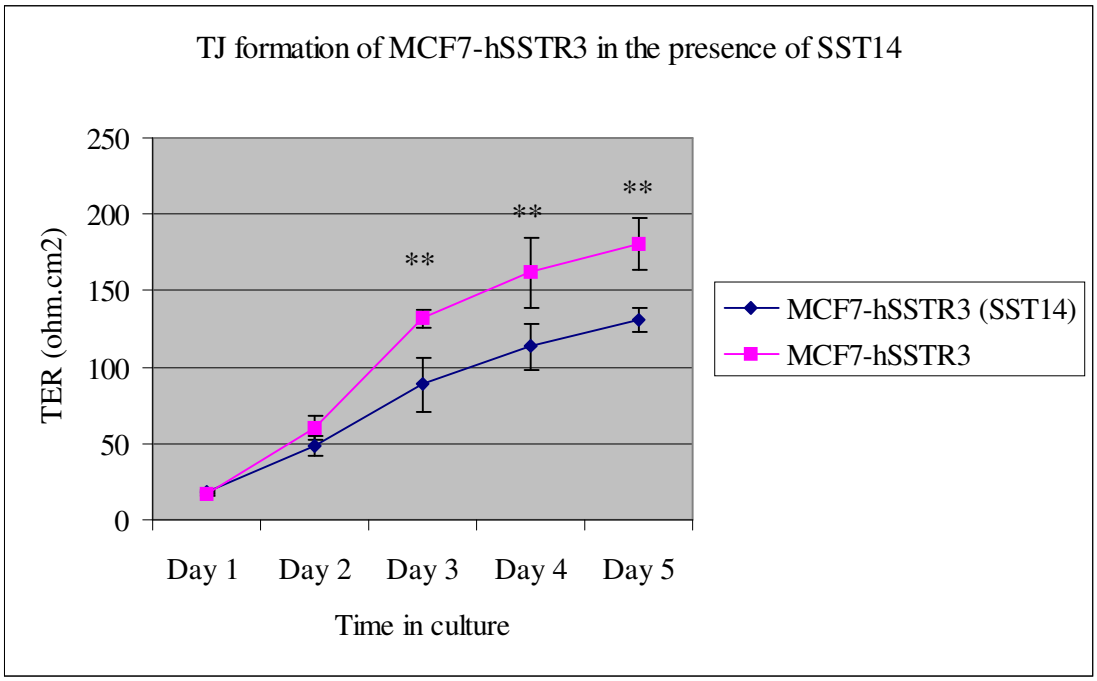

(B)

Figure 3.22 Effect of SST14 on tight junction formation
(A) Agonist SST14 was added to the growth medium daily one day after the wild type MCF-7 cells were seeded onto the transwell membranes and the TERs of the respective monolayer were measured everyday. n = 6.
(B) Stably transfected MCF7-hSSTR3 cells were grown, treated and monitored as in (A). n = 6; **, $p < 0.01$.

In order to confirm these results in a different experimental paradigm, a calcium switch assay was performed on both the wild type and stably transfected MCF-7 cell lines. Calcium is essential for the maintenance of the adherent junction, which in turn controls the integrity of the tight junction. Upon depletion of extracellular calcium ions, both the adherent and tight junctions are disrupted. For these experiments, cells were again grown on transwell filters. After a tight monolayer was formed, cells were washed twice with PBS buffer and placed in serum-free low calcium DMEM for 1 h at 37°C before the TER was again measured to monitor the extent of TJ disruption. After this, the calcium was replaced with DMEM containing 10 % FBS (normal calcium medium: 1.8 mM [Ca^{2+}]) with or without the SST14 agonist. TER was measured at various time points after the calcium switch.

15.5 hr after the calcium switch, TER of both the agonist treated wild type MCF-7 and the MCF7-hSSTR3 monolayer were found to be significantly lower than that of the untreated corresponding samples. At the subsequent time points, only the TER of the agonist treated MCF7-hSSTR3 cells was found to be significantly lower than the untreated samples. The

effect of SST14 on the wild type MCF-7 monolayer seemed to diminish over time (Figure 3.23).

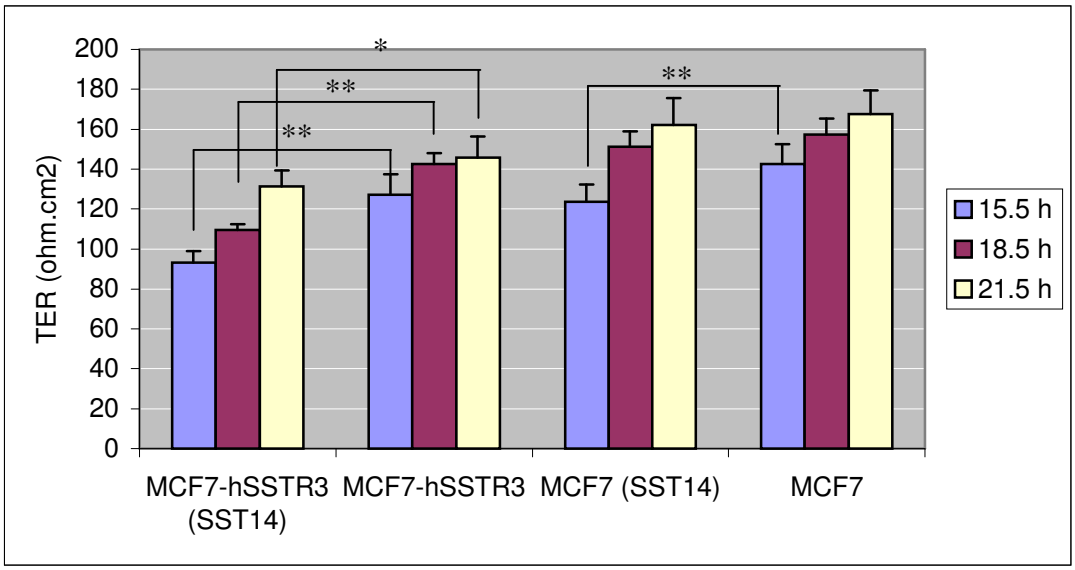

Figure 3.23 Effect of SST14 on tight junction biogenesis after calcium switch assay
Cells were grown on transwell filters until a tight monolayer was formed. The cell junctions were disrupted by incubation in low calcium medium and reformed by calcium replenishment with normal medium with or without SST14 (1µM). TERs were measured after the calcium switch at the time points indicated. Data presented are the mean ± S.D. n = 6. *, $p< 0.05$; **, $p< 0.01$.

3.8.2 Regulation of the TJ Integrity in MDCK II Stable Cell Line

So far, we have seen the regulatory effect of the hSSTR3 on tight junctions in MCF-7 cells. However, the MCF-7 cells might not be the ideal cell line to elucidate the exact mechanisms of tight junction regulation by the receptor, because there is endogenous expression of the receptor in MCF-7, it would be impossible to have a receptor free background. Furthermore, up to this point only few studies have been done on MCF-7 cell lines regarding the tight junction regulation. Therefore, it was necessary to verify the results obtained so far in another standard epithelial cell line, namely MDCK cells.

The lack of endogenous expression of canine SSTR3 receptor in MDCK II cells was verified by RT-PCR using the canine SSTR3 specific primers (data not shown). The stable cell lines established as discussed in section 3.8.3. were grown on the transwell filters for transepithelial electrical resistance measurement. Further experiments were done only on the confluent cell monolayer, which was confirmed by stable TER values.

As it has been done for MCF-7 cells, the agonist SST14 for wild type hSSTR3 or agonist SST28 for the fusion and truncated fusion receptor were added apically onto the

MDCK II monolayers, followed by 30 min incubation at 37°C. SST28 was used in this case for the fusion and truncated receptor because it has a higher affinity for SSTR5 than SST14 (Kreienkamp *et al*., 1997). Thereafter, the TER of the monolayer was measured. Surprisingly, no effect was observed in all the tested wild type and stable cell lines even after overnight incubation with the agonist. In addition, no effect was observed when the agonist was added to the monolayer basolaterally. These could probably be due to the inaccessibility of the receptor located at the tight junction.

In order to make the receptor accessible, the calcium switch assay was used where the junctions were first disrupted (receptor becomes accessible to the agonist) and then allowed to reform in the presence of normal calcium concentration. After the calcium switch, cell monolayers were allowed to recover and the electrical resistances of the monolayers were measured at various time points.

As shown in Figure 3.24(A), 15 h after the calcium switch, the TER of agonist treated MDCK II T7-mSSTR5-hSSTR3-C and MDCK II T7-hSSTR3 cell monolayers were significantly higher than the untreated counterpart. The high TER values induced by SST treatment diminished quickly over time (Figure 3.24B). No significant difference in TER value were recorded for treated and untreated monolayers of both the wild type MDCK II and the truncated fusion receptor, T7-mSSTR5-hSSTR3-8C. These results illustrate that the effect induced by the SST is mediated by the activation of the transfected receptor in MDCK II cells and furthermore the effect of the receptor depends on interaction with MUPP1 and localization at the tight junction.

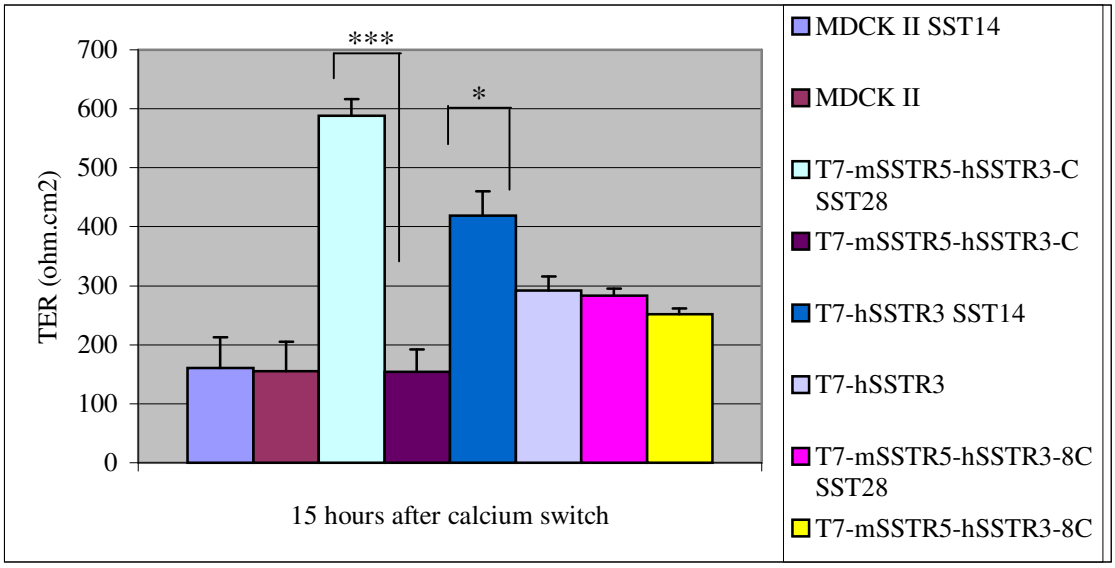

(A)

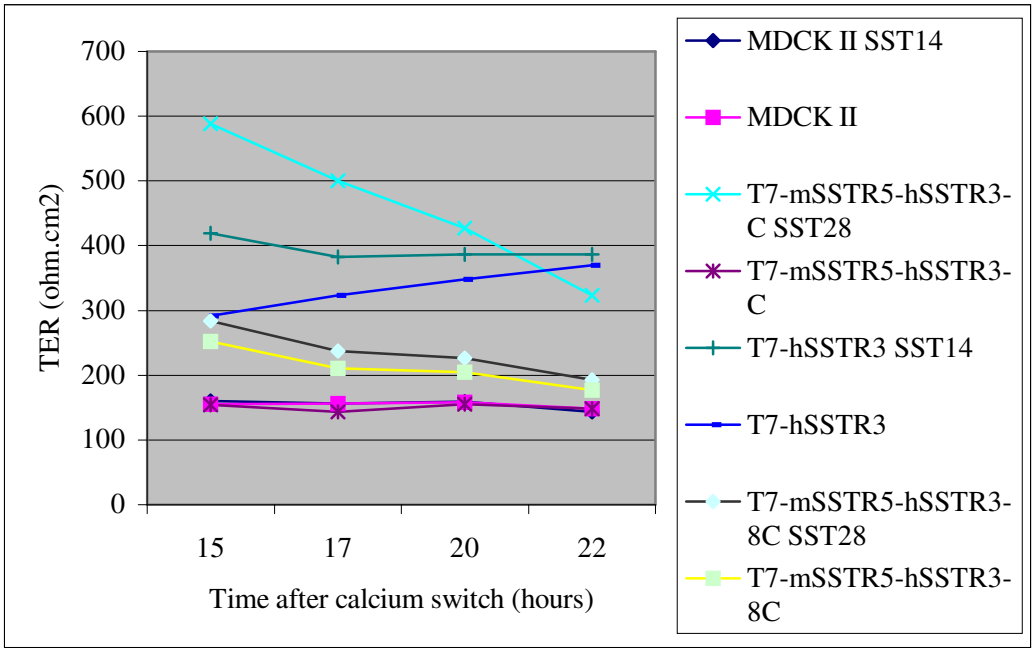

(B)

Figure 3.24 Effect of somatostatin agonist on tight junction biogenesis in MDCK II cell lines
Cells were grown and the calcium switch assay was done as in 3.23. (A) TERs were measured 15 hour after the calcium switch. Data presented are the mean ± S.D. n = 6. *, $p < 0.05$; ***, $p < 0.001$. (B) TERs were measured after the calcium switch at the time points indicated.

So far, the effects of agonist treatment on tight junction biogenesis observed in MDCK II cell lines are contradictory to those seen in the MCF-7 derived cell lines (Figure 3.23). In order to investigate this discrepancy, a calcium switch assay was again performed on the MDCK II and MDCK II fusion receptor cell lines, however this time the recovery of the tight junction was monitored at earlier time points. The stable MDCK II cell line expressing the wild type hSSTR3 receptor was omitted in the following study, because more than 50% of the cells no longer expressed the receptor, which would complicate interpretation of the results.

As described previously, the cell-cell junctions were first disrupted by removing the extracellular calcium. Upon re-addition of the extracellular calcium with or without the agonist, the tight junction recovery was monitored every two hours by measuring the electrical resistance across the monolayer.

Different sets of cells were used for measurement for different time points, as the removal of the cells from the incubator every two hours for measuring was shown to slow down the overall recovery process. As shown in Figure 3.25, the data obtained clearly demonstrates that the earlier the cells were removed from the incubator during the process of tight junction recovery, the greater the effect on the overall recovery process. For example, the mSSTR5-

hSSTR3-C SST28 (10 h) cells recover faster, but have a lower TER than mSSRTR5-hSSTR3-C SST28 (8 h) cells. In other words, the slower the initial recovery process (2-10 h), the greater the TER values observed at the later time point (23 h).

Different sets of cells were cultured for measurement at different early time points. Surprisingly, agonist treatment seems to significantly retard the tight junction recovery of the MDCK II cells expressing the fusion receptor compared to untreated cells at the early phase after calcium switch (Figure 3.26). However, the electrical resistance of the agonist treated cells also seems to rise rapidly at a later phase of recovery resulting in a much higher TER as seen previously (Figure3.24B). Furthermore, the TER level of untreated fusion receptor MDCK II cells was consistently lower than the wild type MDCK II cells.

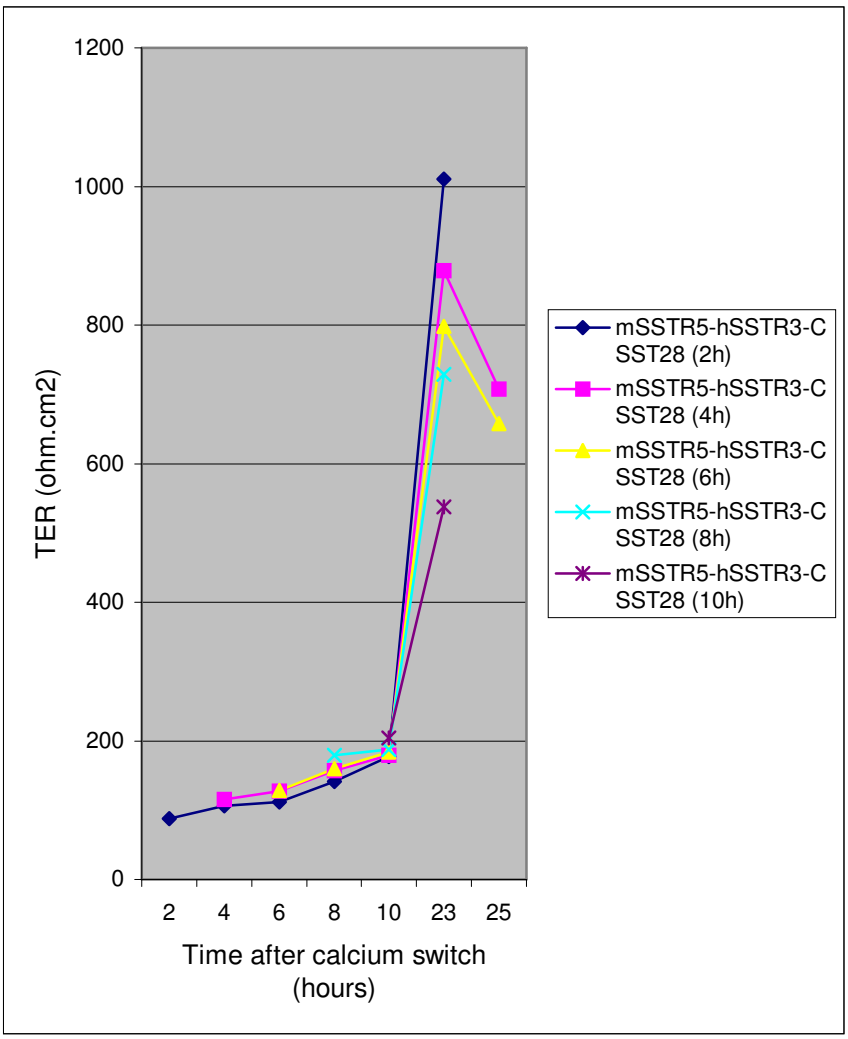

Figure 3.25 Effect of change in incubation conditions on tight junction recovery after calcium switch in MDCK II cells expressing the fusion receptor

Different sets of cells were grown and the calcium switch assay was performed as in 3.23. SST28 (1 µM) was added to the medium and the TER was measured at the time points indicated.

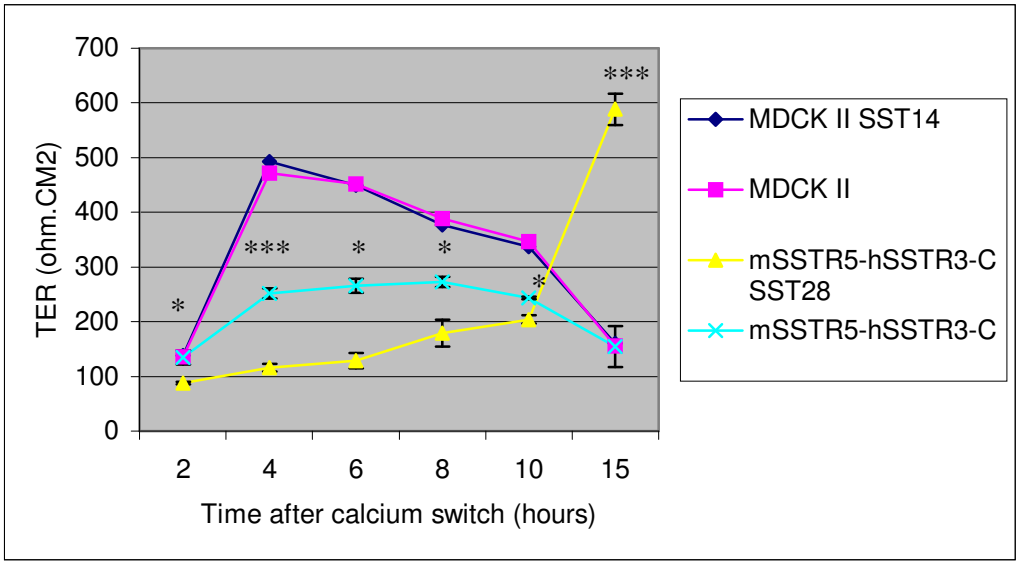

Figure 3.26 Effect of agonist treatment on MDCK II fusion receptor cells at early recovery phase after calcium switch
Cells were grown and the calcium switch assays were performed as in 3.23. The TER was measured every two hours after the re-addition of calcium. Different sets of samples were used for different time points. Data presented are the mean ± S.D. n = 3. *, $p < 0.05$; ***, $p < 0.001$.

3. 9 Biochemical Analysis of Wild Type and Stable MDCK II Cell Line after Calcium Switch Assays

From the results of the calcium switch assays on the MDCK II T7-mSSTR5-hSSTR3-C cell line, we now know that the agonist treatment leads to a change in the biogenesis of the tight junction. Could this change in tight junction biogenesis result from a change in the tight junction protein composition? Which signaling pathway mediates this effect of somatostatin receptor?

For this purpose, a set of cells expressing the fusion receptor and MDCK II wild type cells were treated with the calcium switch paradigm, followed by SST28 as above. After recording TER at the late time point (Figure 3.27A), cells were lysed with RIPA buffer on ice for 15 min and insoluble materials were removed by centrifugation. The total protein content of each sample was quantified. Equal amounts of protein for each sample were then analyzed by Western blotting with antibodies against various tight junction transmembrane proteins (claudin-1, -2, -3 and -4) and plaque proteins (MUPP1, ZO-1 and ZO-2) as well as MAPK (p44/42 ERK) antibodies. An α-tubulin antibody was used as loading control for each sample. Results of the Western blots (Figure 3.27B) showed that the amount of claudin-1, -3

and -4; MUPP1; ZO-1 and ZO-2 were found to be relatively unchanged in both the agonist treated and untreated wild type MDCK II, as well as the mSSTR5-hSSTR3-C stable cell line. Claudin-2 was found to be selectively reduced in cells in which had been treated with agonist whereas no change for claudin-2 was seen in wild type MDCK II control samples. The presence of claudin-2 at the tight junction has been shown to convert the 'tight' tight junction (high TER) to 'leaky' tight junction (low TER) (Furuse *et al.*, 2001). Besides the change in claudin-2 level, p44/42 ERK was found to be phosphorylated in agonist treated, fusion receptor expressing MDCK II cells compared to untreated cells and the wild type MDCK II control. The total amounts of the phosphorylated and unphosphorylated p44/42 ERK in the samples were shown to be equal.

(A)

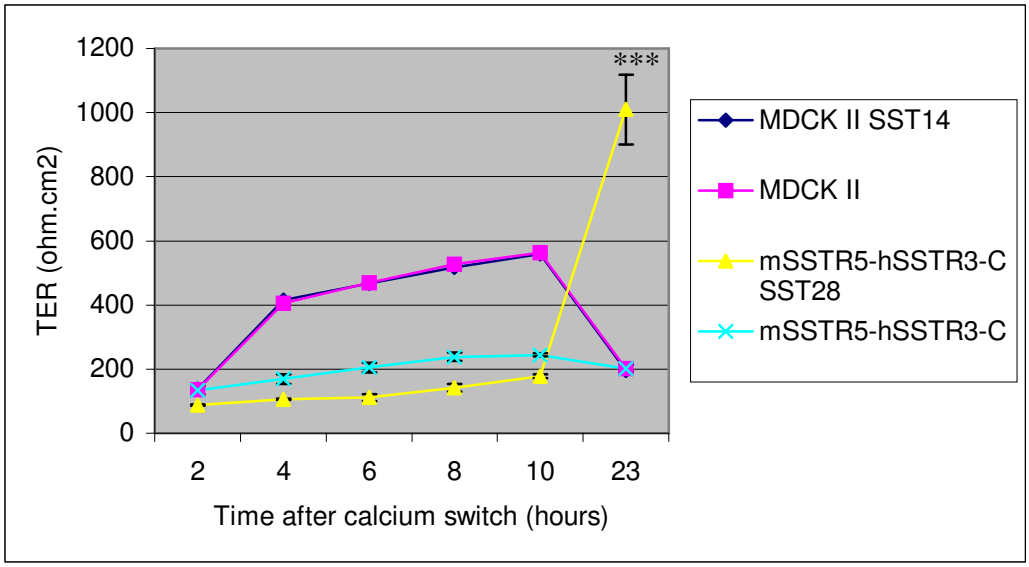

(B)

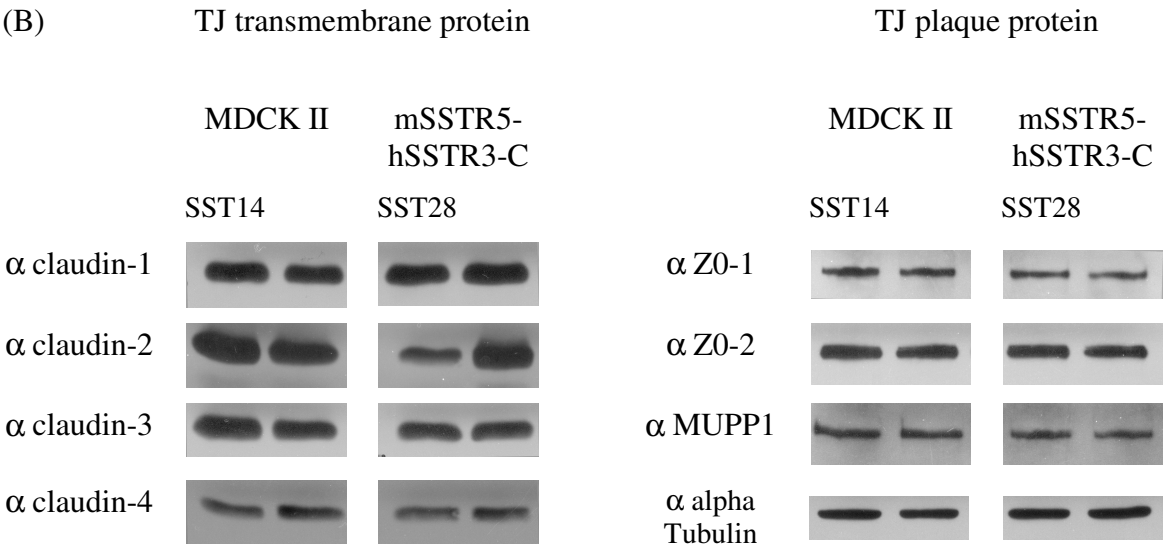

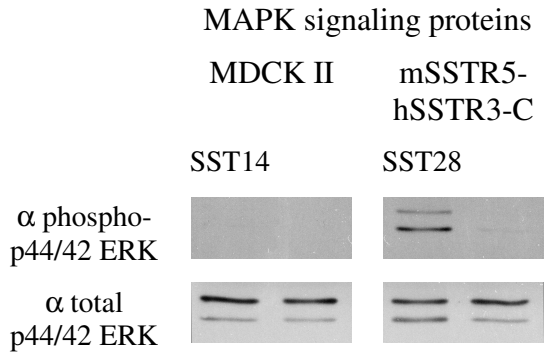

Figure 3.27 Tight junction and signaling proteins analysis in wild type and mSSTR5-hSSTR3-C expressing MDCK II cells
Wild type MDCK II cells and those expressing the fusion receptor were subjected to calcium switch and recovery with treatment of SST. After measurement of TER at the late time point (A) cells were lysed and subjected to Western blotting with the antibodies indicated (B). Data presented are the mean ± S.D. n = 3. ***, $p < 0.001$.

Now we know that levels of the tight junction protein claudin-2 are selectively reduced after agonist treatment at the late time point. So, what happens to the tight junction protein at a much earlier time point after the calcium switch; furthermore, could the reduction of claudin-2 result from the activation of heterotrimeric G-proteins upon activation of the fusion receptor? In order to investigate these issues, samples were monitored for their recovery of the electrical resistance every two hours after the calcium switch. At the same time, different sets of samples were cultured under the same conditions and treated with inhibitors of Gαi/o proteins (pertussis toxin, PTX), MAP kinase (MEK1/2, U0126), 26S proteasome (MG-132), protein synthesis (cycloheximide) and RNA synthesis (Actinomycin D) in order to elucidate the possible pathway mediating the effects seen by the agonist treatment. The monolayer was incubated overnight with PTX (400 ng/ml) prior to the calcium switch assay on the following day. The same concentration of the toxin was used in the low calcium medium when the cell junctions were disrupted as well as in the normal medium after the calcium switch. The inhibitors U0126, MG-132, cycloheximide and Actinomycin D were used at a concentration of 2 μM, 10 μM, 10 μg/ml and 1 μg/ml respectively in the low calcium medium and the normal calcium medium before and after the calcium switch.

As shown in Figure 3.28, all fusion receptor monolayers were activated with the agonist except the mSSTR5-hSSTR3-C (PTX) sample, which was treated only with PTX. All samples treated with agonist were also treated with various inhibitors except the control sample. TERs of the monolayers were monitored every two hours after calcium switch. As shown, inhibition of Gαi/o proteins by PTX could partially reverse the effect exerted by the

agonist treatment. The increase in TER of the agonist/PTX treated samples was significant compared to the control sample treated with agonist only. The MEK inhibitor only very slightly increase of TER recovery compared to the untreated control. Inhibitors MG-132, cycloheximide and Actinomycin D did not affect the inhibition of TER recovery caused by the agonist.

After the TER measurements, some samples from different time points were also lysed in RIPA buffer for analysis by Western blotting with various antibodies. As shown in Figure 3.29, the agonist-induced reduction in claudin-2 levels starts as early as two hours after the calcium switch. In addition, p44/42 ERK was shown to be phosphorylated upon agonist treatment. No changes were found for the rest of the tight junction proteins tested in this study when comparing agonist treated and untreated samples. Pertussis toxin pretreatment was shown to be able to block the agonist-induced claudin-2 reduction as well as the ERK activation. Taking these results together, it seems clear that agonist-induced retardation of TER recovery in the fusion receptor MDCK II stable cell line was due to the combined effect of G-protein activation and other as yet unidentified mechanisms.

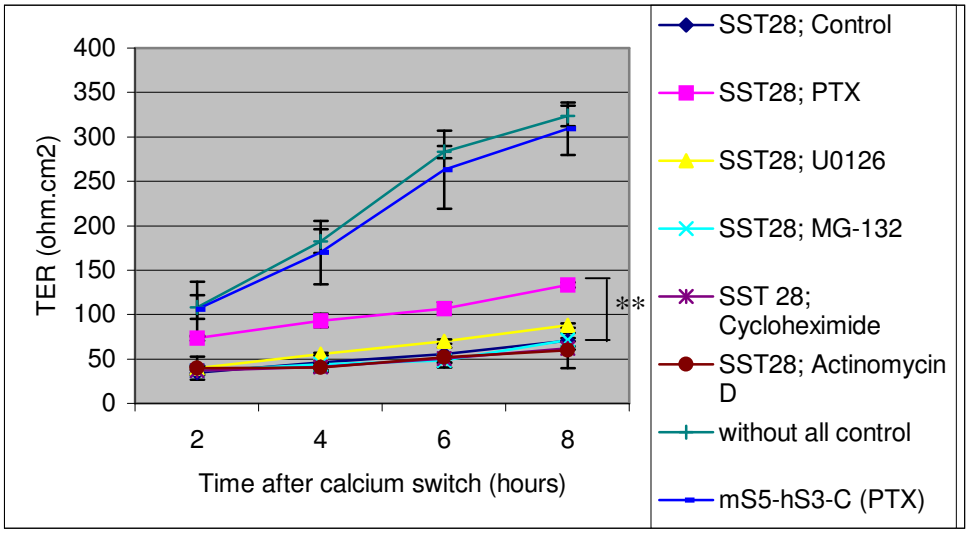

Figure 3.28 Effects of inhibitors on SST regulation of TER at the early phase of recovery
Cells expressing the fusion receptor were subjected to calcium switch and recovery with treatment by SST28 alone or SST28 with the inhibitors indicated. TER was measured every two hours after the calcium switch. Data presented are the mean ± S.D. n = 6. **, $p < 0.01$.

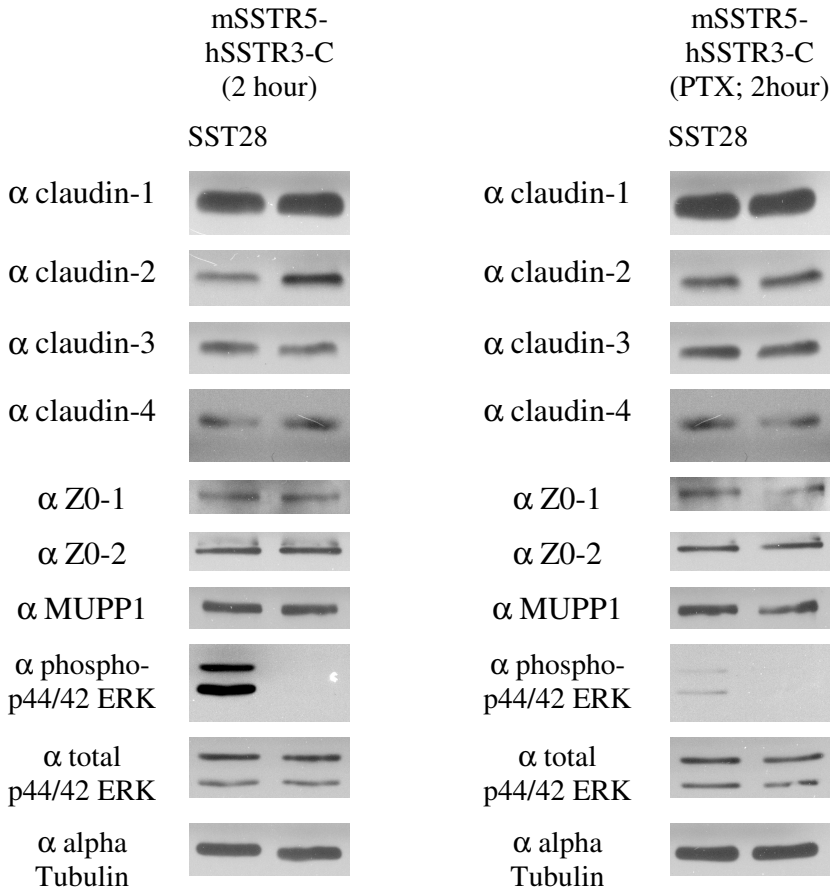

Figure 3.29 Western blot analysis of tight junction and signaling proteins of fusion receptor stable MDCK II cell line 2 hours after calcium switch assay
Cells expressing the fusion receptor were subjected to calcium switch and recovery; as well as treatment with SST28 alone or SST28 with the PTX. After measurement of TER at the early time point, cells were lysed and subjected to Western blotting with the antibodies indicated.

Results of the electrical resistance measurements after the calcium switch at the later time points (23 hour and 25 hour; Figure 3.30) showed that in the presence of agonist, the MEK1/2 inhibitor (U0126) significantly reduced the increase of TER compared to the samples without inhibitor. Similarly, the TER of the PTX treated samples also showed a significantly lower TER compared to the untreated control. Interestingly, both the 26S proteasome inhibitor (MG-132) and the inhibitor of protein synthesis (cycloheximide) completely blocked the increase in late phase TER previously shown to be induced by the agonist. The viability of the Actinomycin D treated monolayer deteriorated after 6 hours of incubation, so that the role of transcription could not be assessed. Taken together, G-proteins and MEK signaling seem to be involved in the agonist induced late phase TER increase. In addition, protein degradation was shown to determine the level of electrical resistance of the monolayer.

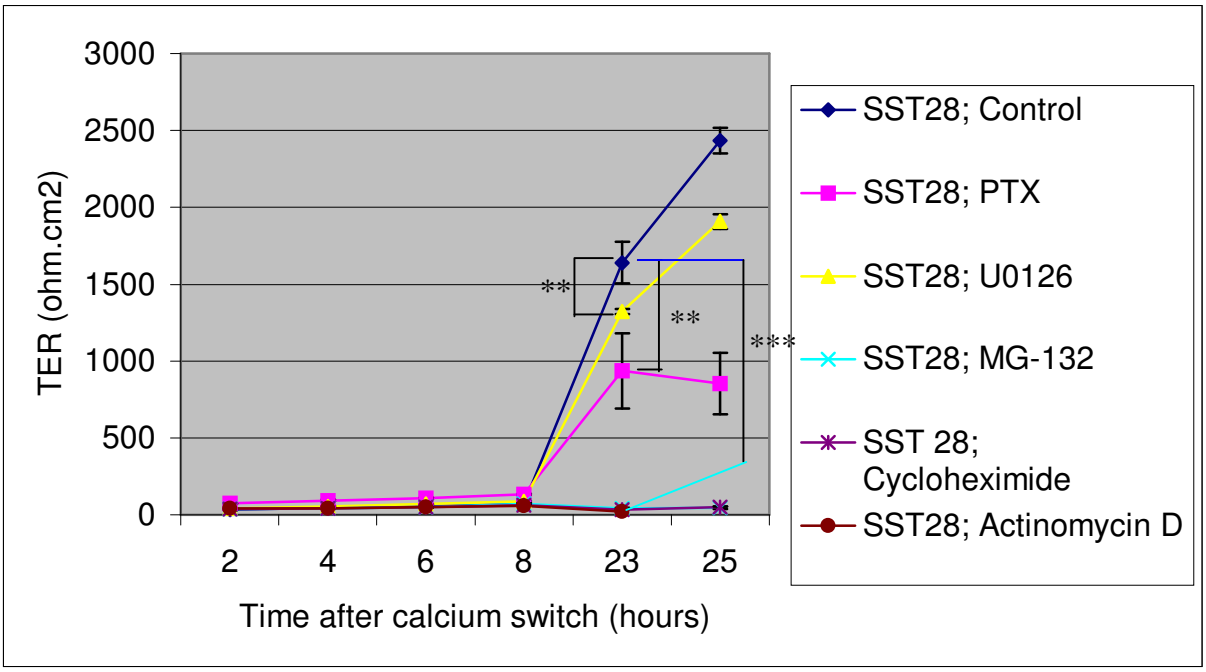

Figure 3.30 Effects of inhibitors on agonist treated fusion receptor expressing MDCK II cells
Fusion receptor expressing MDCK II cells were grown and subjected to calcium switch and recovery with SST28 alone or SST28 with the inhibitors indicated. TER was measured at the time points indicated after the calcium switch. Data presented are the mean ± S.D. n = 6. **, $p < 0.01$; ***, $p<0.001$.

The question now is whether this also corresponds to changes in the amount of tight junction proteins. First, I examined the amounts of claudin-2 at the later time point samples (23 hour) was examined since this protein has been shown previously to be reduced by agonist treatment (Figure 3.27, 3.29).

As shown in Figure 3.31, levels of claudin-2 are negligible in the samples treated with agonist only or agonist/U0126. This is evident even though there is less sample loaded, as shown by the loading control quantification (α-tubulin). There are only traces of claudin-2 in the samples of agonist/PTX and agonist/cycloheximide. In contrast, the amount of claudin-2 from the sample treated with the 26S proteasome inhibitor (MG-132) is comparable to the sample without agonist treatment. The amount of claudin-1 was shown to be reduced in the sample treated with cycloheximide but not in the samples treated with other inhibitors. Cycloheximide treatment generally affected the levels of all claudins tested. The amount of claudin-4 was selectively reduced by the treatment of MEK1/2 inhibitor in the presence of agonist.

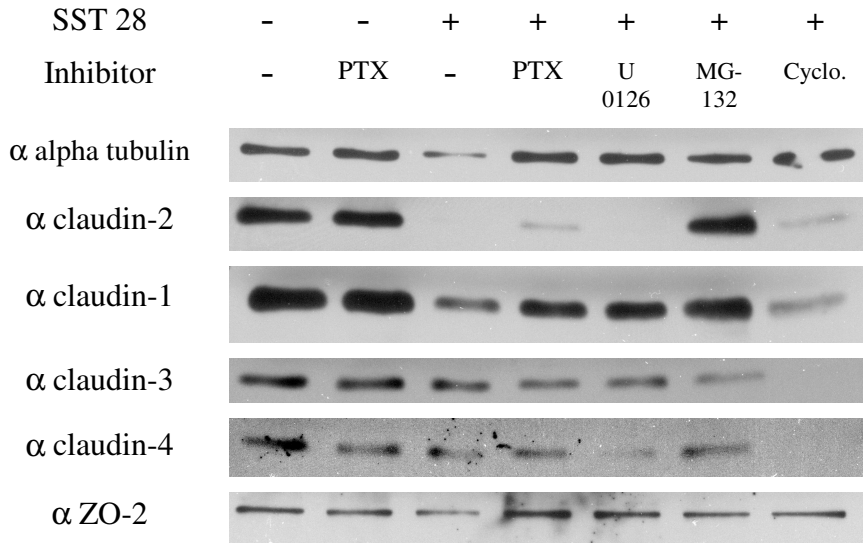

Figure 3.31 Western blot analysis of the effects of different inhibitors on tight junction proteins of fusion receptor expressing MDCK II cells 23 hours after the calcium switch assay
Cells expressing the fusion receptor were subjected to calcium switch and recovery with treatment by SST28 or/and inhibitors. After measurement of TER at the late time point, cells were lysed and subjected to Western blotting with the antibodies indicated.

CHAPTER FOUR DISCUSSION

Although the individual somatostatin receptor subtypes were cloned more than 10 years ago, their *in vivo* functions remain poorly understood. This is despite the recent development of subtype selective agonists and antagonists, subtype and species specific antibodies and the availability of the individual as well as double knock-out mice. Nonetheless, immunohistochemistry analysis using subtype specific antibodies revealed some striking differences in the localization of individual SSTR subtypes. The SSTR1 is primarily localized to axons, SSTR4 in dendrite, SSTR5 was found intracellularly in the AtT-20 cell line and SSTR3 was found at neuronal cilia in rodent brain (review in Schulz *et al*., 2000; Sarret *et al*., 2004). In order to further analyze factors which might affect targeting as well as signaling of SSTR3, we sought to identify interaction partners for the human SSTR3.

For this, a yeast-two hybrid screen was performed using the entire C-terminus of the hSSTR3 as a bait for 'fishing' out potential interaction partners from the human brain cDNA library. 3 putative candidates were isolated from the yeast-two hybrid screen namely MUPP1, BAIAP1 and PIST.

MUPP1, Multiple PDZ Domain Protein 1, is a tight junction protein containing 13 PDZ and one MRE (MAGUK recruitment element) domains for protein-protein interaction. Many interaction partners have been identified since it was first found to interact with the serotonin receptor 5-HT_{2C} (Ullmer *et al*., 1998), including tight junction proteins such as claudin-1, claudin-8, JAM1, Pals1 and CAR; the stem-cell factor receptor (c-kit); virus proteins such as adenovirus 9 E4-ORF1 and high-risk papillomavirus type 18 E6 and etc (review in González-Mariscal *et al*., 2003; Jeansonne *et al*., 2003, Coyne *et al*., 2004; Figure 4.1). BAIAP1 or BAP1, Brain Angiogenesis Inhibitor-Associated Protein 1, is the human homolog of MAGI-1 in rodent. BAIAP1 is also a tight junction protein containing 6 PDZ domains, 2 WW domains and a GK (guanylate kinase) domain (Shiratsuchi *et al*., 1998) for protein-protein interaction. On the other hand, PIST, PDZ Domain Protein Interacting Specifically with TC10, is a Golgi-associated protein containing one PDZ domain, two coiled-coil domain and a leucine zipper (Neudauer *et al*., 2001).

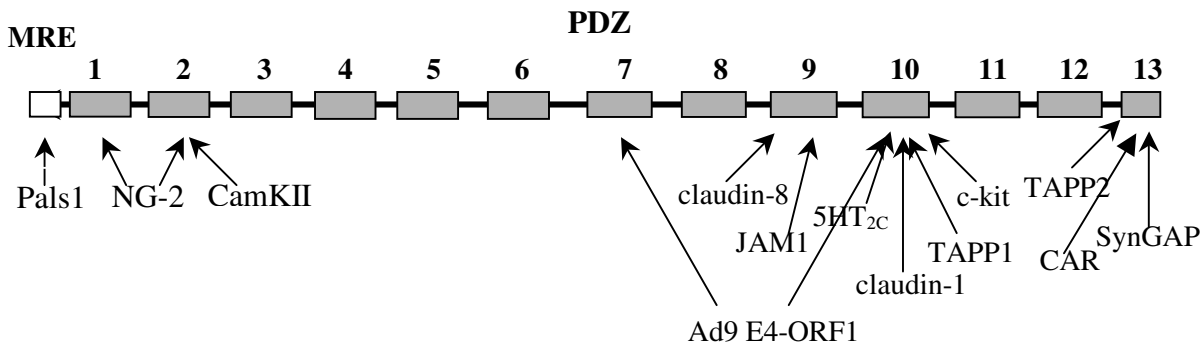

Figure 4.1 Domain structure and interaction partners of MUPP1
Interaction partners of MUPP1 identified so far since it was first described as an interaction partner of serotonin receptor, 5-HT_{2C}. Pals1: *p*rotein *a*ssociated with *L*in-7; NG-2: chondroitin sulfate proteoglycan; CamKII: Ca^{2+}/calmodulin-dependent kinase II; Ad9 E4-ORF1: adenovirus type 9 E4-ORF1; JAM1: *j*unctional *a*dhesion *m*olecule 1; $5HT_{2c}$: serotonin receptor $5HT_{2c}$; TAPP1&2: *ta*ndem *P*H-domain *p*rotein 1&2; c-kit: stem-cell factor receptor; CAR: *c*oxsackievirus and *a*denovirus *r*eceptor; SynGAP: *syn*aptic *G*TPase-*a*ctivating *p*rotein.

Subsequently, the interactions between the hSSTR3 and the interaction partners were shown to be mediated by the PDZ binding motif at the extreme C-terminus of the receptor. This interaction is completely disrupted by deleting the PDZ binding motif from the hSSTR3 C-terminus, providing an important tool for functional analysis. In addition, by using different deletion constructs of MUPP1, it was found that the PDZ domain 10 (PDZ10) was responsible for the interaction with the receptor. Interestingly, the rodent homolog of the SSTR3 was unable to interact with any of interaction partners isolated by the hSSTR3 owing to differences in the amino acid sequences of the respective PDZ binding motif. Interaction between the hSSTR3 with either MUPP1 or BAIAP1 was proven to be receptor subtype specific since no interaction was found between these proteins and the SSTR5, which was however found to interact with the PIST protein. Moreover, MUPP1 and BAIAP1 were never found in yeast-two-hybrid screen done in our laboratory with other receptor subtypes. I assumed that the tight junction proteins MUPP1 and BAIAP1 could function as a scaffolding molecule, which would localize the receptor to tight junction. PIST protein might be involved in the targeting of the receptor in the trans-Golgi network. As MUPP1 could target the receptor to a specific location which might determine the function of the hSSTR3 as well as the possibility that MUPP1 could function as a scaffolding proteins to plug in different proteins into a macromolecular complex, this protein was chosen for subsequent more detailed studies.

Altogether 16 clones of the MUPP1 cDNA were isolated from the yeast-two-hybrid screen, which account for more than 50 % of the total clones isolated from this screen. Sequencing of

all the MUPP1 clones allowed for a careful sequence analysis in which five novel splice variants (A to E) were found. All the splice variants were found to occur around the PDZ domain 10, which is the interaction domain with hSSTR3 and many other interaction proteins. All splice variants were generated by alternative usage of either the splice acceptor or splice donor sites. Two of the splice variants, B and E, were found to encode a truncated version of MUPP1 with the last three or two PDZ domains (11, 12 and 13) missing due to a frame shift mutation. However, the rest of the splice variants did not alter the domain structure of MUPP1 significantly. Results from the RT-PCR analysis showed that splice variant C, which encodes for an extended inter-domain region between PDZ11 and 12, is the predominant splice variant, which is ubiquitously expressed in all tissues examined. The expression of the splice variant B, which caused a frame shift truncation of MUPP1, was found to be tissue specific as it was found predominantly in the brain and lung. Low level expression of this splice variant was also found in liver and pancreas. Corresponding sequences for the novel splice variants identified could also be found in the EST database.

In addition to the splice variants identified from the yeast-two-hybrid clones, three more splice variants were identified by analyzing the EST database. The first splice variant uses the alternative splice acceptor site at exon 6 (EST #AA983518) whereas the second and third splice variant alternatively spliced out exon 24 + 25 (EST #BE263698) and exon 35 (EST #AV646633; AV646631; AV646613; AV646567; AV646667) respectively. The first splice variant was found to encode for a truncated MUPP1 protein due to a frame shift mutation caused by the alternative splicing event. All the above EST sequences were deposited from a study comparing the transcriptome of hepatocellular carcinoma with the non-cancerous liver cells (Xu *et al*., 2001). Interestingly all these MUPP1 splice variants were found exclusively in the hepatocellular carcinoma samples. It seems that the functions as well as the localization of MUPP1 could possibly be altered according to the splice variants expressed in particular cell types. Moreover, it would be possible to modulate the composition of the macromolecular complex (assuming MUPP1 could be a scaffolding protein at the cell-cell junctions) by having MUPP1 with a different domain compositions i.e. a different number of PDZ domains with alternative splicing events. This could prove to be important since MUPP1 has been implicated as a potential tumor suppressor in the context of human adenovirus and human papillomavirus (HPV)-induced cellular transformation, where it was shown that MUPP1 was selectively targeted for degradation by the high risk HPV-16 and HPV-18 as well as the adenovirus type 4 (Lee *et al*., 2000; Banks *et al*., 2003; Massimi *et al*., 2004).

Besides confirming the interaction between the hSSTR3 with MUPP1 in the yeast system, it was crucial to confirm that this interaction occurs in mammalian cells. Co-immunoprecipitations (CoIP) from transiently expressed proteins in COS-7 cells showed that both the full length MUPP1 and the PDZ10 domain interact with the T7-tagged hSSTR3. Unexpectedly, unlike in the yeast system, the rat SSTR3 also co-immunoprecipitated full length MUPP1 protein in COS-7 cells. The reason for this is unclear, but it might be due to the over-expression of both proteins, which might lead to an artificial interaction. In order to confirm that the interaction of the receptor and MUPP1 is relevant *in vivo*, it was necessary to co-immunoprecipitate both proteins from a tissue or cell line where both proteins of interest are expressed endogenously using specific antibodies. In this case, the MCF-7 cell line was used where both the hSSTR3 and MUPP1 are expressed endogenously. Once again, we could show that the receptor could be co-immunoprecipitated with MUPP1 by an antibody targeted to the PDZ domain 10 of MUPP1. Taken together, the results confirm that the interaction between hSSTR3 and MUPP1 occurs both *in vitro* and *in vivo*.

Immunostaining of MDCK cells confirmed the tight junction localization of MUPP1 in the epithelial cells as published by Hamazaki *et al*, 2002. Furthermore, in the absence of cell junctions, MUPP1 is found in the cytoplasm consistent with previous data that MUPP1 is targeted to tight junction by claudin-1 and JAM1 (Hamazaki *et al*., 2002). We subsequently showed that MUPP1 was also present at the cell-cell junction of the MCF-7 and cell-cell contact sites of the HEK293 cells. Immunohistochemistry of the mouse brain sections showed that MUPP1 is highly enriched at the epithelium of the choroid plexus (the blood-cerebrospinal fluid (CSF) barrier). However, no co-localization of MUPP1 and the rodent SSTR3, which is localized at the neuronal cilia, was found. The reason for this will be discussed in greater detail later in this chapter.

As mentioned earlier, MUPP1 is a potential major scaffolding protein at the tight junctions due to its multiple protein-protein interaction domains. It would be of interest to characterize the molecular composition of the MUPP1 macromolecular complex at the tight junctions. The high affinity interaction between the hSSTR3 C-terminal peptide and MUPP1 shown by affinity purification assay on the Western blot provided us with an opportunity to isolate the MUPP1 complex from the tight junction of epithelial cells. Indeed, by using the hSSTR3 C-terminus peptide coupled to sepharose, I could purify an array of proteins from either mouse brain or epithelial cell lines such as MCF-7 and HEK293 cells. The identities of the purified proteins were determined by mass spectrometry. Strikingly, many of the proteins identified have been shown to localize at the cell-cell junctions, which is either the synaptic junction in

the case of PSD-95 (Kornau *et al*., 1995) and CamKIIα (Kennedy, 1998) or the tight junction in the case of ZO-1, ZO-2, MAGI-1, MAGI-3, Scribble and Pals1 (González-Mariscal *et al*., 2003). In order to find out whether the proteins purified interact with hSSTR3 directly or indirectly, an overlay assay was performed using the GST-hSSTR3-50C fusion protein on the precipitates of mouse brain or cell lines. The results clearly showed that the hSSTR3 C-terminus interacts directly only with MUPP1, BAIAP1 and PIST. However, the overlay could not provide an answer whether the rest of the proteins isolated interact with MUPP1. Pals1 and CamKIIα have been shown recently to interact directly with MUPP1 (Roh *et al*., 2002; Krapivinsky *et al*., 2004). Here, PSD-95 and CIPP (channel-interacting PDZ domain protein) were shown to interact with MUPP1 but not directly with hSSTR3 in COS-7 cells. Besides that, by using the anti-scribble antibody, we could co-immunoprecipitate endogenous MUPP1 with endogenous scribble from MCF-7 and HEK293 cells. The results of these assays clearly showed that MUPP1 is indeed a scaffolding protein, which provides a platform to plug together proteins with different functions to form a macromolecular complex at the cell-cell junctions.

The overlay assay was also used to clarify a possible interaction of the rodent SSTR3 and MUPP1, which remained unclear due to contradictory results obtained from the yeast transformation system and the Co-IP assay in COS-7 cells. Results from the overlay assays confirmed that under non-saturating conditions, the rodent SSTR3 does not interact with MUPP1 protein. So, how could we explain the differential binding ability of the rodent and human receptor to MUPP1 since both of the proteins contained a consensus type I PDZ domain binding motif?

The consensus PDZ binding motif is somewhat different for the amino acids at position P-1, P-3 and beyond. These have also been shown to be important for the PDZ binding in term of both binding affinity and specificity in other proteins (Songyang *et al*., 1997; Niethammer *et al*., 1998). The mouse and rat have identical C-termini, which differ from the human homolog. So, is the human SSTR3 C-terminus an exception? Taking advantage of the on-going canine genome project, the dog SSTR3 was first cloned *in silico* and the sequence was then confirmed by sequencing the gene cloned from MDCK II chromosomal DNA. In addition, SSTR3 sequences from several other species were found by searching through the NCBI and PubMed databases. The amino acid sequence of the cloned dog SSTR3 was found to have 88% and 81% sequence similarity against the human and the rodent homolog respectively. This result is consistent with the observation that the SSTR subtypes cloned from species such as dog, pig, cow or sheep generally have higher sequence similarity to the

human homolog than to the receptor subtypes cloned from the rodent (Figure 4.2). As shown in Table 4.1, alignment of the last 8 to 10 amino acids of the extreme C-termini of the SSTR3 from various species revealed that the consensus PDZ binding motif –X-S-X-L-COOH is conserved among all species examined. However, the sequence of the last four amino acids (-I-S-Y-L-COOH) are identical from the human to fishes with the exception of the rodents. The differences in the amino acids at the positions of P-1 and P-3 determine the binding ability of the SSTR3 to the MUPP protein; this is evident in overlay assays with GST fusion protein containing the C-terminus of dog SSTR3 as well as the mutant (humanized) rat SSTR3 where the P-1 was changed from histidine (H) to tyrosine (Y); the P-4 and P-3 was changed to arginine (R) and isoleucine (I).

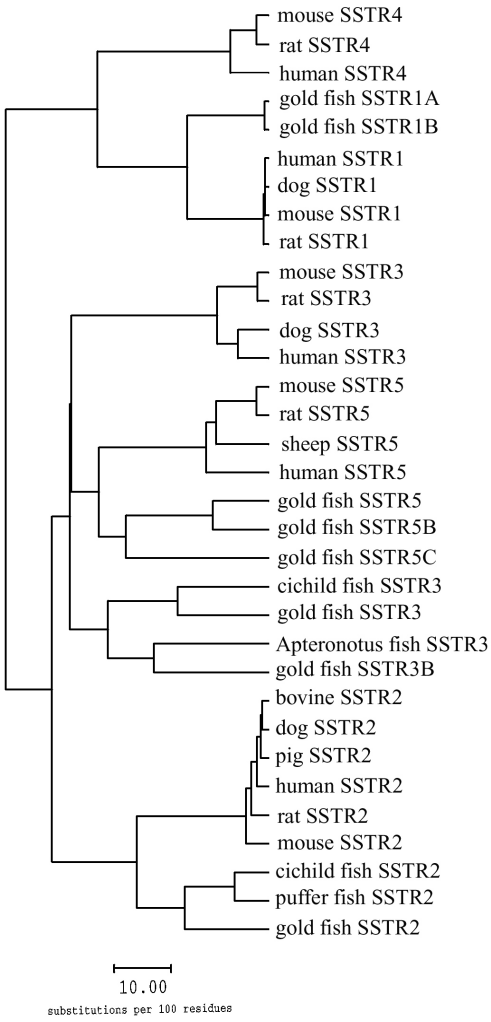

Figure 4.2 Phylogenetic tree based on the alignment of amino acid sequences of the known full-length somatostatin receptor in vertebrates.
The sequences were aligned using the Pileup, Distances and Growtree programs of the Genetics Computer Group (GCG) (Wisconsin Package Version 10.0-UNIX, January 1999). The sequences were obtained from NCBI Genbank or from publication. dog sst1: AY702068 (this work); dog sst2: AY702069 (this work); dog sst3: AY643737 (this work); *Apteronotus albifrons* (gymnotiform fish) sst3 sequence was obtained from Zupanc *et al*. (1999).

Amino acid position, P	-9	-8	-7	-6	-5	-4	-3	-2	-1	0
human SSTR3	K	S	S	T	M	R	I	S	Y	L.
chimpanzee SSTR3	K	S	S	T	M	R	I	S	Y	L.
dog SSTR3	K	P	G	A	L	H	I	S	Y	L.
gold fish SSTR3	K	N	S	S	L	E	I	S	Y	L.
cichlid fish SSTR3	P	S	A	S	L	E	I	S	Y	L.
gymnotiform fish SSTR3	T	D	T	I	L	E	I	S	Y	L.
mouse SSTR3	K	A	S	T	-	-	L	S	H	L.
rat SSTR3	K	A	S	T	-	-	L	S	H	L.
							:	*	:	*

Table 4.1 Comparison of the last 8-10 C-terminal amino acids of the STTR3
Amino acid sequences were obtained from NCBI Genbank or from publication and aligned with Clustal W programme (www.ebi.ac.uk/clustalw; Thompson *et al.*, 1996). "*": identical residues; "**:**": conserved substitutions.

Here, the dog SSTR3 interacts as efficiently as the human homolog with MUPP1 (as well as the BAIAP and the PIST) in contrast to the rat SSTR3 which did not bind to MUPP1. Both of the humanized rat SSTR3 mutants clearly showed improved binding ability to MUPP1. Thus in the case of SSTR3, the exact amino acid sequence of the PDZ binding motif is crucial for its binding ability to the MUPP1 protein. A single amino acid change at a seemingly less important position such as P-1 or P-3 could severely undermines the binding of the receptor to its interaction partner. The results of the overlay assays also showed that binding of the PDZ ligand to the PDZ domain is specific even though it is only mediated by a very short sequence element. This subtle sequence variation provides an explanation why there was no co-localization between MUPP1 and the mouse SSTR3 in mouse brain and why the neuronal cilia staining of rodent SSTR3 was never seen in the human brain (S. Schulz, unpublished observation): because by interacting with MUPP1, the human SSTR3 could localize at a completely different subcellular compartment for a very different function. This may have profound implications in the study of the pharmacological use of SSTR3 ligands, as the cellular functions of SSTR3 might differ between man and his favourite model organisms, rat and mouse.

Now that I have confirmed the interaction of the human SSTR3 with MUPP1, the question arose what the interaction is good for. Is there any functional significance resulting from this interaction? For this, the establishment of a non-rodent epithelial cell line expressing the

receptor either endogenously or after transfection was crucial. This would allow me to find out whether there is any functional role of the receptor in the biogenesis or maintenance of the tight junctions by interacting with MUPP1. Several studies have shown that some heterotrimeric G-proteins, in particular Gαi, Gαo, Gαs and $G\alpha_{12}$ are localized at the tight junction of MDCK cells (De Almeida et al., 1994; Denker et al., 1996; Dodane & Kachar, 1996; Hamilton & Nathanson, 1997). Regulation of the junctional complex by heterotrimeric G proteins was suggested in early pharmacological experiments (Balda *et al*., 1991), and subsequent studies have demonstrated that activation of over-expressed Gαi accelerates tight junction formation, whereas activated $G\alpha_{12}$ reduces transepithelial resistance (Denker *et al*., 1996; Meyer *et al*., 2002).

The MCF-7 cell line, which was used for *in vivo* CoIP seems to be and ideal cell line to use for the functional study. Unfortunately, the endogenous hSSTR3 was never detected in MCF-7 cells immunocytochemically stained with specific hSSTR3 antibody, which was also confirmed by other laboratories (S. Schulz, unpublished observation). This might be due to the extremely low levels of the receptor expressed in individual cells. To overcome this problem, MCF-7 cells stably expressing the T7-tagged hSSTR3 were generated. The immunofluorescence study of the MCF7-hSSTR3-0.5B4 stable cell line showed that the receptor and MUPP1 co-localized at the cell-cell junctions of these cells and should be suitable for functional studies. However, we are also aware that so far there are just a handful of tight junction regulation studies which have been done in MCF-7 cell. In addition, there is no information about a role of heterotrimeric G-proteins in this cell line. In view of this, I also choose another model epithelial cell line, MDCK, to use as a standard cell line for functional study.

Unfortunately, this turned out to be not as simple as in the case of MCF-7 cells. This was due to the apoptotic effect of the hSSTR3 receptor on the transformed cell. No stable MDCK II cell line could be established with the wild type hSSTR3 receptor initially even though the MDCK II tet-off cell line was used. The apoptotic effect observed was independent of the presence of the agonist. The reason for this agonist independent effect is probably due to the fact that one should not just view the receptor activation as an all (ligand binding) or none (absence of ligand) event. Current models for GPCR activation assume that receptors are in equilibrium between inactive (R) and active (R^*) conformations (Samama *et al*., 1993**;** Leff, 1995). R* is promoted by agonists, but can occur in their absence and is capable of spontaneously activating the G proteins, leading to constitutive activity of GPCRs (Costa &

Herz, 1989; Lefkowitz *et al*., 1993; Milligan & Bond, 1995**;** Bond *et al*., 1995). In this case, hSSTR3 would most probably have a high basal activity in the absence of ligand.

These problems were only partly overcome by the use of a suitable strain of MDCK II cells, which allowed for selection of a MDCKII T7-hSSTR3 stable cell line with 50% of the cells expressing the receptor. Results from the immunofluorescence study showed that the receptor co-localized with MUPP1 at the cell-cell junction, but individual cells of the clones also have a wide spectrum of receptor expression level. Still many of the cells die during the cultivation process. One way to overcome the apoptotic effect of the hSSTR3 is to construct a non-apoptosis-inducing receptor. So, various fusion receptor or domain swapping constructs were made between the SSTR5 and SSTR3 receptors. SSTR5 was used because firstly this receptor subtype was shown not to have any apoptotic effect on the transformed cells and secondly both of the subtypes interact with PIST, a Golgi-associated protein, which could imply that they might have a common pathway in the polypeptide processing as well as receptor targeting. Results from the chimeric receptors showed that neither the N-terminal, the C-terminal or the third intracellular loop, which might be involved in the coupling of the SSTR to the heterotrimeric G-proteins, are responsible for the apoptotic effect of the human SSTR3. However at the moment I could not pinpoint the exact domain that is responsible for the apoptotic activity of hSSTR3. But from this study we know that the fusion receptor, T7-mSSTR5-hSSTR3-C, where the entire C-terminal of hSSTR3 was fused to the mSSTR5 after the 7th transmembrane domain, does not have any apoptotic effect on the transformed cells. This fusion receptor was subsequently used for generating a MDCK II stable cell line. Immunofluorescence study of this cell line showed that the receptor co-localized with MUPP1 at the cell-cell junction of MDCK II, particularly at the tight junctions, which is evident in the XZ view of the confocal microscopy. The diffuse immunostaining pattern observed with the MDCK II cell line stably expressing the truncated fusion receptor which lacks the PDZ binding motif showed that the tight junction targeting was mediated by the interaction of the receptor to MUPP1. These results also confirmed that the localization of the receptor is determined by its interaction partner, which in turn could determine the function of the receptor.

The transepithelial electrical resistance (TER) of a cell monolayer grown on the transwell filter is typically used as the functional measure of the integrity of the tight junction (Matter & Balda, 2003). By measuring the TER one can follow the changes occurring at the tight junctions. Therefore, TER was also used in this study to monitor the effect of the receptor at the tight junction upon activation of the receptor.

SSTR3-activation indeed induced changes in the electrical resistance of the monolayer. The TER of the MCF7-hSSTR3 cell line was significantly decreased by 27% and the wild type MCF-7 monolayer was also reduced by 7% compared to the non-agonist treated cells. This result showed that the integrity of the monolayer tight junctions was significantly affected by the activation of the receptor with agonist. A similar but less significant effect was also detected in wild type MCF-7 cells. This is most probably due to the much lower level of the receptor in the wild type cells compared to the stably transformed MCF-7 cell line. Moreover, this result also showed that even though the expression level of the receptor is low (comparable to an *in vivo* situation), it is still high enough to produce a significant effect upon the activation by agonist. This agonist-induced effect on MCF-7 cells was completely blocked by the pretreatment of the monolayer with pertussis toxin (PTX), an Gαi/o inhibitor. In addition, agonist treatment also slowed down tight junction formation during the development of the monolayer. In this case, the wild type MCF-7 cells were not affected by the presence of agonist. This suggested that due to the low level of the receptor in the wild type cells, the effect of the agonist would be the greatest when the receptors are concentrated at the cell junction of a stably formed monolayer compared to a more disperse receptor distribution during the formation of the monolayer. The effect of agonist on a more rapid tight junction biogenesis was also examined in this study by the calcium switch assay (González-Mariscal, *et al*., 1985), where the tight junctions of the stably formed monolayer were first disrupted by removing extracellular Ca^{2+} and tight junction formation was later induced by the re-addition of extracellular Ca^{2+} onto the monolayer. The tight junction formation of both the MCF7-hSSTR3 stable and MCF-7 cell lines were both significantly slowed down in the presence of agonist. Again, the hSSTR3 stable cell line again showed a more pronounced and longer lasting effect compared to the wild type MCF-7 cells. Taking the results together, we can conclude that receptor activation by the agonist, which leads to the activation of the heterotrimeric G-proteins would in turn result in negatively regulating the tight junction formation as well as tight junction stability. However, since a non-selective agonist was used, we cannot exclude at this point the contribution of other SSTR subtypes expressed in MCF-7 cells.

In order to study the regulation of tight junctions by the hSSTR3 receptor in more detail using a receptor free background as a control, we turned to the better studied epithelial cell model, the MDCK cell (Denker *et al*., 1996; Benais-Pont *et al*., 2003). Wild type MDCK II cell as well as those expressing the fusion receptor (T7-mSSTR5-hSSTR3-C), the wild type receptor (T7-hSSTR3) and the truncated fusion receptor (T7-mSSTR5-hSSTR3-8C) were first grown

on the transwell filter to form the monolayer. Respective agonists were applied apically to the monolayer and the TER was monitored. Surprisingly, unlike the MCF-7 cells, no effect was observed in MDCK II cells with this agonist treatment. Similarly, no effect was observed when the agonist was applied basolaterally. This may be due to the inability of the peptide agonist to pass through the tight junction of MDCK II cells (Hayashi *et al*., 1999; Artursson, 1990). So, in order to make the receptor available to the agonist, the calcium switch assay was used throughout the study with MDCK II cells. After the calcium switch, the monolayers were allowed to reform their tight junction for a period of 15 hours before the TER was measured. Unexpectedly, this time an increase of TER was recorded upon activation of the fusion receptor and the wild type hSSTR3 receptor, whereas there were no changes in the electrical resistance of the wild type MDCK II cell and the truncated fusion receptor stable cell line. The lack of effect of the truncated fusion receptor demonstrates that in order to control tight junction formation, the receptor needs to be located at the tight junction, which depends on the interaction with MUPP1. The increase in TER is more significant in the fusion receptor cell line compared to the wild type hSSTR3 cell line, which is probably due to the fact that less than 50% of the cells express the receptor in the stable cell line. It was also observed that the wild type receptor cells consistently have higher basal level than that of other cells. This may be due to the high basal activity of hSSTR3 as discussed earlier.

To investigate the difference in the agonist-induced effects seen in MCF-7 and MDCK II stable cell lines, tight junction formation of the MDCK II monolayer after the calcium switch was monitored at much earlier time points. Here, it became apparent that the tight junction formation was indeed slowed down by the agonist treatment at the early phase (2 to 10 hours) of recovery, similar to what was seen in MCF-7 cells. However, at the later phase, the TERs of the agonist treated samples increase rapidly as seen previously. These differences in response by the MCF-7 and MDCK II cells towards stimuli are not at all surprising since MDCK II is a non-carcinoma cell line unlike the MCF-7 cell line, which might have different cell properties. Furthermore, previous studies have also shown that MDCK II responded in completely different way compared to MCF-7 when the Ras-MEK1 pathway was activated (Chen *et al*., 2000; Macek *et al*., 2003).

It should be noted that the recovery of the tight junction after calcium switch is very much affected by the incubation conditions of the monolayer, due to the experimental setup. Interruption due to the measurements during the early phase of the tight junction formation would significantly slow down the recovery rate. Thus one should keep in mind that when the

tight junctions are disrupted *in vivo*, the rate of recovery may be much faster and the time span may be shorter than what we have observed in our experimental setup.

In order to investigate what happened to the tight junction during the biogenesis after the calcium switch, the amounts of tight junction proteins such as claudin-1 to –4; ZO-1 and ZO-2; MUPP1 as well as the phosphorylated p44/42 ERK proteins in the cell were examined by Western blotting. A possible role of activated p44/42 ERK was examined because Singh & Harris (2004) have shown that the MAPK/ERK pathway is involved in the increase of TER in MDCK II cells upon the treatment with epidermal growth factor (EGF). First samples of both the wild type MDCK II and the fusion receptor stable cell line at a later time point (23 hours) were examined. At this time point the total amount of claudin-2 was reduced several fold by activation of the fusion receptor whereas there were no noticeable changes in the amount of claudin-1, claudin-3, claudin-4, ZO-1, ZO-2 and MUPP1. Claudins constitute a family of transmembrane tight junction proteins which determine the tightness of the tight junction by the combination and mixing ratios of different claudin species. Out of the 24 family members, claudin-1 to –4 are known to be present in MDCK II cells. It has been demonstrated that the presence of claudin-2 could transform a high resistance (tight) MDCK I to a low resistance (leaky) MDCK II monolayer (Furuse *et al*., 2001). In addition, when claudin-4 was selectively removed from the tight junction the TER was significantly reduced (Sonoda *et al*., 1999). So, the presence of high amounts of claudin-2 and claudin-4 would correlate with the 'loose' and the 'tight' tight junction respectively. Thus, there is a good correlation of the agonist-induced high TER in the fusion receptor sample with a low amount of claudin-2 in the cell. At this point, it was tempting to speculate that the increase in TER observed in the agonist treated sample was due to selective degradation of claudin-2 induced by the agonist.

To further elucidate the signaling pathway of the receptor, several inhibitors were tested for their ability to affect the tight junction regulation by the receptor. At the early phase of recovery, PTX could partially reverse the inhibition of the tight junction recovery caused by the agonist and the MEK1/2 inhibitor (U0126) treatment could only accelerate the tight junction recovery very marginally, whereas 26S proteasome inhibitor (MG-132), protein synthesis inhibitor (cycloheximide) and RNA synthesis inhibitor (Actinomycin D) did not seem to prevent the early phase of tight junction formation inhibition. These results imply that the inhibition of tight junction recovery after the calcium switch is partially mediated by the activation of the PTX-sensitive heterotrimeric Gαi protein at the tight junction. This result is contradictory to the study shown by Denker *et al*. (1996) where expression of a

constitutively active $G\alpha_{i2}$ leads to high TER and accelerates tight junction biogenesis. However, the paradigm used here is different from that study, as the fusion receptor is activated only for a certain period of time.

On the other hand, U0126 inhibits late phase TER increase, but did not seem to play any role in the inhibition of early phase tight junction formation. This is actually consistent with the observation that MAPK/ERK mediated TER increase occurs later in the tight junction recovery shown by Singh & Harris (2004). This also suggests that other mechanisms, which are involved in the inhibition of agonist-induced tight junction formation remain unidentified. One should keep in mind that besides modulating tight junction formation via activation of its effectors molecules, upon activation by agonist, the receptor can also be internalized (Roth *et al*., 1997). This internalization could severely alter the tight junction complex composition if the scaffolding molecule, MUPP1, is internalized together with the receptor.

Western blot analysis of tight junction proteins showed that the decreased levels of claudin-2 in the agonist treated sample was already observed 2 hours after the calcium switch and this reduction in claudin-2 could be prevented by the pretreatment of PTX. Activation of p44/42 ERK was observed in the same sample, and its activation could be almost completely blocked by the pretreatment with PTX. These results suggest that the activation of $G\alpha i$ leads to the selective degradation of the claudin-2, which then leads to the observed late phase TER increase.

At the late phase of the tight junction recovery, U0126 and PTX did significantly lower TER, whereas MG-132 and cycloheximide completely prevented the late phase increase of the TER induced by the agonist. Actinomycin D samples were found not to be viable at this late time point, so, the role of transcription could not be accessed. Results obtained from MG-132 and cycloheximide treated samples seem to be somewhat contradictory since cycloheximide blocks protein synthesis and MG-132 prevents proteins degradation but both inhibitors result in TER inhibition. Western blotting analysis of the late time point samples showed that claudin-2 is selectively targeted for degradation via the proteasome pathway as the loss of claudin-2 is completely prevented by the 26S proteasome inhibitor, whereas cycloheximide treatment leads to loss of all claudins. These results provide an explanation for the contradiction observed in the TER of both the MG-132 and cycloheximide samples. Since claudins constitute the tight junction, loss of all claudins would definitely lead to loss of the TER whereas MG-132 selectively prevented the loss of claudin-2 induced by agonist, which leads to selective change in the component of claudins, therefore resulting in the low TER

recorded. On the other hand, the levels of the tight junction plaque proteins such as ZO-2 seem to be relatively unchanged in all the samples examined.

From the inhibitor studies, it became clear that there is a complex interplay between different effectors coupling to the fusion receptor, which leads to selective regulation of the claudin proteins, which in turn results in the complex regulation of the tight junction by the receptor. Claudin-2 seems to be the major claudin species which was selectively degraded by the 26S proteasome after the activation of the fusion receptor by agonist.

In conclusion, my data show that MUPP1 targets the hSSTR3 to the tight junction via its PDZ interaction. This interaction connects the receptor to the MUPP1 macromolecular complex, which is involved in the regulation of tight junction maintenance and biogenesis. The receptor localized at the tight junction regulates tight junction formation upon activation by its agonist, which leads to selective degradation of the claudin-2 tight junction protein by the proteasome.

CHAPTER FIVE SUMMARY

The regulatory peptide, somatostatin, acts as an inhibitory regulator of various cellular functions throughout the brain and periphery. These actions are mediated by the somatostatin receptor (SSTR) family, which comprises five distinct subtypes (SSTR1-5). In a yeast two-hybrid screen, I identified the tight junction multi-PDZ domain protein MUPP1 as an interaction partner for the C-terminus of human SSTR3. This interaction was shown to be mediated by the PDZ binding motif at the extreme C-terminus of hSSTR3 and the PDZ domain 10 of MUPP1. Subsequently, the interaction was confirmed biochemically in both over-expressing as well as native systems. Interestingly, the rodent homolog of SSTR3 was demonstrated not to interact with MUPP1 due to a subtle difference in its PDZ binding motif. MUPP1 was found to be part of a large protein complex at the synaptic and tight junction. Wild type hSSTR3 was shown to co-localize with MUPP1 at the cell-cell junction in fully polarized MCF-7 and MDCK II cells stably expressing the receptor. Due to the pro-apoptotic properties of the wild type hSSTR3, a fusion receptor was constructed which consisted of mouse SSTR5 and the entire C-terminus of hSSTR3. The fusion receptor was shown by confocal microscopy, to co-localize with MUPP1 at the tight junction. As a fusion receptor lacking the PDZ binding motif was found to be diffusely distributed and did not co-localize with MUPP1, I concluded that the receptor is targeted to a large protein complex at the tight junction through its PDZ-mediated interaction with MUPP1.

Functional studies in the breast carcinoma MCF-7 cell line revealed that the receptor was able to disrupt and slow down formation of the tight junction in an agonist-dependent manner. This effect requires a G-protein mediated signaling pathway, as it could be prevented by pretreatment of cells with pertussis toxin (PTX), an inhibitor of Gαi/o. However, activation of the receptor in MDCK II stable cell lines yielded a contrasting picture. Agonist treatment was shown to slow down the tight junction formation initially and facilitate the formation later in a calcium-switch paradigm. The agonist-induced effects could be partially reversed by PTX both at the early and late phase of tight junction formation. The 26S proteasome inhibitor, MG-132, was shown to only block the late phase of tight junction formation. Biochemical analyses showed that upon agonist treatment, the tight junction transmembrane protein claudin-2, a determinant for leaky junctions, was selectively targeted for degradation by the 26S proteasome. The PDZ-domain dependent localization to and regulation of tight junctions by the hSSTR3 add a new aspect to the signaling repertoire of G-protein coupled receptors.

CHAPTER SIX REFERENCES

Aguila, M.C., Rodriguez, A.M., Aguila-Mansilla, H.N. and Lee, W.T. 1996. Somatostatin antisense oligodeoxynucleotide-mediated stimulation of lymphocyte proliferation in culture. *Endocrinology* 137: 1585-1590.

Artursson, P. 1990. Epithelial transport of drugs in cell culture. I: A model for studying the passive diffusion of drugs over intestinal absorptive (Caco-2) cells. *J. Pharm. Sci*. 79: 476-482.

Balda, M.S., Gonzalez-Mariscal, L., Contreras, R.G., Macias-Silva, M., Torres-Marquez, M.E., Garcia-Sainz, J.A. and Cereijido, M. 1991. Assembly and sealing of tight junctions: possible participation of G-proteins, phospholipase C, protein kinase C and calmodulin. *J. Membr. Biol*. 122: 193-202.

Banks, L., Pim, D. and Thomas, M. 2003. Viruses and the 26S proteasome: hacking into destruction. *Trends Biochem. Sci*. 28: 452-459.

Bauer, W., Briner, U., Doepfner, W., Halber, R., Huguenin, R., Marbach, P., Petcher, T.J. and Pless, J. 1982. SMS 201-995: A very potent and selective octapeptide analogue of somatostatin with prolonged action. *Life Sci*. 31: 1133-1140.

Bécamel, C., Figge, A., Poliak, S., Dumius, A., Peles, E., Bockaert, J., Lübbert, H and Ullmer, C. 2001. Interaction of serotonin 5-hydroxytryptamine type 2C receptors with PDZ10 of the multi-PDZ domain protein MUPP1. *J. Biol. Chem.* 276(16): 12974-12982.

Benais-Pont, G., Punn, A., Flores-Maldonado, C., Eckert, J., Raposo, G., Fleming, T.P., Cereijido, M., Balda, M.S. and Matter, K. 2003. Identification of a tight junction-associated guanine nucleotide exchange factor that activates Rho and regulates paracellular permeability. *J. Cell Biol*. 160: 729-740.

Bilder, D. 2003. PDZ domain polarity complexes. *Curr. Biol*. 13: R661-R662.

Bond, R.A., Leff, P., Johnson, T.D., Milano, C.A., Rockman, H.A., McMinn, T.R., Apparsundaram, S., Hyek, M.F., Kenakin, T.P., Allen, L.F. and Lefkowitz, R.J. 1995. Physiological effects of inverse agonists in transgenic mice with myocardial overexpression of the beta 2-adrenoceptor. *Nature* 374: 272-276.

Brazeau, P., Vale, W., Burgus, R., Ling, N., Rivier, J. and Guillemin, R. 1972. Hypothalamic polypeptide that inhibits the secretion of immunoreactive pituitary growth hormone. *Science* 129: 77-79

Breder, C.D., Yamada, Y., Yasuda, K., Seino, S., Saper, C.B and Bell, G.I. 1992. Differential expression of somatostatin receptor subtypes in brain. *J. Neurosci*. 12: 3920-3934.

Bruno, J.F., Xu, Y., Song, J. and Berelowitz, M. 1992. Molecular cloning and functional expression of a brain-specific somatostatin receptor. *Proc. Natl. Acad. Sci. USA* 89: 11151-11155.

Bruno, J.F., Xu, Y., Song, J. and Berelowitz, M. 1993. Tissue distribution of somatostatin receptor subtype messenger ribonucleic acid in the rat. *Endocrinology* 133: 2561-2567.

Cervera, P., Videau, C., Viollet, C., Petrucci, C., Lacombe, J., Winsky-Sommerer, R., Csaba, Z., Helboe, L., Daumas-Duport, C., Reubi, J.C. and Epelbaum, J. 2002. Comparison of somatostatin receptor expression in human gliomas and medulloblastomas. *J. Neuroendocrinol*. 14: 458-471.

Chen, Y., Lu, Q., Schneeberger, E.E. and Goodenough, D.A. 2000. Restoration of tight junction structure and barrier function by down-regulation of the mitogen-activated protein kinase pathway in ras-transformed Madin-Darby canine kidney cells. *Mol. Biol. Cell* 11: 849-862.

Cordelier, P., Esteve, J.P., Bousquet, C., Delesque, N., O' Carroll, A.M., Schally, A.V., Vaysse, N., Susini, C. and Buscail, L. 1997. Characterization of the antiproliferative signal mediated by the somatostatin receptor subtype sst5. *Proc. Natl. Acad. Sci. USA* 94: 9343-9348.

Costa, T. and Herz, A. 1989. Antagonists with negative intrinsic activity at delta opioid receptors coupled to GTP-binding proteins. *Proc. Natl. Acad. Sci. USA* 86: 7321-7325.

Coyne, C.B., Voelker, T., Pichla, S.L. and Bergelson, J.M. 2004. The coxsackievirus and adenovirus receptor interacts with the multi-PDZ domain protein-1 (MUPP-1) within the tight junction. *J. Biol. Chem.* 2004 Sep 9 [Epub ahead of print]

de Almeida, J.B., Holtzman, E.J., Peters, P., Ercolani, L., Ausiello, D.A. and Stow, J.L. 1994. Targeting of chimeric G alpha i proteins to specific membrane domains. *J. Cell Sci.* 107: 507-515.

de Lecea, L., Criado, J.R., Prosperogarcia, O., Gautvik, K.M., Schweitzer, P., Danielson, P.E., Dunlop, C.L.M., Siggins, G.R., Henriksen, S.J. and Sutcliffe, J.G. 1996. A cortical neuropeptide with neuronal depressant and sleep-modulating properties. *Nature* 381: 242-245.

Denker, B.M., Saha, C., Khawaja, S. and Nigam, S.K. 1996. Involvement of a heterotrimeric G protein alpha subunit in tight junction biogenesis. *J. Biol. Chem.* 271: 25750-25753.

Dodane, V. and Kachar, B. 1996. Identification of isoforms of G proteins and PKC that colocalize with tight junctions. *J. Membr. Biol.* 149: 199-209.

Doe, C.Q. 2001. Cell polarity: the PARty expands. *Nat. Cell Biol.* 3: E7-E9.

Dong, H., O'Brien, R.J., Fung, E.T., Lanahan, A.A., Worley, P.F. and Huganir, R.L. 1997. GRIP: a synaptic PDZ domain-containing protein that interacts with AMPA receptors. *Nature* 386: 279-284.

Dong, H., Zhang, P., Liao, D. and Huganir, R.L. 1999. Characterization, expression, and distribution of GRIP protein. *Ann. N. Y. Acad. Sci.* 868: 535-540.

Dournaud, P., Gu, Y.Z., Schonbrunn, A., Mazella, J., Tannenbaum, G.S. and Beaudet, A. 1996. Localization of the somatostatin receptor SSTR2A in rat brain using a specific anti-peptide antibody. *J. Neurosci.* 16: 4468-4478.

Doyle, D.A., Lee, A., Lewis, J., Kim, E., Sheng, M. and MacKinnon, R. 1996. Crystal structures of a complexed and peptide-free membrane protein-binding domain: molecular basis of peptide recognition by PDZ. *Cell* 85: 1067-1076.

Epelbaum, J., Dussaillant, M., Enjalbert, A., Kordon, C. and Rostene, W. 1986. Autoradiographic localization of a non-reducible somatostatin analog (125I-CGP 23996) binding sites in the rat brain: comparison with membrane binding. *Peptides* 6: 713-719.

Epelbaum, J., Dournaud, P., Fodor, M. and Viollet, C. 1994. The neurobiology of somatostatin. *Crit. Rev. Neurobiol.* 8: 25-44.

Evans, C.J., Keith, D.E. Jr., Morrison, H., Magendzo, K. and Edwards, R.H. 1992. Cloning of a delta opioid receptor by functional expression. *Science* 258: 1952-1955.

Fukusumi, S., Kitada, C., Takekawa, S., Sakamoto, J., Miyamoto, M. Kitano, K. and Fujino, M. 1997. Identification and characterization of a novel human cortistatin-like peptide. *Biochem. Biophys. Res. Commun*. 232: 157-163.

Furuse, M., Furuse, K., Sasaki, H. and Tsukita, S. 2001. Conversion of *Zonulae Occludentes* from tight to leaky strand type by introducing claudin-2 into Madin-Darby Canine Kidney I cells. *J. Cell Biol*. 153: 263-272.

González-Mariscal, L., Betanzos, A., Nava, P. and Jaramillo, B.E. 2003. Tight junction proteins. *Prog. Biophysics Mol. Biol.* 81: 1-44.

González-Mariscal, L., Chavez de Ramirez, B. and Cereijido, M. 1985. Tight junction formation in cultured epithelial cells (MDCK). *J. Membr. Biol*. 86: 113-125.

Gossen, M. and Bujard, H. 1992. Tight control of gene expression in mammalian cells by tetracycline-responsive promoters. *Proc. Natl. Acad. Sci. USA* 89: 5547-5551.

Gossen, M., Freundlieb, S., Bender, G., Muller, G., Hillen, W. and Bujard, H. 1995. Transcriptional activation by tetracyclines in mammalian cells. *Science* 268: 1766-1769.

Gromada, J., Hoy, M., Buschard, K., Salehi, A and Rorsman, P. 2001. Somatostatin inhibits exocytosis in rat pancreatic a-cell by G_{i2}-dependent activation of calcineurin and depriming of secretory granules. *J. Physiol*. 535: 519-532.

Guillermet, J., Saint-Laurent, N., Rochaix, P., Cuvillier, O., Levade, T., Schally, A.V., Pradayrol, L., Buscail, L., Susini, C. and Bousquet, C. 2003. Somatostatin receptor subtype 2 sensitizes human pancreatic cancer cells to death ligand-induced apoptosis. *Proc. Natl. Acad. Sci. USA* 100: 155-160.

Hall, R.A., Premont, R.T., Chow, C-W., Blitzer, J.T., Pitcher, J.A., Claing, A., Stoffel, R.H., Barak, L.S., Shenolikar, S., Weinman, E.J., Grinstein, S. and Lefkowitz, R.J. 1998. The β2-adrenergic receptor interacts with the Na^+/H^+-exchanger regulatory factor to control Na^+/H^+ exchanger. *Nature* 392: 626-630.

Hamazaki, Y., Itoh, M., Sasaki, H., Furuse, M. and Tsukita, S. 2002. Multi-PDZ domain protein 1 (MUPP1) is concentrated at tight junctions through its possible interaction with claudin-1 and junctional adhesion molecule. *J. Biol. Chem.* 277(1): 455-461.

Hamilton, S.E. and Nathanson, N.M. 1997. Differential localization of G-proteins, G alpha o and G alpha i-1, -2, and -3, in polarized epithelial MDCK cells. *Biochem. Biophys. Res. Commun*. 234: 1-7.

Hanahan, D. 1983. Studies on transformation of Escherichia coli with plasmids. *J. Mol. Biol*. 166: 557-580.

Harris, B.Z. and Lim, W.A. 2001. Mechanism and role of PDZ domains in signaling complex assembly. *J. Cell Sci*. 114: 3219-3231.

Hassel, B., Schreff, M., Stuebe, EM., Blaich, U and Schumacher, S. 2003. CALAB/NGC interacts with Golgi-associated protein PIST. *J. Biol. Chem.* 278(41): 40136-40143.

Hayashi, M., Sakai, T., Hasegawa, Y., Nishikawahara, T., Tomioka, H., Iida, A., Shimizu, N., Tomita, M. and Awazu, S. 1999. Physiological mechanism for enhancement of paracellular drug transport. *J. Control Release* 62: 141-148.

Hillier, B.J., Christopherson, K.S., Prehoda, K.E., Bredt D.S. and Lim, W.A. 1999. Unexpected modes of PDZ domain scaffolding revealed by structure of nNOS-syntrophin complex. *Science* 284: 812-815.

Hokfelt, T., Effendic, S., Hellerstrom, C., Johansson, O., Luft, R. and Arimura, A. 1975. Cellular localization of somatostatin in endocrine-like cells and neurons of the rat with special references to the A_1 cells of the pancreatic islets and to the hypothalamus. *Acta Endocrinol*. 80 (Suppl. 200): 5-41.

Hoyer, D., Bell, G.I., Berelowitz, M., Epelbaum, J., Feniuk, W., Humphrey, P.P., O'Carroll, A.M., Patel, Y.C., Schonbrunn, A. and Taylor, J.E. 1995. Classification and nomenclature of somatostatin receptors. *Trends Pharmcol. Sci*. 16: 86-88.

Hung, A.Y. and Sheng, M. 2002. PDZ domains: structural modules for protein complex assembly. *J, Biol. Chem*. 277: 5699-5702.

Im, Y.J., Park, S.H., Rho, S.H., Lee, J.H., Kang, G.B., Sheng, M., Kim, E. and Eom, S.H. 2002. Crystal structure of GRIP1 PDZ6-peptide complex reveals the structure basis for class II PDZ target recognition and PDZ domain-mediated multimerization. *J. Biol.Chem*. 278: 8501-8507.

Jeansonne, B., Lu, Q., Goodenough, D.A. and Chen, Y.H. 2003. Claudin-8 interacts with multi-PDZ domain protein 1 (MUPP1) and reduces paracellular conductance in epithelial cells. *Cell Mol. Biol. (Noisy-le-grand)*. 49: 13-21.

Karalis, K., Mastrorakos, G., Chrousos, G.P. and Tolis, G. 1994. Somatostatin analogues suppress the inflammatory reaction *in vivo*. *J. Clin. Invest*. 93: 2000-2006.

Kennedy, M.B. 1998. Signal transduction molecules at the glutamatergic postsynaptic membrane. *Brain Res. Brain Res. Rev*. 26: 243-257.

Kennedy, M.B. 2000. Signal-processing machines at the postsynaptic density. *Science* 290: 750-754.

Kennedy, M.E. and Limbird, L.E. 1993. Mutations of the α2-adrenergic receptor that eliminate detectable palmitoylation do not perturb receptor/G protein coupling. *J. Biol. Chem*. 268: 8003-8011.

Kim, E., Niethammer, M., Rothschild, A., Jan Y.N. and Sheng, M. 1995. Clustering of shaker-type K^+ channels by interaction with a family of membrane-associated guanylate kinases. *Nature* 378: 85-88.

Kluxen, F.W., Bruns, C. and Lubbert, H. 1992. Expression cloning of a rat brain somatostatin receptor cDNA. *Proc. Natl. Acad. Sci. USA* 89: 4618-4622.

Komatsuzaki, K., Murayama, Y., Giambarella, U., Ogata, E., Seino, S. and Nishimoto, I. 1997. A novel system that reports the G-proteins linked to a given receptor: A study of type 3 somatostatin receptor. *FEBS Lett*. 406: 165-170.

Kong, H., DePaoli, A.M., Breder, C.D., Yasuda, K., Bell, G.I. and Reisine, T. 1994. Differential expression of messenger RNAs for somatostatin receptor subtypes SSTR1, SSTR2 and SSTR3 in adult rat brain: analysis by RNA blotting and *in situ* hybridization histochemistry. *Neuroscience* 59: 175-184.

Kornau, H.C., Schenker, L.T., Kennedy, M.B. and Seeburg, P.H. 1995. Domain interaction between NMDA receptor subunits and the postsynaptic density protein PSD-95. *Science* 269: 1737-1740.

Kozlov, G., Gehring, K. and Ekiel, I. 2000. Solution structure of the PDZ2 domain from human phosphatase hPTP1E and its interactions with C-terminal peptides from the Fas receptor. *Biochemistry* 39: 2572-2580.

Krapivinsky, G., Medina, I., Krapivinsky, L., Gapon, S. and Clapham, D.E. 2004. SynGAP-MUPP1-CaMKII synaptic complexes regulate p38 MAP kinase activity and NMDA receptor-dependent synaptic AMPA receptor potentiation. *Neuron* 43: 563-574.

Kreienkamp, H-J., Akgun, E., Baumeister, H., Meyerhof, W. and Richter, D. 1999. Somatostatin receptor subtype 1 modulates basal inhibition of growth hormone release in somatotrophs. *FEBS Lett*. 462: 464-466.

Kreienkamp, H-J., Hoenck, H-H. and Richter, D. 1997. Coupling of rat somatostatin receptor subtypes to a G-protein gated inwardly rectifying potassium channel (GIRK1). *FEBS Lett*. 419: 92-94.

Krempels, K., Hunyady, B., O'Carroll, A.M. and Mezey, E. 1997. Distribution of somatostatin receptor messenger RNAs in the rat gastrointestinal tract. *Gastroenterology* 112: 1948-1960.

Krulich, L., Dhariwal, A.P.S. and McCann, S.M. 1968. Stimulatory and inhibitory effects of purified hyphothalamic extracts on growth hormone release from rat pituitary *in vitro*. *Endocrinology* 83: 787-790.

Kulaksiz, H., Eissele, R., Roessler, D., Schulz, S., Hoellt, V., Cetin, Y. and Arnold, R. 2002. Identification of somatostatin receptor subtypes 1, 2, 3, and 5 in neuroendocrine tumours with subtype specific antibodies. *Gut* 50: 52-60.

Kurschner, C., Mermelstein, P.G., Holden, W.T. and Surmeier, D.J. 1998. CIPP, a novel multivalent PDZ domain protein, selectively interacts with Kir4.0 family members, NMDA receptor subunits, neurexins, and neuroligins. *Mol. Cell. Neurosci*. 11: 161-172.

Kumar, U., Sasi, R., Suresh, S., Patel, A., Thangaraju, M., Metrakos, P., Patel, S.C. and Patel, Y.C. 1999. Subtype-selective expression of the five somatostatin receptors (hSSTR1-5) in human pancreatic islet cells. *Diabetes* 48: 77-85.

Laemmli, U.K. 1970. Cleavage of structural proteins during the assembly of the head of bacteriophage T4. *Nature* 227: 680-685.

Lee, S.S., Glaunsinger, B., Mantovani, F., Banks, L. and Javier, R.T. 2000. Multi-PDZ domain protein MUPP1 is a cellular target for both adenovirus E4-ORF1 and high-risk papillomavirus type 18 E6 oncoproteins. *J. Virol*. 74: 9680-9693.

Leff, P. 1995. Inverse agonism: theory and practice. *Trends Pharmacol. Sci*. 16: 256.

Lefkowitz, R.J., Cotecchia, S., Samama, P. and Costa, T. 1993. Constitutive activity of receptors coupled to guanine nucleotide regulatory proteins. *Trends Pharmacol. Sci*. 14: 303-307.

Li, X.J., Forte, M., North, R.A., Ross, C.A. and Snyder, S.H. 1992. Cloning and expression of a rat somatostatin receptor enriched in brain. *J. Biol. Chem*. 267: 21307-21312.

Macek, R., Swisshelm, K. and Kubbies, M. 2003. Expression and function of tight junction associated molecules in human breast tumor cells is not affected by the Ras-MEK1 pathway. *Cell Mol. Biol. (Noisy-le-grand)* 49: 1-11.

Mascardo, R.N., Barton, R.W. and Sherline, P. 1984. Somatostatin has an antiproliferative effect on concanavalin-activated rat thymocytes. *Clin. Immunol. Immunopathol*. 33: 131-138.

Massimi, P., Gammoh, N., Thomas, M. and Banks, L. 2004. HPV E6 specifically targets different cellular pools of its PDZ domain-containing tumour suppressor substrates for proteasome-mediated degradation. *Oncogene* 2004 Sep 20 [Epub ahead of print]

Matter, K. and Balda, M.S. 2003. Functional analysis of tight junctions. *Methods* 30: 228-234.

Meyer, T.N., Schwesinger, C. and Denker, B.M. 2002. Zonula occludens-1 is a scaffolding protein for signaling molecules. Galpha (12) directly binds to the Src homology 3 domain and regulates paracellular permeability in epithelial cells. *J. Biol. Chem*. 277: 24855-24858.

Meyerhof, W. 1998. The elucidation of somatostatin receptor functions: a current view. *Rev. Physiol. Biochem. Pharmacol*. 133: 55-108.

Meyerhof, W., Paust, H-J., Schoenrock, C. and Richter, D. 1991. Cloning of a cDNA encoding a novel putative G-protein-coupled receptor expressed in specific rat brain regions. *DNA Cell Biol*. 10: 689-694.

Meyerhof, W., Wulfsen, I., Schoenrock, C., Fehr, S. and Richter, D. 1992. Molecular cloning of a somatostatin-28 receptor and comparison of its expression pattern with that of a somatostatin-14 receptor in rat brain. *Proc. Natl. Acad. Sci. USA* 89: 10267-10271.

Milligan, G. and Bond, R.A. 1997. Inverse agonism and the regulation of receptor number. *Trends Pharmacol. Sci*. 18: 468-474.

Milligan, G. and White, J.H. 2001. Protein-protein interactions at G-protein-coupled receptors. *Trends Pharmacol. Sci*. 22: 513-518.

Neudauer, C.L., Joberty, G. and Macara, I.G. 2001. PIST: A novel PDZ/coiled-coil domain binding partner for the Rho-family GTPase TC10. *Biochem. Biophys. Res. Commun*. 280: 541-547.

Niethammer, M., Valtschanoff, J.G., Kapoor, T.M., Allison, D.W., Weinberg, T.M., Craig, A.M. and Sheng, M. 1998. CRIPT, a novel postsynaptic protein that binds to the third PDZ domain of PSD-95/SAP90. *Neuron* 20: 693-707.

O'Carroll, A.M., Lolait, S.J., Koenig, M. and Mahan, L.C. 1992. Molecular cloning and expression of a pituitary somatostatin receptor with preferential affinity for somatostatin-28. *Mol. Pharmacol*. 42: 939-946.

O'Dowd, B.F., Hnatowich, M., Caron, M.G., Lefkowitz, R.J. and Bouvier, M. 1989. Palmitoylation of the human beta2-adrenergic receptor: mutation of Cys341 in the carboxyl tail leads to an uncoupled nonpalmitoylated form of the receptor. *J. Biol. Chem*. 264: 7564-7569.

Pagliacci, M.C., Tognellinin, R., Grignani, F. and Nicoletti, F. 1991. Inhibition of human breast cancer cell (MCF-7) growth in vitro by the somatostatin analog SMS 201-995: Effects on cell cycle parameters and apoptotic cell death. *Endocrinology* 129: 2555-2562.

Panetta, R., Greenwood, M.T., Warszynska, A., Demchyshyn, L.L., Day, R., Niznik, H.B., Srikant, C.B. and Patel, Y.C. 1994. Molecular cloning, functional characterization and chromosomal localization of a human somatostatin receptor (somatostatin receptor type 5) with preferential affinity for somatostatin 28. *Mol. Pharmacol*. 45: 417-427.

Patel, Y.C. 1992. General aspects of the biology and function of somatostatin. In: Weil, C., Muller, E.E. and Thorner, M.O. Eds. *Basic and Clinical Aspects of Neuroscience*. Berlin: Springer-Verlag. Vol. 4: 1-16.

Patel, Y.C. 1999. Somatostatin and its receptor family. *Front. Neuroendocrinol*. 20: 157-198.

Patel, Y.C. and Galanopoulou, A. 1995. Processing and intracellular targeting of prosomatostatin-derived peptides: the role of mammalian endoproteases. *Ciba Found. Symp*. 190: 26-40.

Patel, Y.C., Greenwood, M.T., Panetta, R., Demchyshyn, L., Niznik, H. and Srikant, C.B. 1995. The somatostatin receptor family. *Life Sci*. 57: 1249-1265.

Patel, Y.C., Greenwood, M.T., Warszynska, A., Panetta, R. and Srikant, C.B. 1994. All five cloned human somatostatin receptor subtypes (hSSTR1-5) are functionally coupled to adenylyl cyclase. *Biochem. Biophys. Res. Commun*. 198: 605-612.

Patel, Y.C. and Srikant, C.B. 1994. Subtype selectivity of peptide analogs for all five cloned human somatostatin receptors (hsstr1-5). *Endocrinology* 135: 2814-2817.

Patel, Y.C. and Reichlin, S. 1978. Somatostatin in hypothalamus, extrahypothalamic brain and peripheral tissues of the rat. *Endocrinology* 102: 523-530.

Pradayrol, L., Jornval, H., Mutt, V. and Ribet, A. 1980. N-terminal expended somatostatin: the primary structure of somatostatin-28. *FEBS Lett*. 109: 55-58.

Raulf, F., Perez, J., Hoyer, D. and Bruns, C. 1994. Differential expression of five somatostatin receptor subtypes, SSTR1-5, in the CNS and peripheral tissue. *Digestion* 55: 46-53.

Raynor, K., Murphy, W.A., Coy, D.H., Taylor, J.E., Moreau, J-P., Yasuda, K., Bell, G.I. and Reisine, T. 1993a. Cloned somatostatin receptors: identification of subtype-selective peptides and demonstration of high-affinity binding of linear peptides. *Mol. Pharmacol*. 43: 838-844.

Raynor, K., O'Carroll, A.M., Kong, H.Y., Yasuda, K., Mahan, L.C., Bell, G.I. and Reisine, T. 1993b. Characterization of cloned somatostatin receptors SSTR4 and SSTR5. *Mol. Pharmacol*. 44: 385-392.

Reichlin, S. 1983. Somatostatin. *N. Engl. J. Med*. 309: 1495-1501, 1556-1563.

Roh, M.H., Makarova, O., Liu, C.J., Shin, K., Lee, S., Laurinec, S., Goyal, M., Wiggins, R. and Margolis, B. 2002. The Maguk protein, Pals1, functions as an adapter, linking mammalian homologues of Crumbs and Discs Lost. *J. Cell Biol*. 157: 161-172.

Roth, A., Kreienkamp, H.-J., Nehring, R.B., Roosterman, D., Meyerhof, W. and Richter, D. 1997. Endocytosis of the rat somatostatin receptors: subtype discrimination, ligand specificity, and delineation of carboxy-terminal positive and negative sequence motifs. *DNA Cell Biology* 16(1): 111-119.

Saha, C., Nigam, S.K. and Denker, B.M. 1998. Involvement of Galphai2 in the maintenance and biogenesis of epithelial cell tight junctions. *J. Biol. Chem*. 273: 21629-21633.

Samama, P., Cotecchia, S., Costa, T. and Lefkowitz, R.J. 1993. A mutation-induced activated state of the beta 2-adrenergic receptor. Extending the ternary complex model. *J. Biol. Chem*. 268: 4625-4636.

Sambrook, J., Maniatis, T. and Fritsch, E.F. 1989. Molecular Cloning: A Laboratory Manual. Cold Spring Harbor Laboratory, Cold Spring Harbor, New York.

Sanger, F., S. Nicklen, and A.R. Coulson. 1977. DNA sequencing with chain-terminating inhibitors. *Proc. Natl. Acad. Sci. USA*. 74: 5463-5467.

Sarret, P., Esdaile, M.J., McPherson, P.S., Schonbrunn, A., Kreienkamp, H-J. and Beaudet, A. 2004. Role of amphiphysin II in somatostatin receptor trafficking in neuroendocrine cells. *J. Biol. Chem*. 279: 8029-8037.

Schindler, M., Sellers, L.A., Humphrey, P.P.A. and Emson, P.C. 1997. Immunohistochemical localization of the somatostatin SST2 (A) receptor in the rat brain and spinal cord. *Neuroscience* 76: 225-240.

Schoeffter, P., Perez, J., Langenegger, D., Schupbach, E., Bobirnac, I., Luebbert, H., Bruns, C. and Hoyer, D. 1995. Characterization and distribution of somatostatin SS-1 and SRIF-1 binding sites in rat brain: identity with SSTR-2 receptors. *Eur. J. Pharmacol*. 289: 163-173.

Schultz, J., Hoffmuller, U., Krause, G., Ashurst, J., Macias, M.J., Schmieder, P., Schneider-Mergener, J. and Oschkinat, H. 1998. Specific interactions between the syntrophin PDZ domain and voltage-gated sodium channels. *Nat. Struct*. Biol. 5: 19-24.

Schulz, S., Handel, M., Schreff, M., Schmidt, H. and Hollt, V. 2000. Localization of five somatostatin receptors in the rat central nervous system using subtype-specific antibodies. *J. Physiol. Paris* 94: 259-264.

Sellers, L.A., Alderton, F., Carruthers, A.M., Schindler, M. and Humphrey, P.P.A. 2000. Receptor isoforms mediate opposing proliferative effects through $G_{\beta\gamma}$-activated p38 or Akt pathways. *Mol. Cell. Biol*. 20: 5974-5985.

Sharma, K. and Srikant, C.B. 1998. Induction of wild-type p53, Bax, and acidic endonuclease during somatostatin-signaled apoptosis in MCF-7 human breast cancer cells. *Int. J. Cancer* 76: 259-266.

Sharma, K., Patel, Y.C. and Srikant, C.B. 1996. Subtype-selective induction of wild-type p53 and apoptosis, but not cell cycle arrest, by human somatostatin receptor 3. *Mol. Endocrinol*. 10: 1688-1696.

Sheng, M. and Kim, E. 2000. The Shank family of scaffold proteins. *J. Cell Sci*. 113: 1851-1856.

Sheng, M and Sala, Carlo. 2001. PDZ domains and the organization of supramolecular complexes. *Annu. Rev. Neurosci*. 24: 1-29.

Shevchenko, A., Wilm, M., Vorm, O. and Mann. M. 1996. Mass spectrometric sequencing of proteins silver-stained polyacrylamide gels. *Anal. Chem*. 68: 850-858.

Shiratsuchi, T., Futamura, M., Oda, K., Nishimori, H., Nakamura, T. and Tokino, T. 1998. Cloning and characterization of BAI-associated protein1: a PDZ domain-containing protein that interacts with BAI1. *Biochem. Biophys. Res. Commun*. 247: 597-604.

Siehler, S., Seuwen, K. and Hoyer, D. 1998. [^{125}I]Tyr^{10}-cortistatin14 labels all five somatostatin receptors. *Naunyn Schmiedebergs Arch. Pharmacol*. 357: 483-489.

Singh, A.B. and Harris, R.C. 2004. Epidermal growth factor receptor activation differentially regulates claudin expression and enhances transepithelial resistance in Madin-Darby canine kidney cells. *J. Biol. Chem*. 279: 3543-3552.

Sonoda, N., Furuse, M., Sasaki, H., Yonemura, S., Katahira, J., Horiguchi, Y. and Tsukita, S. 1999. Clostridium perfringens enterotoxin fragment removes specific claudins from tight junction strands: Evidence for direct involvement of claudins in tight junction barrier. *J. Cell Biol*. 147: 195-204.

Songyang, Z., Fanning, A.S., Fu, C., Xu, J., Marfatia, S.M., Chishti, A.H., Crompton, A., Chan, A.C., Anderson, J.M. and Cantley, L.C. 1997. Recognition of unique carboxyl-terminal motifs by distinct PDZ domains. *Science* 275: 73-77.

Srikant, C.B. 1995. Cell cycle dependent induction of apoptosis by somatostatin analog SMS 201-995 in AtT-20 mouse pituitary tumor cells. *Biochem. Biophys. Res. Commun*. 209: 400-407.

Stricker, N.L., Christopherson, K.S., Yi, B.A., Schatz, P.J., Raab, R.W., Dawes, G., Bassett, D.E. Jr., Bredt, D.S. and Li, M. 1997. PDZ domain of neuronal nitric oxide synthase recognizes novel C-terminal peptide sequences. *Nat. Biotechnol*. 15: 336-342.

Strowski, M.Z., Kohler, M., Chen, H.Y., Trumbauer, M.E., Li, Z., Szalkowski, D., Gopal-Truter, S., Fisher, J.K., Schaeffer, J.M., Blake, A.D., Zhang, B.B. and Wilkinson, H.A. 2003. Somatostatin receptor subtype 5 regulates insulin secretion and glucose homeostasis. *Mol. Endocrinol*. 7: 93-106.

Strowski, M.Z., Parmar, R.M., Blake, A.D. and Schaeffer, J.M. 2000. Somatostatin inhibits insulin and glucagon secretion via two receptors subtypes: an in vitro study of pancreatic islets from somatostatin receptor 2 knockout mice. *Endocrinology* 141: 111-117.

Takano, K., Yasufuku-Takano, J., Teramoto, A. and Fujita, T. 1997. G_{i3} mediates somatostatin-induced activation of an inwardly rectifying K^+ current in human growth hormone-secreting adenoma cells. *Endocrinology* 138: 2405-2409.

Thoss, V.S., Perez, J., Probst, A. and Hoyer, D. 1996. Expression of five somatostatin receptor mRNAs in the human brain and pituitary. *Naunyn Schmiedebergs Arch. Pharmacol*. 354: 411-419.

Tochio, H., Zhang, Q., Mandal, P., Li, M. and Zhang, M. 1999. Solution structure of the extended neuronal nitric oxide synthase PDZ domain complexed with an associated peptide. *Nat. Struct. Biol*. 6: 417-421.

Thompson, J.D., Higgins, D.G. and Gibson, T.J. 1996. CLUSTAL W: improving the sensitivity of progressive multiple sequence alignment through sequence weighting, position-specific gap penalties and weight matrix choice. *Nucleic Acids Res*. 22: 4673-4680.

Tsukita, S., Furuse, M. and Itoh, M. 2001. Multifunctional strands in tight junctions. *Nat. Rev. Mol. Cell Biol*. 2: 285-93.

Tsunoda, S., Sierralta, J., Sun, Y., Bodner, R., Suzuki, E., Becker, A., Socolich, M. and Zuker, C.S. 1997. A multivalent PDZ-domain protein assembles signalling complexes in a G-protein-coupled cascade. *Nature* 388: 243-249.

Tu, J.C., Xiao, B., Naisbitt, S., Yuan, J.P., Petralia, R.S., Brakeman, P., Doan, A., Aakalu, V.K., Lanahan, A.A., Sheng, M. and Worley, P.F. 1999. Coupling of mGluR/Homer and PSD-95 complexes by the shank family of postsynaptic density proteins. *Neuron* 23: 583-592.

Ullmer, C., Schmuck, K., Figge, A. and Lübbert, H. 1998. Cloning and characterization of MUPP1, a novel PDZ domain protein. *FEBS Lett*. 424: 63-68.

Vanetti, M., Kouba, M., Wang, X., Vogt, G. and Hoellt, V. 1992. Cloning and functional expression of a novel mouse somatostatin receptor (SSTR2B). *FEBS Lett*. 311: 290.

Weckbecker, G., Lewis, I., Albert, R., Schmid, H.A., Hoyer, D. and Bruns, C. 2003. Opportunities in somatostatin research: biological, chemical and therapeutic aspects. *Nat. Rev. Drug Discov*. 2: 999-1017.

Weckbecker, G., Raulf, F., Stolz, B. and Bruns, C. 1993. Somatostatin analogs for diagnosis and treatment of cancer. *Pharmac. Ther*. 60: 245-264.

Wente, W. 2004. Funktionelle Untersuchungen von Somatostatinrezeptor-5 interagierenden Proteinen in der Maus (*Mus musculus*). Dissertation, University of Hamburg.

Wulfsen, I., Meyerhof, W., Fehr, S and Richter, D. 1993. Expression patterns of rat somatostatin receptor genes in pre- and postnatal brain and pituitary. *J. Neurochem*. 61: 1549-1552.

Xia, J., Zhang, X., Staudinger, J. and Huganir, R.L. 1999. Clustering of AMPA receptors by the synaptic PDZ domain-containing protein PICK1. *Neuron* 22: 179-187.

Xu, X.R., Huang, J., Xu, Z.G., Qian, B.Z., Zhu, Z.D., Yan, Q., Cai, T., Zhang, X., Xiao, H.S., Qu, J., Liu, F., Huang, Q.H., Cheng, Z.H., Li, N.G., Du, J.J., Hu, W., Shen, K.T., Lu, G., Fu, G., Zhong, M., Xu, S.H., Gu, W.Y., Huang, W., Zhao, X.T., Hu, G.X., Gu, J.R., Chen, Z. and Han, Z.G. 2001. Insight into hepatocellular carcinogenesis at transcriptome level by comparing gene expression profiles of hepatocellular carcinoma with those of corresponding noncancerous liver. *Proc. Natl. Acad. Sci. USA* 98: 15089-15094.

Xu, X.Z., Choudhury, A., Li, X. and Montell, C. 1998. Coordination of an array of signaling proteins through homo- and heteromeric interactions between PDZ domains and target proteins. *J. Cell Biol*. 142: 545-555.

Yamada, Y., Post, S.R., Wang, K., Tager, H.S., Bell, G.I. and Seino, S. 1992. Cloning and functional characterization of a family of human and mouse somatostatin receptors expressed in brain, gastrointestinal tract and kidney. *Proc. Natl. Acad. Sci. USA* 89: 251-255.

Zitzer, H., Honck, H., Bachner, D., Richter, D. and Kreienkamp, H-J. 1999. Somatostatin receptor interacting protein defines a novel family of multidomain proteins present in human and rodent brain. *J. Biol. Chem*. 274: 32997-33001.

Zupanc, G.K., Siehler, S., Jones, E.M., Seuwen, K., Furuta, H., Hoyer, D. and Yano, H. 1999. Molecular cloning and pharmacological characterization of a somatostatin receptor subtype in the gymnotiform fish Apteronotus albifrons. *Gen. Comp. Endocrinol*. 115: 333-345.

APPENDIX I LIST OF CONSTRUCTS

Construct	Vector	Primer	Cloning site
pGBKT7-hSSTR3-C	pGBKT7	SSTR3-F (C-terminal) SSTR3-R	EcoRI / BamHI
pGBKT7-rSSTR3-C	pGBKT7	rSSTR3-F rSSTR3-R (PstI)	EcoRI / PstI
pGBKT7-hSSTR3-8C	pGBKT7	SSTR3-F (C-terminal) hSSTR3-8R	EcoRI / BamHI
pAS-hSSTR5-C	pAS2.1	Wente, 2004	
pACT-3D1 (MUPP1)	pACT2	Clontech, YTH library	EcoRI / XhoI
pACT-3D6 (MUPP1)	pACT2	Clontech, YTH library	EcoRI / XhoI
pACT-PDZ10-13	pACT2	mu4694 mu6180	EcoRI / XhoI
pACT-PDZ11-13	pACT2	mu4916 mu6180	EcoRI / XhoI
pACT-PDZ12-13	pACT2	mu5207 mu6180	EcoRI / XhoI
pACT-PDZ13	pACT2	mu5525 mu6180	EcoRI / XhoI
pACT-PDZ10	pACT2	mu4694 mu5171	EcoRI / XhoI
pACT-3D7 (BAIAP1)	pACT2	Clontech, YTH library	EcoRI / XhoI
pACT-BAIAP (PDZ1-5)	pACT2	BAP-GW-F BAP-GW-R	BamHI / EcoRI
pACT-BAIAP (GK-WW)	pACT2	BAP-PDZ-F BAP-PDZ-R	BamHI / EcoRI
pACT-PIST	pACT2	Wente, 2004	
pACT-PIST (PDZ)	pACT2	Wente, 2004	
pACT-PIST(-PDZ)	pACT2	Wente, 2004	
pCDNA3-T7-Ntag-hSSTR3	pCDNA3-T7-Ntag	hSSTR3-F hSSTR3-R	BamHI / EcoRI
pCDNA3-T7-Ntag-rSSTR3	pCDNA3-T7-Ntag	rSSTR3-F rSSTR3-R(XhoI)	EcoRI / XhoI
pXMD1-rMUPP1	-	Ullmer *et al.*, 1998	-
pCMV-Tag-3D1	pCMV-Tag-2C	EcoRI/XhoI fragment from pACT2-3D1	EcoRI / XhoI
pGEX-4T-1-PDZ10	pGEX-4T-1	PDZ10-F PDZ10-R	EcoRI / SalI

pGEX-6P-1-hSSTR3-50C	pGEX-6P-1	hSSTR3-50C-F hSSTR3-R	BamHI / EcoRI
pEGFP-rPSD95	pEGFP-C3	S. Kindler, UKE	-
CMV-26-mCIPP	p3XFLAG-*myc*-CMV-26	mCIPP-F mCIPP-R	EcoRI / XbaI
pGEX-6P-1-rSSTR3-50C	pGEX-6P-1	rSSTR3-50C-F rSSTR3-50C-R	BamHI / EcoRI
pGEX-6P-1-cSSTR3-50C	pGEX-6P-1	cSSTR3-50CF cSSTR3-50CR	BamHI / EcoRI
pGEX-6P-1-rSSTR3-50C-Y	pGEX-6P-1	rSSTR3-50C-F rSSTR3-Y-R	BamHI / XhoI
pGEX-6P-1-rSSTR3-50C-RI	pGEX-6P-1	rSSTR3-50C-F rSSTR3-RI-R	BamHI / XhoI
pCDNA3-T7-Ntag-hSSTR3-8C	pCDNA3-T7-Ntag	hSSTR3-F hSSTR3-8CR	BamHI / EcoRI
pCDNA3-T7-Ntag-hSSTR3-R3	pCDNA3-T7-Ntag	hSSTR3-F hSSTR3-R3	BamHI / EcoRI
pCDNA3-T7-Ntag-hSSTR3-C terminal	pCDNA3-T7-Ntag	hSSTR3-F2 hSSTR3-R	BamHI / EcoRI
pCDNA3-T7-Ntag-hSSTR3-mSSTR5-IC3	pCDNA3-T7-Ntag-hSSTR3	hSSTR3-mSSTR5-IC3-F hSSTR3-mSSTR5-IC3-R	Blunt end ligation
pCDNA3-T7-Ntag-mSSTR5 (without C-terminal)	pCDNA3-T7-Ntag	mSSTR5-F mSSTR5-R	BamHI / EcoRV
pCDNA3-T7-Ntag-mSSTR5-hSSTR3-C	pCDNA3-T7-Ntag-mSSTR5	phSSTR3-F hSSTR3-R	EcoRV / EcoRI
pCDNA3-T7-Ntag-mSSTR5-hSSTR3-N-C	pCDNA3-T7-Ntag-mSSTR5-hSSTR3-C	mSSTR5-NF/mSSTR5-NR hSSTR3-F/hSSTR3-NR	BamHI / blunt
pTRE2-hyg-T7-hSSTR3	pTRE2-hyg	T7-hSSTR3-F T7-hSSTR3-R	BglII(BamHI) / blunt
pCDNA3-T7-Ntag-mSSTR5-hSSTR3-8C	pCDNA3-T7-Ntag-mSSTR5	phSSTR3-F hSSTR3-8CR (XhoI)	EcoRV / XhoI
Topo-cSSTR1	pCRII-TOPO	cSSTR1-F cSSTR1-R	-
Topo-cSSTR2	pCRII-TOPO	cSSTR2-F cSSTR2-R	-
Topo-cSSTR3	pCRII-TOPO	cSSTR3-F cSSTR3-50CR	-

APPENDIX II LIST OF PRIMERS

	Sequence/Restriction site
SSTR3-F (C-terminal)	CCC **GAA TTC** TCC TAC CGC TTC AAG CAG GGC **EcoRI**
SSTR3-R	CCC **GGA TCC** CTA CAG GTA GCT GAT GCG CAT C **BamHI**
rSSTR3-F	C C**GA ATT C**CC ATG GCC GCT GTT ACC TAT C **EcoRI**
rSSTR3-R	CC**C TGC AG**T TAC AGA TGG CTC AGC GTG CTG **PstI**
hSSTR3-8R	CC**G GAT CC**C TAC TCC CCA GTG GAA GCC TC **BamHI**
mu4694	CCC **GAA TTC** AAG ACA GCA AAG ATG ACA GTA AAA C **EcoRI**
mu4916	CCC **GAA TTC** CCT GGC TGC GAA ACA ACC ATC **EcoRI**
mu5207	CCC **GAA TTC** TGT GAC ACC CTC ACT ATT GAG C **EcoRI**
mu5525	CCC **GAA TTC** GCA TTG GCA TCT GAA ATA CAG GG **EcoRI**
mu5903	CCC **GAA TTC** GAT TTA GGA CCT CCT CAA TGT AAG **EcoRI**
mu6180	CCC **CTC GAG** GCC AAT TCA AGA GAG AAC CAT CAA **XhoI**
mu5171	CCA **CTC GAG** AGG GTG TCA CAC ACT TCC TCC **XhoI**
BAP-GW-F	CCA **GGA TCC** TGC ACA ACC CGA TCT CCC AG **BamHI**
BAP-GW-R	CCC **GAA TTC** TTT CCG CAG CTT TGT GTG AAT G **EcoRI**
BAP-PDZ-F	CCA **GGA TCC** GGC AAG TTC ATT CAC ACA AAG **BamHI**
BAP-PDZ-R	CCC **GAA TTC** GAC TTT CCT GCT GCC GTT C **EcoRI**
hSSTR3-F	CC **GGA TCC** GCC ATG GAC ATG CTT CAT C **BamHI**
hSSTR3-R	CC**G AAT TC**C TAC AGG TAG CTG ATG CGC **EcoRI**
rSSTR3-F	C C**GA ATT C**CC ATG GCC GCT GTT ACC TAT C **EcoRI**
rSSTR3-R	CC**C TCG AG**T TAC AGA TGG CTC AGC GTG CTG **XhoI**

PDZ10-F	CCC **GAA TTC** AAA GAC AAT CCC CAG ACT CC **EcoRI**
PDZ10-R	CAA **GTC GAC** GGG GCC TCA TCT CGG TAG AG **SalI**
hSSTR3-50C-F	GAA **GGA TCC** AAG GAG ATG AAC GGC CGG **BamHI**
mCIPP-F	G GG**G AAT TC**C TGC AGC ATG GTC CAC GG **EcoRI**
mCIPP-R	GGG **TCT AGA** TTA ATC AGC CGT CCT CTG C **XbaI**
rSSTR3-50C-F	CTT **GGA TCC** GAG ATG AAT GGG AGG CTC **BamHI**
rSSTR3-50C-R	CCC **GAA TTC** TTA CAG ATG GCT CAG CGT GC **EcoRI**
cSSTR3-50CF	CCT **GGA TCC** ATG AAC GGC CGG GTC AGC **BamHI**
cSSTR3-50CR	CCC **GAA TTC** CTA CAG ATA GCT GAT GTG CA **EcoRI**
rSSTR3-Y-R	CC **CTC GAG** TTA CAG *GTA* GCT CAG CGT GCT GGC **XhoI**
rSSTR3-RI-R	CC **CTC GAG** TTA CAG ATG ACT *GAT GCG* CAG CGT GCT GGC **XhoI**
hSSTR3-8CR	CTT **GAA TTC** GGA CTT CTC CCC AGT GGA AGC **EcoRI**
hSSTR3-R3	CCT **GAA TTC** CTA GCC CTG CTT GAA GCG GTA GG **EcoRI**
hSSTR3-F2	CCT **GGA TCC** TAC CGC TTC AAG CAG G **BamHI**
hSSTR3-mS5-IC3-F	*TCA* CG*A* CG*G* *A*G*A* CGC TC*A* GAA CGC *AAG* GTG ACT CGC ATG GTG
hSSTR3-mS5-IC3-R	*GGA* *GCC* CAC CCG *CAT* CCC AGC *AGC* *CTT* CAC CTT CAC CAC GAT GAG
mSSTR5-F	CCC **GGA TCC** ATG GAG CCC CTC TCT TTG G **BamHI**
mSSTR5-R	CC**G ATA TC**A GAG AGA AAG CCA TAG AG **EcoRV**
mSSTR5-NR	CCA AAG AGA GGG GCT CCA T
mSSTR5-NF	GCG GTA TTA GTG CCT GTG C
hSSTR3-NR	ACT GAC CGC CAG CCC TG
T7-hSSTR3-F	CC **AGA TCT** CAA GCA ATG GCT AGC ATG ACT GG **BglII**
T7-hSSTR3-R	CGC GGC CGC CTA CAG GTA GCT GAT GCG CAT C
phSSTR3-F	CGC TTC AAA CAG GGC TTC CG

hSSTR3-8CR (XhoI)	CCG **<u>CTC GAG</u>** CTA GGA CTT CTC CCC AGT GGA A **XhoI**
hMUSV2F(n)	CAC CCT CAC TAT TGA GCT GCA GAA G
hMUSV2R(n)	TGC TGA TTC CCA GTG AGT CAG TAG G
hMUSV2R2(n)	GTA CTG GAT CCA GCT TTG ATT CTT CC
hMUSV2F3	GCC TAG GAT TAA AAA CGA TAC TGG AG
cSSTR1-F	ATG TTC CCC AAT GGC ACT GC
cSSTR1-R	TCA GAG AGT CGT GAT CCG AG
cSSTR2-F	ATG GAT ATG GAG TAT GAG CT
cSSTR2-R	TCA GAT ACT GGT CTG GAG GT
cSSTR3-F	C ATG GAT ACC CTT GGC TAT C

Underlined: silent change of nucleotide to avoid primer secondary structure
Underlined and italic: site-directed mutagenesis to change or add amino acid.

CURRICULUM VITAE

PERSONAL PARTICULARS

Name	CHONG WEE LIEW
Place of Birth	Kuala Lumpur, Malaysia
Nationality	Malaysian

EDUCATIONAL BACKGROUND

July 1992- June 1995	**The National University of Singapore (NUS), Singapore** Bachelor of Science (B. Sc.) Degree with merit, major in Microbiology and Biochemistry
July 1995- June 1996	**The National University of Singapore (NUS), Singapore** Bachelor of Science with Honours (Class II, Upper Div.) in Microbiology
Oct. 1999- March 2001	**The National University of Singapore (NUS), Singapore** Master of Science in Microbiology
June 2001- Dec. 2004	**University of Hamburg, Germany** PhD study

PUBLICATIONS

Yip, C.W., Liew, C.W. and Nga, B.H. 1997. Ribosomal RNA genes of *Endomyces fibuliger*: isolation, sequencing and the use of the 26S rRNA gene in integrative transformation of *Saccharomyces cerevisiae* for efficient expression of the α-amylase gene of *Endomyces fibuliger*. *World J. Microbiol. Biotechnol*. 13: 103-117.

Liew, C.W., Nga, B.H., Tan, H.M., H, B., Nakase, T. and Suzuki, K. 1998. Isolation of actinomycetes from soil and screening for the presence of bioactive substances produced by them. *Proceedings of the International Conference on Asian Network on Microbial Research*. pp.155-164.

Liew, C.W., Leong, M.L. and Nga, B.H. 2001. Characterisation of genes of actinomycete that produce aromatic polyketide which are antitumour agents. *Microbial Biotechnology in the Asia-Pacific Region: Prospects and Challenges for the 21st Century. 4th Asia-Pacific Biotechnology Congress and 30th Annual Philippine Society for Microbiology, Inc. (PSM) Convention.*

Liew, C.W., Richter, D. and Kreienkamp, H-J. Interaction of human SSTR3 receptor with tight junction protein, MUPP1, via PDZ domain. *23rd Blankenese conference, Hamburg, 2003.*

Liew, C.W., Richter, D. and Kreienkamp, H-J. Interaction of human SSTR3 receptor with tight junction protein, MUPP1, via PDZ domain. *Oral presentation at the 15th International Symposium on Regulatory Peptides, September, 2004, Toulouse, France.*

Kreienkamp, H-J., Liew, C.W., Baechner, D., Mameza, M-G., Soltau, M., Quitsch, A., Christenn, M., Wente, W. and Richter, D. Physiology of somatostatin receptors: from genetics to molecular analysis.

Quitsch, A., Berhoerster, K., Liew, C.W., Richter, D. and Kreienkamp**,** H-J. Postsynaptic shank antagonizes dendrite branching induced by the leucine rich repeat protein densin-180. Journal of Neuroscience.

Liew, C.W., Schulz, S., Brandner, J.M., Buck, F., Glassmeier, G., Schwarz, J., Richter, D. and Kreienkamp, H-J. Regulation of tight junction biogenesis by the G-protein coupled somatostatin receptor subtype 3. Manuscript Submitted to Journal of Cell Biology.